69

979

69-21,979

CALVERT, Floyd Olan, 1925-
CONCEPTUAL DESIGN OF A FIVE KW RADIOISOTOPE-FUELED POWER SYSTEM FOR TERRESTRIAL APPLICATIONS.

The University of Oklahoma, D.Engr., 1969
Engineering, mechanical

University Microfilms, Inc., Ann Arbor, Michigan

THE UNIVERSITY OF OKLAHOMA

GRADUATE COLLEGE

CONCEPTUAL DESIGN OF A FIVE KW RADIOISOTOPE-FUELED POWER SYSTEM FOR TERRESTRIAL APPLICATIONS

A DISSERTATION

SUBMITTED TO THE GRADUATE FACULTY

in partial fulfillment of the requirements for the

degree of

DOCTOR OF ENGINEERING

BY

FLOYD OLAN CALVERT

Norman, Oklahoma

1969

CONCEPTUAL DESIGN OF A FIVE KW RADIOISOTOPE-FUELED

POWER SYSTEM FOR TERRESTRIAL APPLICATIONS

APPROVED BY

[illegible]

[illegible]

Raymond Kasey

Darrel G. Harden

David M. Elliott

DISSERTATION COMMITTEE

ACKNOWLEDGMENT

It is a pleasure to record my sincere appreciation of the counsel, direction, and encouragement which Dr. Tom J. Love, Jr. has given me both in this present work and in other aspects of my professional life. Any achievement is far easier if in the doing of the thing one is attempting to satisfy the expectation that some other person has of him. Dr. Love has been such a person to me as I have made this effort. He has thereby, surely, fulfilled one of the major roles of a teacher.

I am also most grateful to Dr. C. Phillip Colver, Dr. Darrel G. Harden, Dr. David M. Elliott, and Dr. Raymond V. Kaser for their time and assistance as they have served on my doctoral committee. I also want to acknowledge the able assistance of Dr. John E. Francis who helped me over a troublesome spot. I especially thank Mary Ann Parton who somehow was able to transform my almost illegible writing into pages of neatly typed material. I am most appreciative of the help that has been given me by Louise Sizemore, engineering librarian, on very many occasions.

Finally, I must acknowledge my wife and children who have made the accomplishment of this dissertation a real challenge. I hope they will ultimately know it has all been for them.

TABLE OF CONTENTS

		Page
LIST OF TABLES		v
LIST OF ILLUSTRATIONS		vi
Chapter		
I.	INTRODUCTION; THE NEED FOR TERRESTRIAL RADIOISOTOPE-FUELED KILOWATT POWER SYSTEMS	1
II.	COMPARISON OF VARIOUS POWER SYSTEM CONCEPTS AND SYSTEM SELECTION	8
III.	SELECTION OF A WORKING FLUID	32
IV.	SELECTION OF THE RADIOISOTOPE FUEL	44
V.	TURBINE DESIGN	51
VI.	CYCLE THERMODYNAMICS	64
VII.	DESIGN OF THE HEAT SOURCE - BOILER	79
VIII.	A LATER DESIGN PHASE: PRELIMINARY DESIGN	113
IX.	RELIABILITY CONSIDERATIONS	116
X.	DESIGN CONCEPT SUMMARY	124
BIBLIOGRAPHY		129
APPENDIX		132

LIST OF TABLES

Table		Page
2.1	Space Power Plants	11
2.2	Reactants for Chemical Heat Source Systems	25
2.3	Power System Selection Table	27
4.1	Radioisotopic Power Fuels Data	45
4.2	Thermal Conductivity of Shield Materials	47
4.3	Fuel Selection Decision Table	49
5.1	Working Fluid Conditions	55
5.2	Comparison of Turbine Designs	63
6.1	Turbine Power Summary	64
6.2	Steam Cycle Properties	67
6.3	Mercury State Point Properties	73
6.4	Comparison of Cycles	75

LIST OF ILLUSTRATIONS

Figure		Page
1.1	Power System Application Ranges	5
2.1	Schematic Illustration, Stirling Engine	13
2.2	Radioisotope Brayton Cycle Power System	14
2.3	Indirect Rankine Power System Concept	17
2.4	Supercritical Cycle Arrangement	20
2.5	Pseudo-Supercritical Cycle for CO_2	21
2.6	Supercritical Thermodynamic Cycle	21
2.7	Chemical Dynamic Power System	24
3.1	Cycle Work Areas	35
3.2	Rankine Cycle Thermal Efficiency	39
4.1	Cobalt - 60 Decay Scheme	50
5.1	Application Regimes of Various Turbine Types	54
5.2	Turbine Expansion Process - Alternative A	57
5.3	Maximum Efficiency for Optimum Turbine Design, Axial Flow, Multi-Stage, Single Disk Turbines	59
6.1	Cycle Arrangement for Steam Cycles	66
6.2	Steam Turbine Expansion Process	70
6.3	Heat Interchanger Schematic	70
6.4	Superheated Mercury Cycle	72
6.5	Cycle Efficiency	77
7.1	Heat Source Design - Alternative No. 1	83

LIST OF ILLUSTRATIONS CONTINUED

Figure		Page
7.2	Experimental Boiling Heat Transfer Coefficient	84
7.3a	Schematic Illustration, Once-Through Boiler	87
7.3b	Typical Heat Flux Distribution in a Liquid-Heated, Counter-Flow Boiler Tube	88
7.4	Heat Source Cycle Arrangement, Alternative No. 3	90
7.5	Heat Source-Boiler Design, Alternative No. 4	91
7.6	Flat Slab Model-Temperature	99
7.7	Cross Section, Cylindrical Heat Flow Model	104
7.8	Cross Section of RIT Heat Source-Boiler	111
9.1a	Parallel Redundant System	118
9.1b	Series-Parallel Redundant System	118
9.2	System Arrangement for Redundancy	120
10.1	Design Concept, Direct Cycle Power System	125
A7.1	Mercury Boiler Schematic	141
A7.2	Slip Ratio Curve	143
A7.3	Martinelli-Nelson Friction Multiplier Correlation	146
A7.4	Flat Slab Model of Heat Source	152
A7.5	Fuel Heat Flow	152

CONCEPTUAL DESIGN OF A FIVE KW RADIOISOTOPE-FUELED POWER SYSTEM FOR TERRESTRIAL APPLICATIONS

CHAPTER I

INTRODUCTION; THE NEED FOR TERRESTRIAL RADIOISOTOPE-FUELED KILOWATT POWER SYSTEM

Introduction

The purpose of this conceptual design study is to design a 5 kw radioisotope-fueled power system for terrestrial applications. One obvious application is in manned underseas stations. The ocean depths have been characterized as "energy deserts". Most conventional power plants are "air breathing" and such systems may not be readily applied in the ocean depths. Another characteristic of the type of application envisioned in this study is the requirement for long periods of operation without maintenance or refueling. Thus one is led to consider radioisotope-fueled systems.

The nature of the design function is that it is a highly iterative process. The designer considers and analyzes a concept often with comparatively crude tools of analysis and with perhaps an incomplete grasp of the principles involved in the early iterations of the design process. He is content to achieve order-of-magnitude results at the beginning. As the number of iterations increases, the design achieves sophistication and the analysis occurs in greater detail and to greater accuracy. Thus if one presents only the last iteration, the finished product of the design effort, he may be able to present little tangible evidence of the tortuous, backtracking route to the final design scheme. It is for this reason that in some sections of this report "false-starts" or multiple iterations are included. In fact, time limitations are such that this entire presentation should be considered as an early iteration. The following remarks, taken from reference 25, seem appropriate here:

> After the frequency of changes has diminished, detailed design parameters can be better determined with a more complicated representation that includes extensive neutronic and shielding information. In such a representation, detailed digital computer models of the major components are integrated into a single system computer representation. This type of system representation has the advantage of producing detailed and more accurate optimized parameters. It is not feasible to utilize such a representation for conceptual studies because of the large effort required to incorporate modifications, and to develop and integrate the individual component models. Final design characteristics are the end result of this type of system representation.

As the design study has developed, (and this is a typical result in design work), it has become apparent that some other alternative may be more desirable (or at least equally desirable) than the design alternative pursued to this point. However, the main function of a later stage in the design cycle (the preliminary design stage) is to optimize various alternative systems and to select that system which is best. The aim of this study is to propose one candidate design which must ultimately be compared with other alternative systems when any particular application is considered. Additionally, a fact-of-life is that many problems will arise, and true comparative performance may be obtained, only during the hardware phase of the design cycle.

In brief, it may be stated that the concept here presented (direct cooling of heat source by the mercury working fluid) is a valid concept worthy of further development. However, it is clear that cycles involving double loops (indirect cycles) and cycles using steam as the working substance appear to have equal merit and worthiness of further development. And, ultimately, the once-through boiler concept may prove superior to natural circulation units.

A description of the design proposed herein is contained in Chapter 10.

Design Goals

The design goals of this conceptual design study are as follows:

1. High reliability for up to 10000 hours of operation
2. Maximum safety
3. Producibility of the design concept using current "state-of-the-art".
4. Maximum thermodynamic cycle efficiency with concomitant minimum radioisotope fuel inventory.
5. System to be capable of adaptation for underseas applications.

The Need for Terrestrial Radiosotope-Fueled Kilowatt Power System

It has been estimated that 40 per cent of the world's oil reserves are under the continental shelves and petroleum industry spokesmen predict an investment to $25 billion in offshore development over the next 10 years. In addition to petroleum industry operations, proposed underseas missions include underseas stations for research, underseas mining and manufacturing, communications systems; and even underseas pleasure resorts. Such missions as these will obviously require contiguous power sources.

References 6 and 12 list the following as applications where long life reliable electrical power plants in the low kilowatt range are needed:

1. Undersea applications, both manned (such as Seahabitat) and unmanned (such as underwater sound propagation)
2. Inland Arctic and Antarctic stations
3. Remote communication facilities, navigational aids, and weather stations
4. Stand-by power for military installations.

Ranges of Application for Power Systems

Figure 1.1 is derived from reference 12 and illustrates the typical ranges of application of nuclear energy power systems. Radioisotope power systems are usually applied in the power interval range 1 mw up to about 15 kw. Dynamic conversion is generally more efficient than thermoelectric or thermionic conversion in the 2 to 15 kw power range.

Comparison of Space and Terrestrial Environmental Constraints

Considerable development of dynamic energy conversion systems has been accomplished in the various space programs. It is useful to compare environmental constraints on earth and in space.

Space Constraints

1. Either complete recovery or complete burn-up of radioiso-

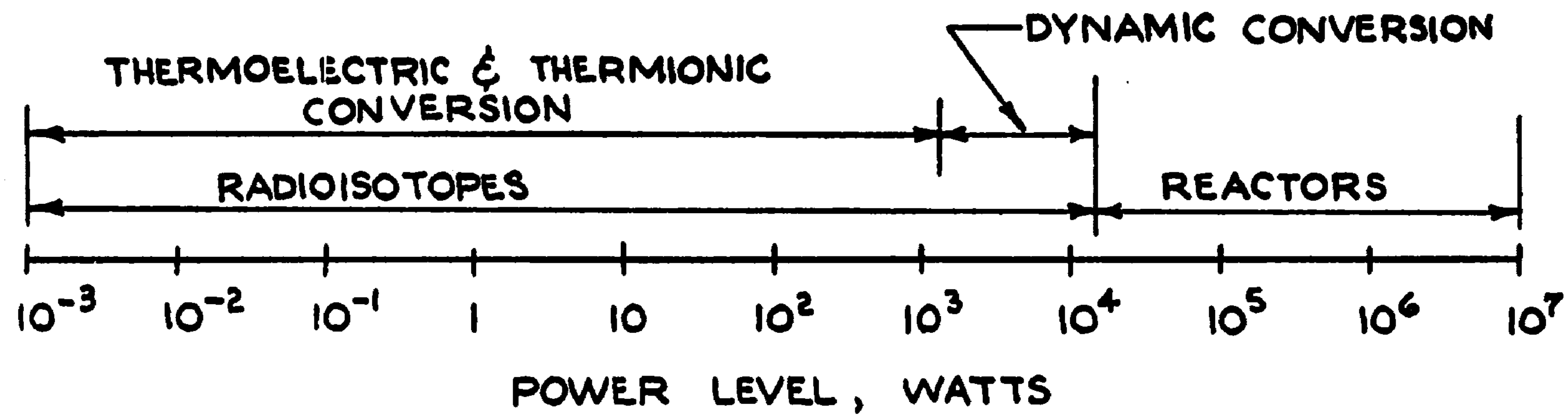

Power System Application Ranges

Figure 1.1

tope fuel is necessary.

2. The heat sink is provided by very low temperature space. Mode of heat rejection is by radiation from "space radiators". Thus it becomes expedient to design for minimum weight of the space radiator in order to minimize the cost of placing the power package in orbit. The minimum weight radiator requirement leads to a ratio of upper cycle temperature (for Rankine Cycles) to condensing temperature of approximately 0.75 when the power cycle is optimized with respect to the minimum radiator area criterion.
3. Weight penalties also influence the shielding design for the power plant.
4. Little maintenance can be accomplished in space.
5. Liquid metal working substances are particularly suited for space application since they have comparatively high condensing temperatures.

Terrestrial Constraints (Ocean Application)

1. Weight of the power plant is not of major importance. Thus the power system is not optimized with respect to minimum condensing surface area. It is, however, necessary to minimize the initial fuel inventory in order to limit costs. Thus cycle efficiency is all important.
2. Mode of cycle heat rejection is by convection and conduction to the ocean or atmospheric heat sink. Ocean temperatures range from $34^{o}F$ to $86^{o}F$. Therefore the liquid metal working substances with their high condensing temperatures

are at a distinct disadvantage compared to water or organic fluid working substances. Note that the thermal efficiency of a Carnot cycle can be increased more by decreasing the temperature of heat rejection than by raising the temperature of heat addition by the same number of degrees.

3. It probably is not possible to design for complete burn-up of the radioisotope fuel. Rather it is necessary to design for integrity of the radioisotope containers under all credible accidents and under corrosion and erosion forces.
4. Weight constraints on shielding are not as severe as in space.
5. Limited maintenance activities may be designed for. Somewhat greater opportunity exists for resupply or exchange of fuel inventory as compared to space applications.

CHAPTER II

COMPARISON OF VARIOUS POWER SYSTEM

CONCEPTS AND SYSTEM SELECTION

Introduction

A brief survey of various types of power systems which may have potential for application in confined, limited access, environments in the power range 2 to 10 kw is contained in this chapter. A qualitative comparison and evaluation of power system concepts of potential interest is contained in table 2.3.

Selection Criteria

The selection criteria listed in reference 19 are generally applicable to the power system application herein considered. These criteria, (as presented in reference 19) are:

1. Performance
2. Reliability
3. Weight
4. Vehicle Integration
5. Development Risk
6. Maintainability
7. Safety
8. Survivability
9. Logistics

10. Flexibility
11. Development Cost
12. Acquisition Cost
13. Operational Cost

Selection Technique

Also useful from reference 19 are the following weighting factor indices and rating scales:

Weighting Factor	Relative Value
10	Critical
9	Major concern
8	Very important
7	Important
6	Normal concern
5	Minor concern
4	Least concern

After each criterion is assigned a weighting factor, the various power system concepts are given a numerical rating on each criterion. Useful rating values would be

Rating	Relative Value
8 to 10	Very good to excellent
6 to 8	Good to very good
4 to 6	Satisfactory to good

A typical evaluation form would be as follows:

CRITERIA	RATING	WEIGHTING FACTOR	SCORE
SAFETY	10	6	60

etc.

Dynamic Power System Concepts

Table A2.1, (located in the appendix), is from reference 6 and provides a brief comparison of energy conversion techniques. Table A2.2, (in the appendix), is also from reference 6 and gives a brief listing of advantages and disadvantages of steam, organic vapor and liquid metal Rankine cycles. Table 2.1 is extracted from reference 7 and provides information on power systems which were designed for space applications.

Stirling Cycle

The Stirling cycle engine is a reciprocating piston engine in which the thermodynamic processes may be ideally depicted as shown in figure 2.1. Since the Stirling engine has a potentially high efficiency it is of much interest for applications which use radioisotope fuels as heat energy sources. However the Stirling engine may be still considered to be in the developmental stage and as having, at present, comparatively unknown maintenance and reliability characteristics. For this reason the Stirling engine will not be considered as a design alternative for the application contemplated. (The design and performance of a 7.3 kw(e) radioisotope energized undersea Stirling engine is described in reference number 26.)

Closed Brayton Cycle

Reference 8 presents a conceptual design study for a space application of a Brayton-cycle power system fueled by a radioisotope heat source. A schematic illustration of the proposed cycle is shown in figure 2.2. Also shown are the ideal thermodynamic processes on the pv and Ts diagrams. The design is based on the use of either

Table 2.1*

Space Power Plants

	Vendor and Type of Cycle		
	Sunstrand, Biphenyl Rankine Cycle (System 1A)	TRW-TAPCO Mercury Rankine Cycle	AiResearch, Argon Brayton Cycle, (Radiator Heat Sink) (System No. 5)
1. Regenerator Temperature, (^{o}R)			
(Hot side) In and out	1100, 837	-	1539
(Cool side) In and out	808, 1010 $\eta_{reg} = 0.90$	-	465
2. Condenser temp. and pressure	800^{o}R 1.5 psia	1050 to 1110^{o}R 611.5 psia	-
3. Alternator Power Out, (KW_e)	1.5 plus 0.15 parasitic	1.8	1.5
4. Radiator area, (ft^2)	63 to 65	48 (using Hg) 60 (using glycol)	120 - 150
5. Weight Summary			
Gross	600	850	1020
Usable By-Product	0	0	0
Net (lb)	600	850	1020
6. Power Source	Po^{210} RIT Heat Source ½ Life: 138 days Power Density 134 w/gm	Po^{210} RIT Heat Source ½ Life: 138 days Power Density 134 w/gm	Po^{210} RIT Heat Source ½ Life: 138 days Power Density 134 w/gm

*Extracted from Reference 6

7.	Power Conversion System	Turbo-Pump and 3200 cps A.C. Alternator η_{alt} = 0.85	Turbo-Pump and 400 cps A.C. Alternator η_{alt} = 0.85	Turbo-Compressor and 3200 cps Alternator η_{alt} = 0.85-0.90
8.	Working Fluid	Biphenyl	Mercury in PCS Loop	Argon
9.	Compressor/Pump:			
	Inlet Pressure, P_1(psia)	1.5(η_c = 0.25)	4-10, η_p = 0.25	1.0, η_2 = 0.78
	Discharge Pressure, P_2(psia)	166.5	408-500, η_p = 0.25	2.5
	Inlet Temp, T_1 (^oR)	790	760 to 810	300
	Discharge Temp, T_3(^oR)	794	760 to 810	465
10.	Turbine/Expander:			
	Inlet Temp, T_3(^oR)	1210	1810, η_t = 0.55	2000, η_t = 0.83
	Outlet Temp, T_4(^oR)	1100	1050 - 1110	1539
	Inlet Temp, P_3(psia)	158.6	408 - 500	2.5
	Outlet Temp, P_4(psia)	1.50	6 - 11.5	1.0
11.	Combined Rotating Unit Speed, (RPM)	24000	40000	64000

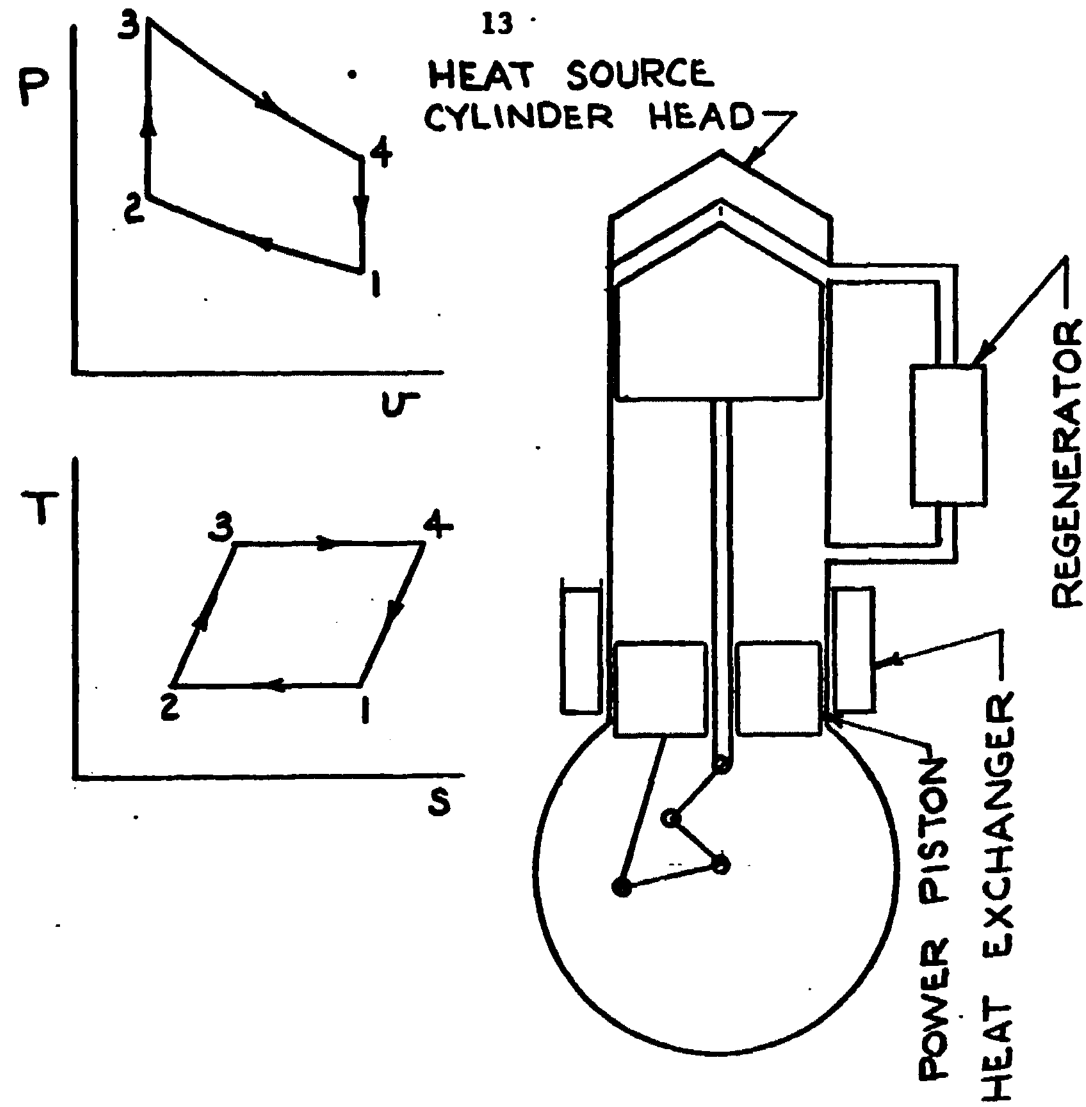

Schematic Illustration
Stirling Engine
Figure 2.1

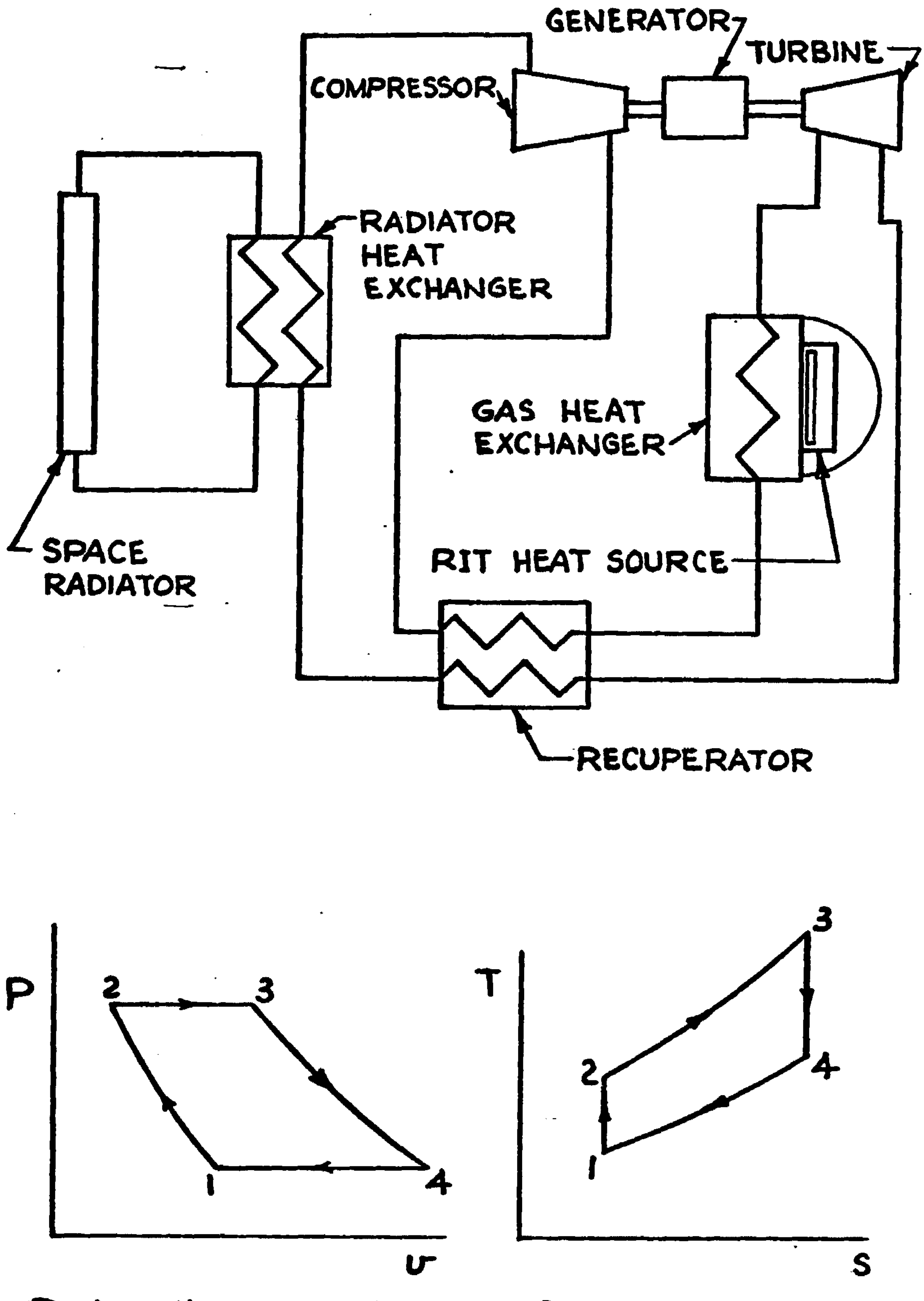

Radioisotope Brayton Cycle Power System

Figure 2.2

(ORNL, REFERENCE 8)

Pu-238, Cm-244, or Pm 147 as radioisotope fuels. The design study indicates that, "Probably the most important problem with respect to the long-term containment of the two alpha-emitting fuels, Pu-238 and Cm-244, is the internal capsule pressure resulting from the helium produced during decay." The design goal is for a cycle efficienty of 20% (based on the shaft power and on the thermal input at the end of one year). The design specification for the turbine inlet temperature is 1960°R.

It is to be noted that weight and size, while not of primary concern in terrestrial applications, are of critical importance for space applications. Thus the Brayton cycle power plant which utilizes high-speed dynamic components is particularly attractive for space use. The Brayton cycle power plant should most certainly be considered for any specific application in the power range of interest in this report. And the design goal for the cycle efficiency, indicated above, will be useful for comparison with power plant efficiencies predicted for the various Rankine cycles.

Rankine Cycle

Physical feasibility of the Rankine cycle concept using radioisotope fuels may be expected if it is possible to show that sufficient quantities of radioisotope fuels are available or may become available and if safety features associated with the use of the fuel are acceptable. Economic feasibility will be more difficult to predict since under most usual circumstances one is not willing to pay, say for example, $15.00 per kw-hr for energy.

The Rankine cycle may use either the turbine or a reciprocating engine as the thermal-energy-to-mechanical-work conversion device. Currently some work is being devoted to the development of new concepts in steam engines, particularly for application as automobile power plants, (reference 9). However since the reliability of the reciprocating engines probably is not presently as high as that for turbines they will not be considered further in this study.

Rankine cycles may be direct or indirect. A direct cycle, by definition, is one wherein the radioisotope coolant is used as the power cycle working fluid. An indirect cycle has a power cycle working fluid which is separate from the radioisotope coolant fluid and exchanges heat energy with it.

Westinghouse, reference 10, has a conceptual design for an underseas application of a radioisotope power plant which uses the indirect Rankine cycle. The radioisotope heat source is to be cooled by air circulated by blowers and the turbine working fluid will be steam. The schematic diagram for this cycle is shown in figure 2.3. The reasons listed by Westinghouse for choice of the indirect cycle are:

1. Because of its simplicity, the gas-cooled heat source requires a minimum of development effort. Furthermore, since it is relatively well developed, there is little uncertainty as to its operational characteristics.
2. Loss-of-coolant and general cooling problems encountered during transit are diminished when gas is used. (An emergency gas supply can be carried.)
3. The coolant loop is isolated from the working fluid loop.
4. The path of the coolant loop is minimized.
5. A loss of working fluid does not affect the heat source if

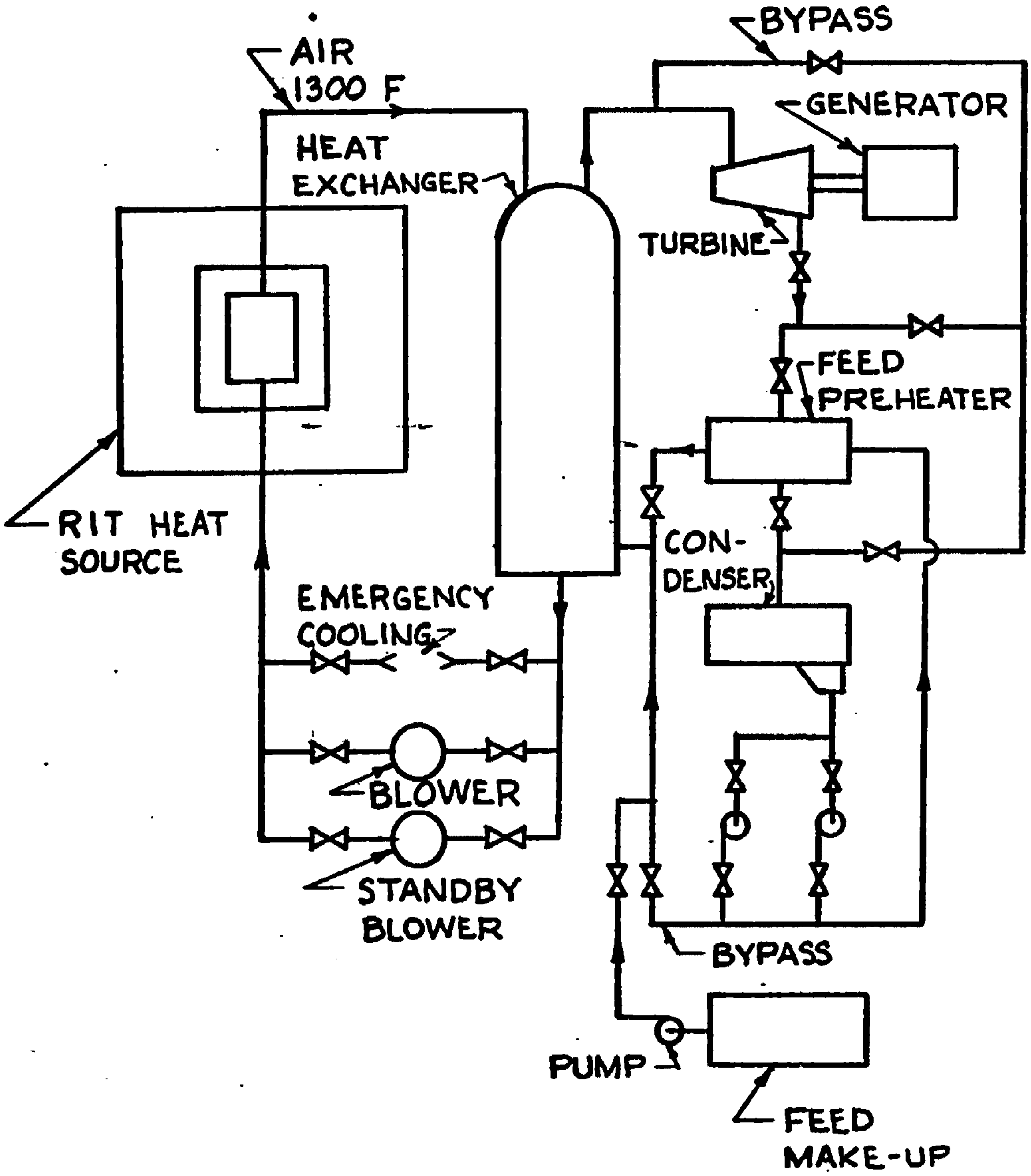

Indirect Rankine
Power System Concept
(WESTINGHOUSE, REFERENCE 10)
Figure 2.3

an emergency heat rejection system is provided.

6. The heat source can be designed and developed separately.

7. Secondary system components are not subjected to radiation contamination.

8. The heat source may be coupled to alternate types of power conversion systems.

The General Dynamics Corporation design for an underwater power system, reference 11, used a naturally circulating lead-bismuth eutectic as a heat-transfer and a radiation-shielding fluid and steam as the Rankine cycle working fluid.

It is the author's conclusion that the direct Rankine cycle has the following advantages over the indirect cycle which cannot be easily ignored:

1. Higher overall cycle efficiency than the indirect cycle,

2. Reduced system complexity and therefore greater reliability than the indirect cycle.

A possible disadvantage is the increased susceptibility to radiation contamination of the direct cycle when compared to indirect cycles. For the indicated reasons the direct Rankine power cycle will be employed in this design. (See Table 2.3)

Rankine cycle boiler type. An additional design alternative has to do with the boiler circulation concept. There are basically two types of boilers, recirculating and "once-through" boilers. Considerable data is available on the design of recirculating boilers. Less design data is available relative to "once-through" designs and such designs are usually accomplished by empirical methods. (Both boiler concepts are considered in Chapter 7.)

Supercritical Thermodynamic Power Cycles

Thermodynamic power cycles have been described (reference 14), which operate entirely above the critical pressure of the working fluid. Such a cycle when operating in conjunction with a gas-cooled nuclear reactor or radioisotope heat source is a potential power system for terrestrial applications. A typical cycle using carbon dioxide as a working fluid would have the highly desirable attributes of no blade erosion in the turbine and lack of cavitation in the cycle "pump". Other characteristics of the cycle include single phase fluid in heat transfer processes, high thermal efficiency, and low volume of system components to power ratio.

Pseudo-supercritical cycles are currently employed in large central station steam power plants using water as the working fluid. Another potential working fluid is carbon dioxide.

Pseudo-Supercritical Cycle Using Carbon Dioxide as Working Fluid. Although many cycle variations are possible a representative cycle would be as shown in figures 2.4 and 2.5. In this cycle the flow of working fluid, (CO_2), leaving the low temperature regenerator divides with the mass fraction α going to the condenser and the mass fraction $(1 - \alpha)$ going to the compressor. (Thus the cycle may be considered as a combination Brayton-Rankine cycle since compression occurs partly in the liquid phase and partly in the gaseous phase.) The condensed flow is heated to temperature T_2 by the low temperature regenerator. The flow fraction $(1 - \alpha)$ is heated to the same temperature, T_2, by means of compression in the compressor. The combined flow stream at state 2 is then heated to state 6 by exchanging heat energy

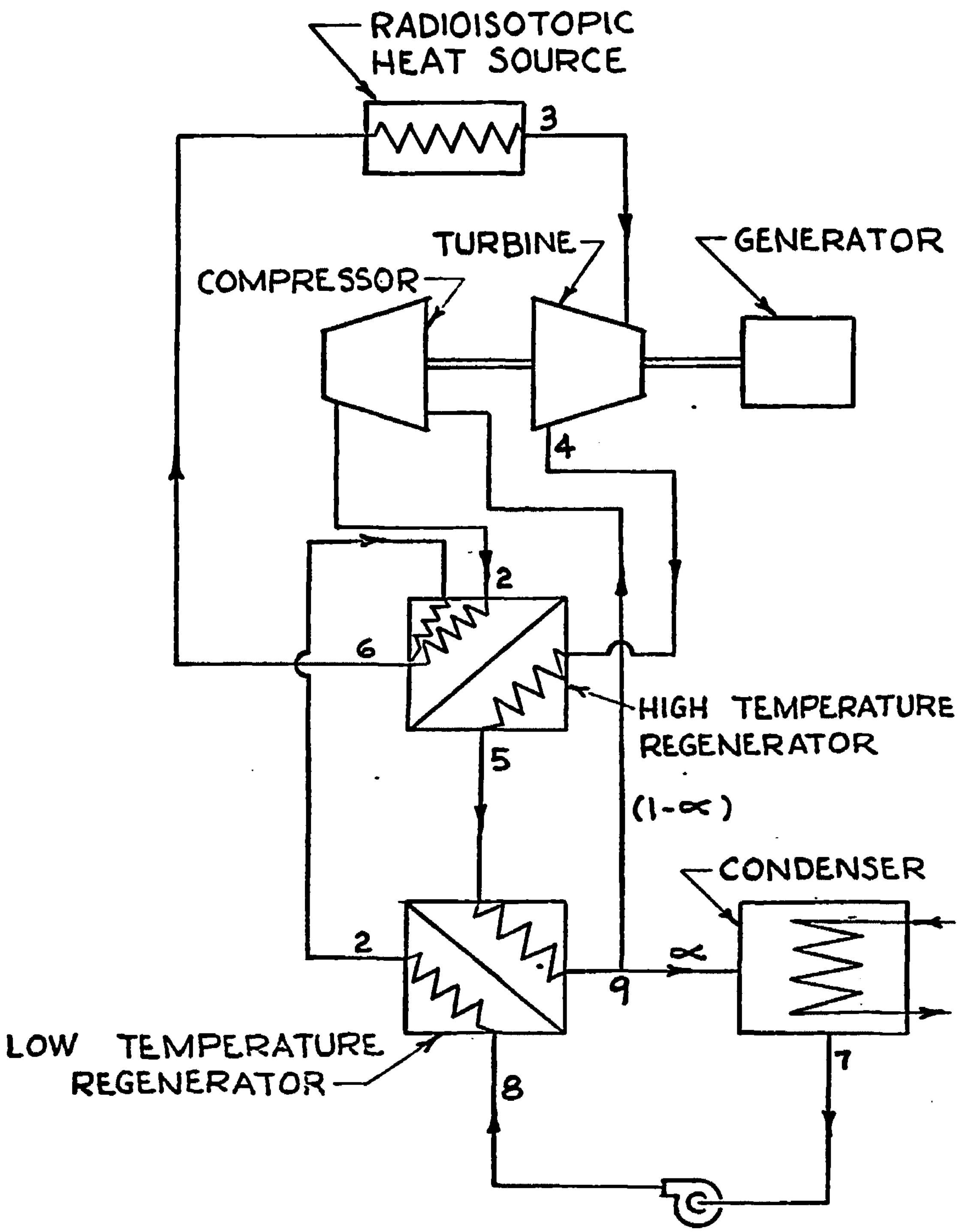

Supercritical Cycle Arrangement
Figure 2.4

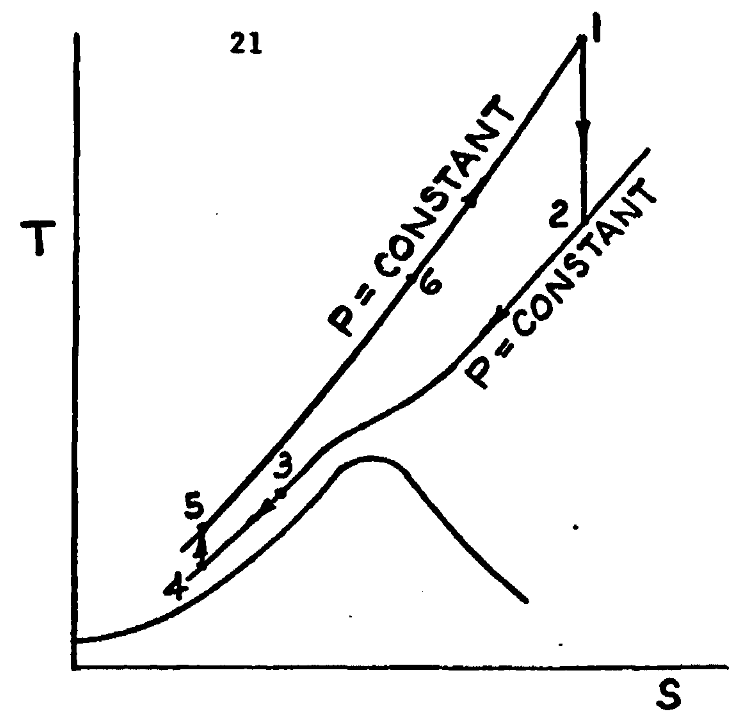

Supercritical Thermodynamic Cycle
Figure 2.6

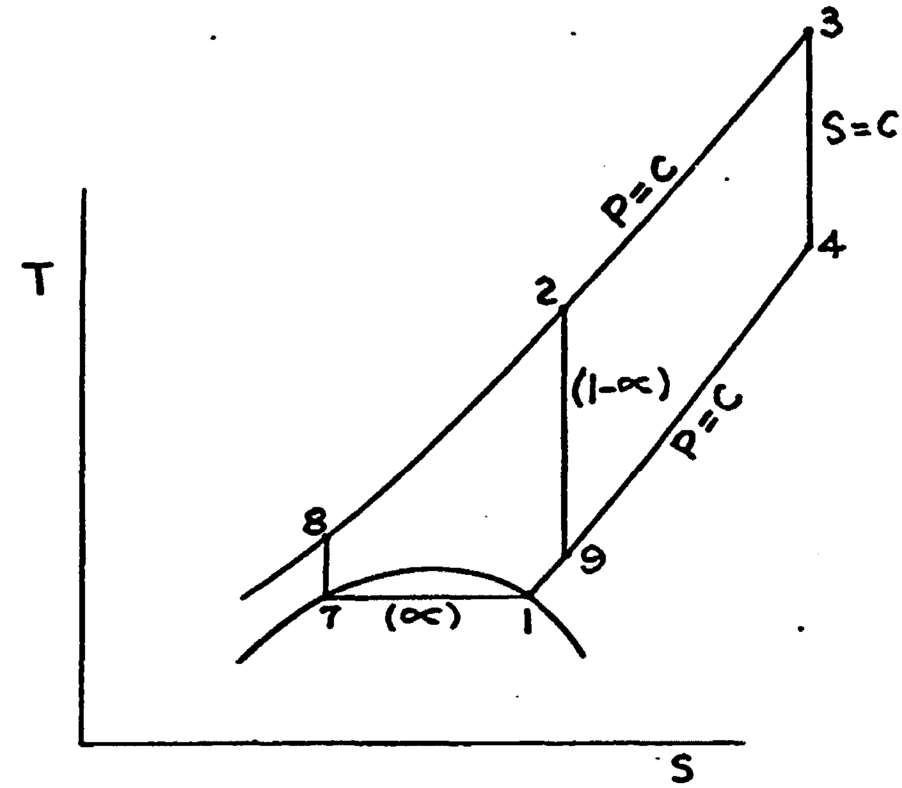

Pseudo - Supercritical Cycle for CO_2
Figure 2.5

with the turbine exhaust flow stream in the high temperature regenerator. Heating from state 6 to state 3 occurs in the heat source component. The expansion work producing process occurs from state 3 to state 4. The expanded flow stream is cooled from state 4 to state 5 in the high temperature regenerator and from state 5 to state 9 in the low temperature regenerator. A necessity for the cycle (using CO_2 as a working fluid) would be the availability of condenser cooling water at temperatures not higher than $50^{o}F$ to $60^{o}F$. Such temperatures would be available at deep ocean installations and also in many other regions of the earth.

Supercritical thermodynamic cycle. The supercritical thermodynamic cycle operates entirely above the critical pressure of the working fluid. Figure 2.6 shows the cycle depicted on the Ts diagram. The ideal cycle processes consist of the following:

1 → 2 Isentropic expansion work producing process

2 – 3 and 5 - 6 Constant pressure regenerative heat exchange processes

3 - 4 Constant pressure heat rejection to external heat sink

6 - 1 Constant pressure heat addition from external heat source.

The cycle efficiency is comparatively high because of the regenerative heat exchange processes employed by the cycle and also because the pump work is a small fraction of the gross cycle work output.

Possible working fluids include ammonia, carbon dioxide, water, and certain hydrocarbons. Carbon dioxide has several desirable attributes when used as a working fluid.

The major disadvantages of supercritical cycles for the applications of interest in this design study are,

(1) Relatively high cycles pressures are involved and

(2) Lack of availability of thermodynamic property data on working fluids of interest.

Real gas property data must be used since high pressures are employed in the cycle and also because of the large deviation of fluid properties from the ideal in the vicinity of the critical point. Parenthetically it may be noted that a fruitful field for engineering graduate research would seem to be in the area of working fluid property determination for supercritical cycles.

Even though it may be expected that a practical Supercritical Cycle Power Plant may be accomplished using present technology it is probable that considerable development would be required and for this reason this cycle will not be further considered as an alternative in this study.

Chemical Dynamic Systems

Many solid, liquid, and gaseous fuel/oxidizer combinations are feasible for closed-cycle energy conversion loop chemical dynamic power plants. Since specific fuel consumption is generally high this class of power plants is attractive for short-duration missions. A schematic diagram of a chemical dynamic power system as given in reference 15 is shown in figure 2.7. Table 2.2, also from reference 15, lists a few chemical reaction systems that have potential use in underseas applications.

Selection of the Power System

The system design will be that for a stationary installation

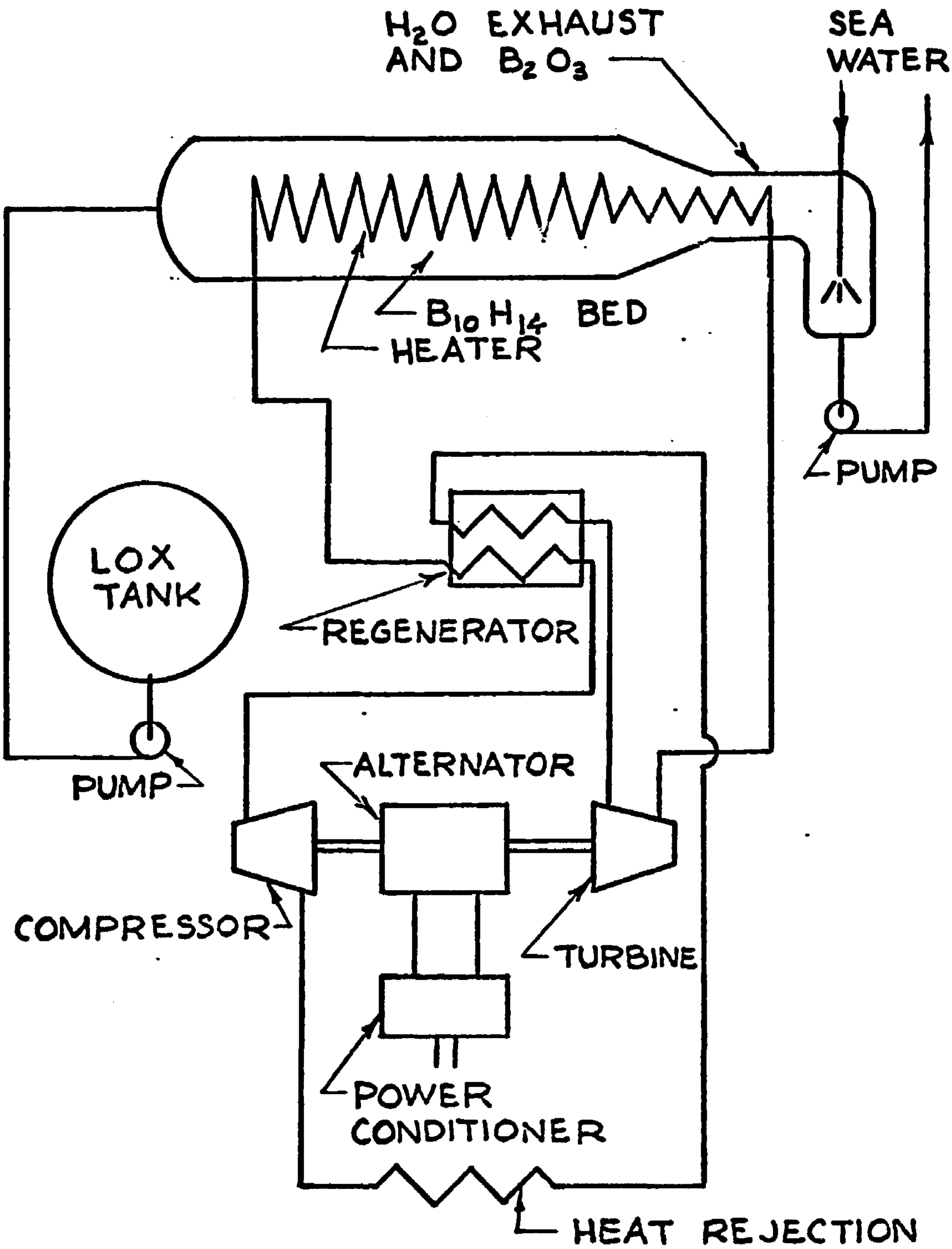

Chemical Dynamic Power System
Figure 2.7

Table 2.2

Reactants for Chemical Heat Source Systems

Chemical System	Class	Btu/lb	Btu/ft^3
N_2H_4	Monopropellant	1,500+	94,900
N_2H_4 and H_2O	Storable liquid bipropellant	3,490	283,500
$LiBH_4$ and O_2(liquid)	High energy fuel cell Source (H_2 from hydrolysis of $LiBH_4$)	4,430	248,000
$B_{10}H_{14}$ and O_2(liquid)	Controllable solid heat source	7,200	446,000

as for example in an underseas manned laboratory. The power system is to be designed for a continuous period of operation of 8,760 hours, (1 year). The criteria and weighting factors used in comparing various system concepts are as follows:

CRITERIA	WEIGHTING FACTOR
1. Reliability	10
2. Thermodynamic performance	10
3. Safety	10
4. Logistics	8
5. Cost (development plus production)	7
6. Development risk	6
7. Applicability to "total energy" concept	5
8. Weight and Size	3

The criteria are given weighting factors on a scale ranging from 1 to 10. A value of 10 denotes primary importance whereas a value of 1 denotes relatively small importance.

The systems are rated in accordance with a scale ranging from 1 through 10. A rating of 10 represents a superior performance. A rating of 1 represents strong system deficiency. Both the criteria weighing factors and the system rating factors are non-dimensionless and the system comparison is qualitative in nature.

The power system rating of interest in this design is 5 kw_e net output. The power system should also be suitable for applications underseas to depths of 6000 ft.

The "applicability to total-energy concept" criterion refers to the feasibility of using waste heat from the cycle for space or water heating purposes.

Table 2.3

Power System Selection Table

System Concept	Reliability	Thermodynamic Performance	Safety	Logistics	Cost	Development Risk	Applicability to T.E. Concept	Weight and Size	Comparison Index
Weight Factor	10	10	10	8	7	6	5	3	
1. Brayton Cycle*	9	10	7	9	7	8	9	8	488
2. Direct Rankine Cycle*	9	10	7	9	8	8	9	9	498
3. Two Fluid Rankine Cycle*	8	9	7	9	7	8	9	8	478
4. Battery	9	6	8	3	7	9	3	3	381
5. Fuel Cell	7	7	6	5	5	6	3	7	347
6. Feher Cycle* (Supercritical)	7	8	5	9	5	5	9	7	403
7. Chemical Dynamic	8	6	6	3	9	8	5	7	381

*Radioisotope heat source

Advantages and Disadvantages of Potential Power Systems

Rankine Cycle:

Advantages.

1. High cycle efficiency
2. Excellent background of technology for design of system components

Disadvantages.

1. Danger of turbine blade erosion by "wet" working substance vapors
2. Radiation shielding problems when fuel is nuclear
3. Possibility of cavitation in pumps and bearings
4. Sensitive to parasitic losses at the power levels of interest in this design study
5. Problems associated with containment of the working fluid, i.e., seal design, high toxicity of mercury vapor even at very low concentrations, etc.
6. Possibility of orientation problems in underseas applications

Brayton Cycle:

Advantages.

1. High Cycle efficiency
2. Background of jet engine technology from aircraft industry upon which to draw
3. No turbine blade errosion

Disadvantages.

1. Sensitive to parasitic losses at the power levels of

interest in this application

2. Larger heat exchangers

3. Working fluid containment problems

Batteries

Advantages.

1. Simple system---thus reliable

2. Silent

3. Various capacity ratings available by increasing or decreasing number of units

Disadvantages.

1. Large space and weight penalty

2. Cannot be adapted to total energy concept

Fuel Cell

Advantages.

1. High Efficiency

2. Silent

3. Modular construction

Disadvantages.

1. Requires continual supply of chemicals

2. Still developmental

Chemical-Dynamic Systems:

Advantages.

1. Adaptable to total energy concept

Disadvantages.

1. Requires continual supply of high energy chemicals

2. Necessity for pumping waste products overboard

Feher Cycle

Advantages.

1. No turbine blade erosion or pump cavitation problems

2. High thermal efficiency

Disadvantages.

1. Concept is developmental---not yet demonstrated in hardware

2. High pressures increase component design complexity

Thus the result of the system evaluation in the selection table is that the direct Rankine cycle power system is the preferred choice. However both the Brayton cycle and the Two-Fluid (Indirect) Rankine cycle have high values for the Comparison Index and both systems should be further developed as system alternatives. More detailed design studies of the various systems would be expected to change particular system rating values. Since the major item of cost for the radioisotope heat source systems is that for the radioisotope fuel the system ultimately selected for development will probably be that one which has the higher cycle efficiency, (assuming high reliability for competing cycles).

Choice of System

On the basis of the Selection Table the Direct Rankine cycle will be chosen for further design study.

Even though the type of cycle is selected there still remains a major decision as to the choice of working substance. The working substance will have a strong influence on thermal efficiency and upon system component designs.

The power plant system may be considered as being composed of the following subsystems:

1. Heat Source
2. Power Conversion
3. Heat Rejection
4. Power Conditioning

Design analyses for the heat rejection and power conditioning subsystems are not included in this report.

CHAPTER III

SELECTION OF A WORKING FLUID

Introduction

Since the radioisotopic fuel cost is extremely high and is the major item of cost in the power system it is necessary that the cycle efficiency for the plant be as high as possible. While several concepts may be listed for converting heat energy into shaft power, the most efficient conversion scheme known today is one which uses a turbine or reciprocating engine. (Fuel cells may be more efficient but they are still in the developmental stage and fuel cell reliability has not been demonstrated for long-term applications.) The cycle working fluid will influence the thermodynamic efficiency of the cycle and will also determine the design complexity of the power cycle components. The aim of this chapter is to compare different candidate working fluids and to select the most efficient with respect to the pertinent criteria.

Possible Working Fluids

Working fluids which may be considered for the power system include the following:

water

ammonia

liquid metals:

mercury

rubidium

sodium

potassium

cesium

organic fluids such as:

Diphenyl

Dowtherm

sulphur

aluminum bormide

Criteria Useful in Selection of Working Fluid

Candidate working fluids may be compared on the basis of the following criteria:

1. Cost of working fluid
2. Vapor pressure
3. Power system thermal efficiency
4. Vapor quality at turbine exhaust
5. Stability at elevated temperatures
6. Materials compatibility
7. Melting points
8. Volume of exhaust vapor
9. Condensing temperatures
10. Flow rate
11. Heat-transfer and pumping characteristics
12. Safety

Mackay (reference 1) writes the cycle thermal efficiency as the product of three efficiency factors, (the equations of this paragraph are from reference 1):

$$\eta = \eta_c \, \eta_t \, \eta_f$$

where

η_c = efficiency of the Carnot cycle,

η_t = turbine adiabatic efficiency,

η_f = fluid efficiency factor.

The fluid efficiency factor η_f is given by the ratio of the efficiency of the ideal Rankine cycle to the efficiency of the Carnot cycle between the same temperature limits, i.e.,

$$\eta_f = \frac{\eta_{\text{theo.Rankine}}}{\eta_c}$$

Also η_f is shown to be given by the following expression:

$$\eta_f = \frac{1}{1 + (\frac{1}{f} - 1)(T_2/T_1)}$$

where f represents the ratio $W_{\text{theo.Rankine}}/W_c$. Figure 3.1 shows the work areas for the Carnot cycle and for the theoretical Rankine cycle, (the analysis of reference 1 does not apply to the superheat cycle). Mackay further shows that f may be given by

$$f = \frac{1 + h_{fg1}/CT_1 + \frac{T_2/T_1}{1 - (T_2/T_1)}(\log_e T_2/T_1)}{h_{fg1}/CT_1 + \log_e(T_2/T_1)}$$

where C is the average specific heat of saturated liquid.

High values of f are desired since high values of f result in high thermal efficiencies. For the temperature range of interest in this application all of the above liquid metals will have values of f in excess of 0.9. Further, figure 10 of reference 1 shows the liquid

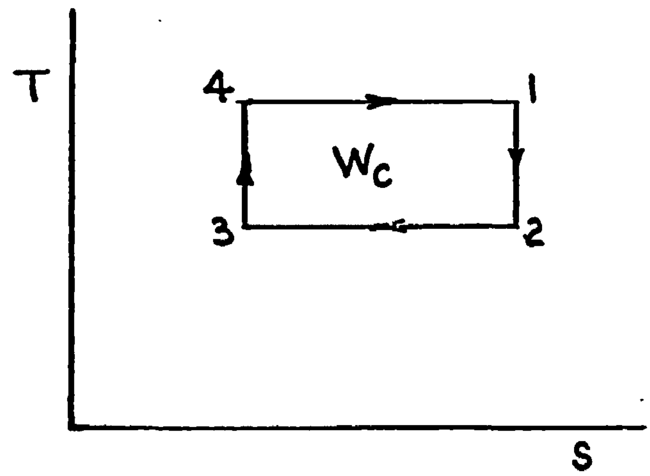

CARNOT CYCLE

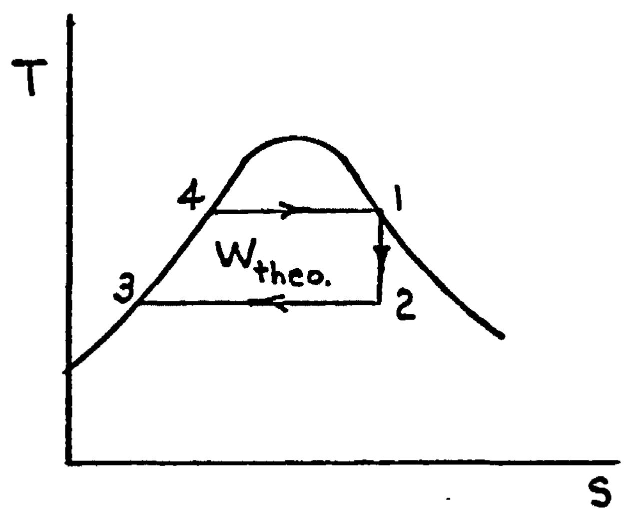

RANKINE CYCLE

Cycle Work Areas
Figure 3.1

metals to have fluid efficiency factors in excess of 90 per cent whereas the other candidate working substances have much lower values for the fluid efficiency factor. Diphenyl, for example, has values in the neighborhood of 50%. (It is noted that the values indicated on the figure are based on a temperature ratio of 0.75, which is characteristic for space power plant applications.) It is additionally observed that all of the liquid metals fall in the range of 94 to 97%. On the basis of fluid efficiency the liquid metals would be clearly indicated as the logical choice. Temperature ratios below 0.75 will be required in this application. Even though the value of f decreases with a reduction of temperature ratio the change in η_f will be small. Thus at a temperature ratio of 0.625 the fluid efficiency factor for liquid mercury is approximately 93 per cent.

Cost of Working Fluid

Prices taken from the Liquid Metals Handbook (reference 2) are as follows:

Cesium	\$ 4.00/g	(=~\$1815.00/lb)
Mercury	195.00/flask	(=~ 2.60/lb)
Potassium	2.50/lb	
Rubidium	4.50/g	(=~ 2040.00/lb)
Sodium	0.16/lb	

Even though the prices listed are for 1951, the current prices may be expected to be of the same order of magnitude.

Prices for the organic liquids may be roughly estimated at \$0.25/lb.

The investment for either cesium or rubidium working fluids would therefore represent a significant proportion of the total plant cost. The cost for the other liquid metals listed would be comparatively negligible.

Vapor Pressure

In order to achieve high cycle thermal efficiencies it is necessary for the working fluid to transport heat energy at as high a temperature level as possible. Saturation Pressures (psia) corresponding to a temperature of 1000°R are

Water	962
Sulphur	~ 1
Diphenyl	~ 30
Cesium	<0.1
Mercury	3.232
Potassium	3.52×10^{-3}
Rubidium	<0.1
Sodium	1.391×10^{-4}
Aluminum Bromide	~ 40

Thus liquid metals have very low vapor pressures, water has very high vapor pressures, and the organic liquids are intermediate between the two. Heavy pressure vessels and piping would be required for a high vapor pressure working substance such as water.

Power Plant Thermal Efficiency

Mackay (1) shows the cycle thermal efficiency to be given by:

$$\eta = \eta_t \frac{1 - T_2/T_1}{1 + (\frac{1}{f} - 1)(T_2/T_1)} .$$

Figure 3.2 shows the cycle thermal efficiency plotted as a function of the turbine adiabatic efficiency for a temperature ratio of 0.625 and for f = 0.9. A value of the work function, f, of 0.9 would apply to liquid metals. Also included in the figure is a plot of the ideal fluid cycle efficiency, (f = 1.0). Figure 8 of reference 1 shows the rather curious fact that for diphenyl, and for a particular temperature ratio, the ideal Rankine cycle thermal efficiency decreases with an increasing upper cycle temperature. Other organic fluids having similar vapor domes would be expected to exhibit the same tendency.

Heat Transfer and Pumping Characteristics

The following data taken from table 10-1 of reference 3 gives the ratio of pumping work to heat removal ability of coolants

Water	1.0
Organic liquids	4 - 10
Liquid metals	3 - 7
Gases	~ 100

The data are normalized with respect to the value of the ratio for water and are for turbulent flow without change of phase. Water is therefore superior to both organic liquids and liquid metals on the basis of pumping work comparisons. Organic liquids generally have poorer heat transfer and pumping characteristics than either water or liquid metals.

Vapor Quality at Turbine Exhaust

The ideal working fluid would be in the superheated state at the turbine exhaust in order that turbine blade erosion problems may not occur. The low pressure steam cycle considered in Chapter VI does have superheated vapor at the turbine exhaust. The mercury cycle

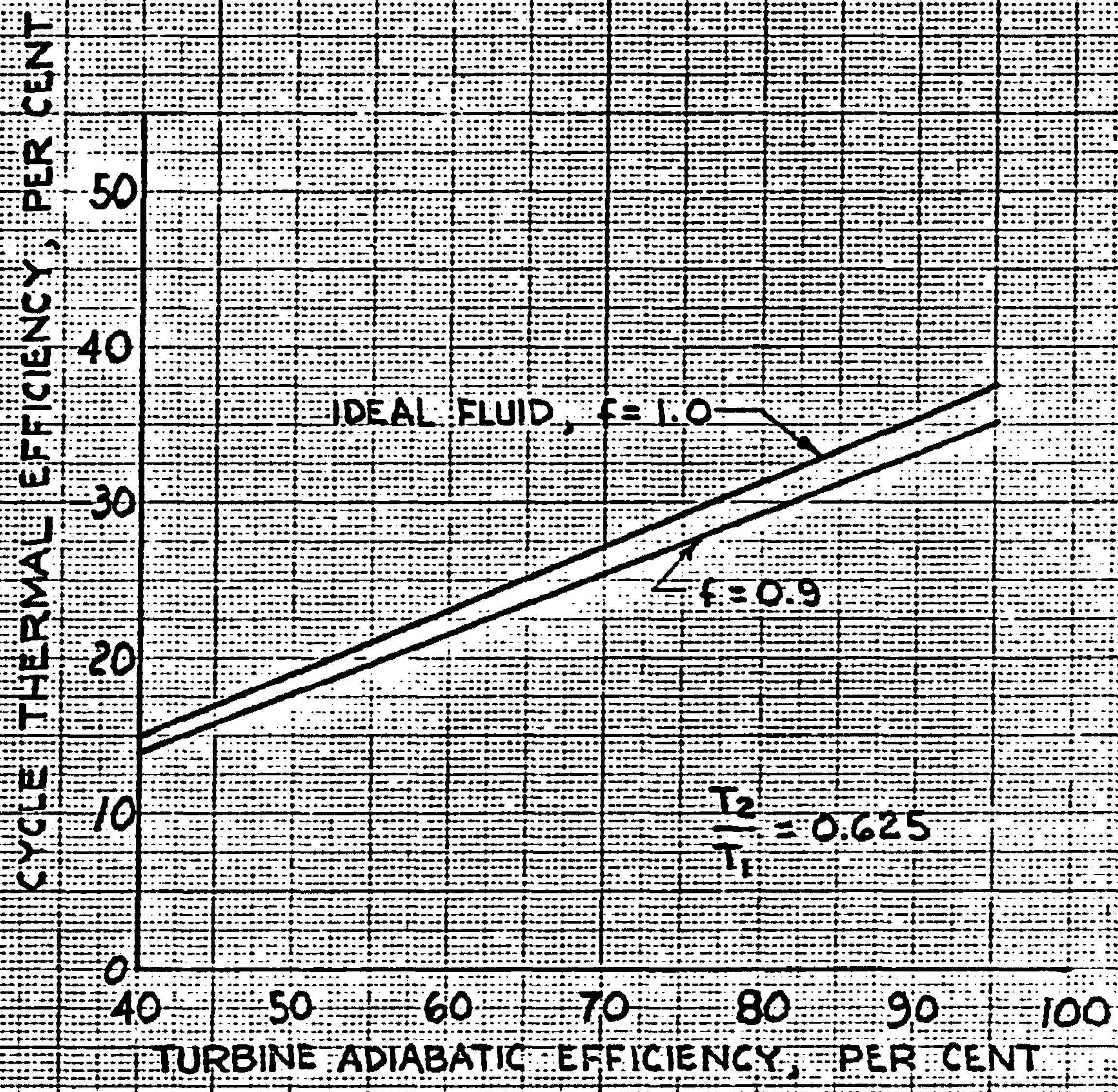

Rankine Cycle
Thermal Efficiency
Figure 3.2

considered in the same chapter results in about 15 per cent moisture for the mercury at the turbine exhaust.

Stability at Elevated Temperatures

All of the liquid metals considered are stable in the temperature range contemplated for this application. Sulphur has a non-constant molecular structure which makes difficult the prediction of performance in an actual power cycle.

Organic materials are unstable at high temperatures and are also subject to damage by nuclear radiations. To prevent plugging of heat transfer surfaces and piping it would be necessary to include a purification process in the cycle in order to remove decomposition products (and replace with fresh coolant) from the power system. This is a definite disadvantage for organic coolants. (However, a real advantage for organic coolants is the low induced radioactivity of the pure coolant.)

Safety

Organic coolants ignite spontaneously when heated in contact with air. For example, the flame-point temperature of diphenyl is 255°F. It may be necessary to provide a blanket of inert gas to shield an organic coolant from possible exposure to air. Such increased complexity would be expected to decrease the reliability of the power system.

Mercury vapor is highly toxic. Air only very slightly saturated can cause mercury poisoning if breathed over a long period. (Reference 2, page 124). In addition, liquid metals are subject to induced radioactivity. The induced radioactivity has relatively long half-lives and strong radiations. For this reason intermediate coolant loops are often provided for power cycles using liquid metal coolants.

The radioisotopes of mercury have half-lives varying in length from 44 minutes to 47.9 days, (reference 3, page 436). The radiations have γ energies varying between 0.13 and 0.37 Mev. Neutron radiation of naturally occurring sodium produces the reaction $Na^{23}(n,\gamma)Na^{24}$. Gamma radiation of 2.76 and 1.38 Mev energy and with a half-life of 15 hr. is emitted by the product Na^{24}.

Naturally occurring potassium contains approximately 7 per cent of the K^{41} isotope which becomes a beta and gamma emitter upon neutron absorption. The half-life of the radioactive isotope is 12.5 hours.

Rubidium is a silvery-white alkali metal which is very reactive and ignites spontaneously in air. Cesium is also an alkali metal which catches fire in dry air. Molten sodium burns in the presence of air and forms dense fumes of sodium monoxide. Sodium reacts violently with water. The gases nitrogen, argon, and helium do not react with sodium and so these gases may be used as a blanketing agent to isolate sodium from the atmosphere. Potassium is, in general, more chemically reactive than sodium.

Melting Points

The following melting points are at 760 mm Hg (Standard Atmospheric Pressure):

	^{o}F
Water	32
Ammonia	-108
Mercury	-38
Rubidium	102
Sodium	208

Potassium	147
Cesium	83
Diphenyl	157

The melting point of a working fluid would be of interest if temperatures in the system were ever such that the fluid could solidify in piping or vessels.

Materials Compatibility

Chemical interaction between polyphenyl working fluids and most power system materials would be expected to be low. Magnesium and zirconium are susceptible to slight chemical reaction. Corrosion of aluminum, stainless steels, and carbon steels would not be significant. In general organic working fluids are compatible with most fuels, cladding, and structural materials.

Tests indicate (reference 4, page 1007, 1008) that low alloy carbon steels have good corrosion properties for liquid mercury up to 1100 - 1200°F. Also it has been discovered that the addition of titanium and magnesium to the mercury resulted in negligible attack on even low-carbon steel.

Table 49.8, page 1016 of reference 4 indicates Armco iron, stainless steels, and nickel alloys have good corrosion resistance properties for sodium up to about 1650°F.

Rubidium and potassium may be expected to have corrosion properties similar to those of sodium.

Sulphur has highly corrosive properties and may be estimated on this basis. In other respects a sulfur cycle can be considered as competitive with a mercury cycle.

Condensing Temperature Comparison

Liquid metals have relatively high condensing temperatures. High condensing temperatures may be utilized advantageously in space applications where the mode of heat rejection is thermal radiation. High heat rejection temperatures result in small radiator surface areas and as a consequence the radiator component will be lighter in weight. For underwater applications, the ocean, with temperatures in the range $34^{o}F$ to $90^{o}F$, will serve as the heat sink. Heat transfer will be essentially by convection. Therefore the high condensing temperatures of the liquid metals are a definite disadvantage for ocean applications. Both water and the organic working fluids could take fuller advantage of low heat sink temperatures than the liquid metals.

Choice of Working Fluid

Organic working fluids will not be further considered because of susceptibility to radiation damage and because of the requirement for clean-up components which increases the complexity of the power cycle.

The essential working fluid choice is between water and liquid mercury. The final choice is postponed until comparative cycle efficiencies are investigated.

CHAPTER IV

SELECTION OF THE RADIOISOTOPE FUEL

Suitable Radioisotopes

Criteria useful in the selection of the radioisotope are as follows:

1. Cost of radioisotope
2. Availability
3. Shielding requirements
4. Length of half-life
5. Specific power density
6. Difficulty of capsule design, (Gas evolution)

The items are listed in the order of importance. Since the initial cost of the radioisotope fuel will be the major determining factor in the owning and operating costs of a radioisotope fueled power system it is of primary importance in the above list. For the same reason the thermal cycle efficiency will be of major importance because it determines fuel quantity. Table 4.1 taken from reference 6 lists fuels which may be considered for this application. Of those radioisotopes listed in the table the alpha emitters would be most desirable from a shielding standpoint. Thus Curium 244 and Plutonium 238 are very promising fuels since they are essentially alpha emitters. Sr 90, Cs 137, Ce 144, and Pm 147 may be purified from fission products whereas Pu 238, Cm 242,

Table 4.1

Radioisotopic Power Fuels Data**

Radioisotopes	^{90}Sr-Y	^{137}Cs-Ba	^{147}Pm	^{144}Ce-Pr	^{238}Pu	^{242}Cm	^{244}Cm	^{60}Co	^{210}Po
Half-life (years)	27.7	30	2.62	0.78	87.6	0.45	18.4	5.24	0.38
Radiation type[a]	β,γ	β,γ	β,γ	β,γ	α,n,γ	α,n,γ	α,n,γ	β,γ	α,n,γ
Radiation energy (curies/W(t))	148	207	2790	126	29.1	28	29	65	31.2
Shield Thickness[b]	8	5.8	1.6	15	(nil)	10*	3.5 (34)*	13	1.4
Typical Form	$SrTiO_3$	Glass	Pm_2O_3	CeO_2	PuO_2	Cm_2O_3 matrix	Cm_2O_3	Metal	Metal
Density (g/cc)[c]	3.7	3.1	6.6	6.3	9	9	9	8.7	9.3
Power (W(t)/cc)	0.82	0.24	1.8	21.9	3.6	150	22.5	27(k) 54(k)	1150
(Kw(t)/yr)									
1967[d]	9.5	3	1	4	11	(i)	(j)	130	14
1970[d]	170	140	7.2	1200	15(h)	--	--	--	-
1980[e]	770	760	33	7000	60	--	--	7500	9400
Present$/W(t)[f]	29.60	25.80	556	18.90	--	--	--	32.50	780
Future$/W(t)[g]	19	21	93	0.90	535	--	480	10	10

Notes for Table 4.1

* Centimeters of H_2O for neutron shielding

(a) The symbol γ includes bremsstrahlung and gamma radiation.

(b) Shield thickness in cm of uranium to reduce a 100 W(t) source to 10 mr/hr at 1 meter.

(c) Power density of the fuel form.

(d) Availability from AEC produced products.

(e) Based on civilian nuclear power operations or special radioisotope production reactors.

(f) Based on large orders and does not include conversion, encapsulation or shipping costs.

(g) Based on studies assuming large scale production of encapsulated products.

(h) Could be increased.

(i) Operation now on a developmental basis with cost at 10 Kw thermal per year capacity estimated at about $100/W(t).

(j) Operation now on a developmental basis with cost at 10 Kw thermal per year estimated at about $1, 110 per thermal watt. Production in the range of 100 Kw in 1972 and 400 Kw in 1980, estimated at a cost of $480 per thermal watt.

(k) Based on 200 curies/gm and 400 curies/gm material respectively.

** From reference 6. (Original from Division of Isotopes Development, "Isotopic Power Fuels Data Sheet", April 1966).

Co 60, and Po 210 are produced by irradiation in reactors. Large scale production of curium and its conversion to a usable fuel form has not been accomplished as yet.

One disadvantage of alpha emitters is that these fuels evolve helium gas as the radioisotope decays. Provision must be made, in the design of the fuel capsules, to accommodate the build-up of the helium gas.

Even though the future price of Ce 144 is a factor of ten less than any other fuel, its relatively short half-life presents a large disadvantage. If this fuel is used refueling would be necessary about every six months and the control scheme for the power plant would be more complex.

The gamma and beta emitting fuels will require a substantial shield thickness. Suitable shield materials are depleted uranium, lead, tungsten and iron. If heat is being transmitted through the shield, which will most certainly be necessary for Co - 60, it is important that the shield material have a high thermal conductivity. Thermal conductivities and densities for the shield materials listed above are listed in table 4.2.

Table 4.2

Thermal Conductivity of Shield Materials

	Density lb_m/ft^3	Thermal Conductivity Btu/ft-hr ^oR	Temperature ^oR
Iron	491	22.8	1572
Lead	708	17.2	1032
Tungsten	approx. 1170	65.1	1572
Uranium	1167	24.2	1572

Thus from the standpoint of thermal cond

most attractive shield material. Also i

shield material for a cylindrical config

cylinder length and diameter are approxi

Fuel Selection

For a system having n differ

comparison index for the j^{th} system is:

$$CI_j = \sum_{i=1}^{n} L_i F_{ij}$$

where

L_i = the i^{th} weighting factor

F_{ij} = the i^{th} normalized figur

The fuel selection decision tabl

fuel selected should be cobalt 60. Th

however use of this fuel involves design

short half-life of this fuel, (0.28 year

Cobalt - 60

According to reference 20 as mic

been produced at Savannah River Laborato

200 curies/gram or greater. Cobalt-60 h

for the application herein proposed. Th

radioisotope is that of shielding the in

its intended application configuration a

cal decay event of cobalt-60 releases t

gamma radiations. One of the gamma rays

Co 60, and Po 210 are produced by irradiation in reactors. Large scale production of curium and its conversion to a usable fuel form has not been accomplished as yet.

One disadvantage of alpha emitters is that these fuels evolve helium gas as the radioisotope decays. Provision must be made, in the design of the fuel capsules, to accommodate the build-up of the helium gas.

Even though the future price of Ce 144 is a factor of ten less than any other fuel, its relatively short half-life presents a large disadvantage. If this fuel is used refueling would be necessary about every six months and the control scheme for the power plant would be more complex.

The gamma and beta emitting fuels will require a substantial shield thickness. Suitable shield materials are depleted uranium, lead, tungsten and iron. If heat is being transmitted through the shield, which will most certainly be necessary for Co - 60, it is important that the shield material have a high thermal conductivity. Thermal conductivities and densities for the shield materials listed above are listed in table 4.2.

Table 4.2

Thermal Conductivity of Shield Materials

	Density lb_m/ft^3	Thermal Conductivity Btu/ft-hr ^oR	Temperature ^oR
Iron	491	22.8	1572
Lead	708	17.2	1032
Tungsten	approx. 1170	65.1	1572
Uranium	1167	24.2	1572

Thus from the standpoint of thermal conductivity tungsten would be the most attractive shield material. Also it is to be noted that minimum shield material for a cylindrical configuration will result if the cylinder length and diameter are approximately equal.

Fuel Selection

For a system having n different figures of merit, the total comparison index for the j^{th} system is:

$$CI_j = \sum_{i=1}^{n} L_i F_{ij}$$

where

L_i = the i^{th} weighting factor

F_{ij} = the i^{th} normalized figure of merit for system j.

The fuel selection decision table, table 4.3, indicates that the fuel selected should be cobalt 60. The second choice is polonium 210 however use of this fuel involves design concepts suitable for the short half-life of this fuel, (0.38 years).

Cobalt - 60

According to reference 20 as much as 125 kw(t) of Cobalt-60 has been produced at Savannah River Laboratories with specific activity of 200 curies/gram or greater. Cobalt-60 has a very attractive half-life for the application herein proposed. The major problem in using this radioisotope is that of shielding the intense gamma radiation both in its intended application configuration and in transit handling. The typical decay event of cobalt-60 releases a 0.31 Mev beta particle and two gamma radiations. One of the gamma rays has an energy of 1.17 Mev

Table 4.3

Fuel Selection Decision Table

	Selection Criteria	Importance Weighting Factor	Sr-90	Cs-137	Pm-147	Ce-144	Pu-238	Cm-242	Cm-244	Co-60	Po-210	Notes
			Normalized Figures of Merit									
1.	Cost	10	5	5	3	10	2	4	2	8	8	(1)
2.	Availability	8	8	8	3	10	5	3	3	10	10	
3.	Shielding Requirement	6	6	6	8	5	10	6	8	5	9	(2)
4.	Length of Half-Life	5	9	9	7	3	8	2	9	10	1	
5.	Specific Power	4	6	5	6	8	7	9	8	8	10	
6.	Gas Evolution	4	10	10	10	10	5	5	5	10	5	
TOTAL COMPARISON INDEX, CI			259	255	201	207	208	166	189	312	279	
Normalized Comparison Index			0.83	0.82	0.64	0.66	0.67	0.53	0.61	1.0	0.89	(3)

1. Future Cost basis used.
2. Very long half-lives are penalized slightly
3. Each comparison index normalized to highest value, (312)

and the other 1.33 Mev. The decay scheme for Cobalt-60 (reference 29) is shown in figure 4.1. The photons of gamma energy are emitted "in cascade". Associated with β particle emission is the emission of a neutrino. In the present work it is assumed that the published fuel energy density is a net value and that no additional allowance for energy loss associated with neutrino emission is necessary.

Even though tungsten is perhaps the best shield material because of its high energy absorption coefficient, (μ), and its relatively high thermal conductivity, its high cost must be "traded off" for less desirable values of these properties which are possessed by competing shield materials, e.g., lead and depleted uranium. Another negative attribute of tungsten is its difficulty of processing. Relative shield thickness requirements for the various isotope fuels are shown in table 4.1.

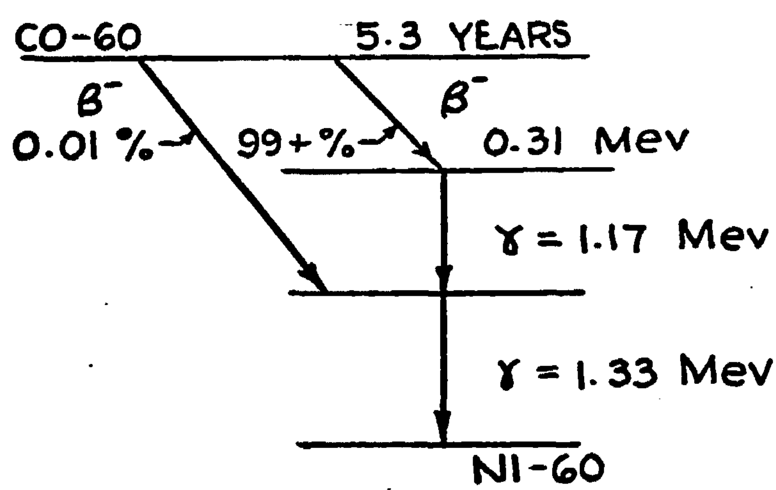

Cobalt-60 Decay Scheme
Figure 4.1

CHAPTER V

TURBINE DESIGN

Introduction

In chapter six the effect of the turbine efficiency upon the power cycle thermal efficiency will be investigated. The efficiency of the turbine exerts a large influence on the cycle efficiency. Thus it is essential to select a working fluid which will be compatible with high turbine expansion efficiencies. Even though the liquid metal working fluids are handicapped in terrestrial power plant applications because of their relatively high condensation temperatures, (when compared to water, for example), it may be that higher turbine efficiencies will compensate for the negative effect of high condensation temperatures. This is one of the principal points to be investigated in this chapter. It is to be noted that the efficiency of conventionally designed steam turbines falls of rapidly below about 15 kw(e).

Turbine Types

Turbines may be classified as axial-flow, radial-flow, or tangential-flow. Axial-flow turbines may be of either the reaction or impulse type. Impulse turbines are those which restrict the fluid expansion to stationary nozzles with no expansion occuring in the rotor. Reaction turbines expand the working fluid in both the stator and rotor of the turbine. In addition the axial-flow turbine may be either partial or full admission with respect to whether stationary nozzles are provided over the whole periphery or only part of the periphery of the turbine.

Small power output axial-flow turbines are generally designed as partial admission turbines. This is because the volume-flow rate is small which results in short blade heights and small turbine wheel diameter. However manufacturing limitations in regard to minimum practical clearances preclude extremely small clearances in relation to the component dimensions of the turbine and for this reason it becomes attractive to design for partial admission. Partial-admission turbines must be of the pure impulse type. In addition since admission occurs over only part of the periphery it becomes possible to multi-stage the turbine using only a single disk.

The multi-staged, axial-flow (single-disk) turbine provides better performance in the specific speed regime below about 10. The optimum number of stages increases with decreasing specific speeds.

Performance diagrams for turbines are generally based on the similarity parameters N_s, (specific speed), and D_s, (specific diameter). The specific speed is given by

$$N_s = \frac{(N)(Q)^{0.5}}{H^{0.75}}$$

and the specific diameter is given by

$$D_s = \frac{DH^{0.25}}{(Q)^{0.5}}$$

where

N = speed, rpm

Q = volume flow rate, cu ft/sec

H = head due to isentropic expansion, ft

D = wheel diameter, ft.

The application regimes of various turbine types are shown in figure 5.1.

Turbine Speeds

The turbine speed to be selected will depend on the desired electric current characteristics and upon whether or not speed increasing or decreasing gears are to be used. The alternator speed is determined by the synchronous speed required for the current frequency.

Thus, if the power system is to supply 400-cycle power, the alternator speed must be 24000 rpm since

$$N = \frac{120\ f}{P}$$

where

N = synchronous speed, rpm

f = frequency, cycles/sec

P = number of poles, ($P \geq 2$).

For an underseas application, reliability and lubrication considerations inhibit against the use of gear boxes between the turbine and the alternator. Thus the present design will be based on the operation of the turbine and alternator at the same speed.

In order to limit turbine blade erosion by means of impinging liquid particles it is necessary to limit the expansion of the working fluid into the wet-vapor region. The practice in steam power plants has been to maintain an exit quality of not less that 85 per cent.

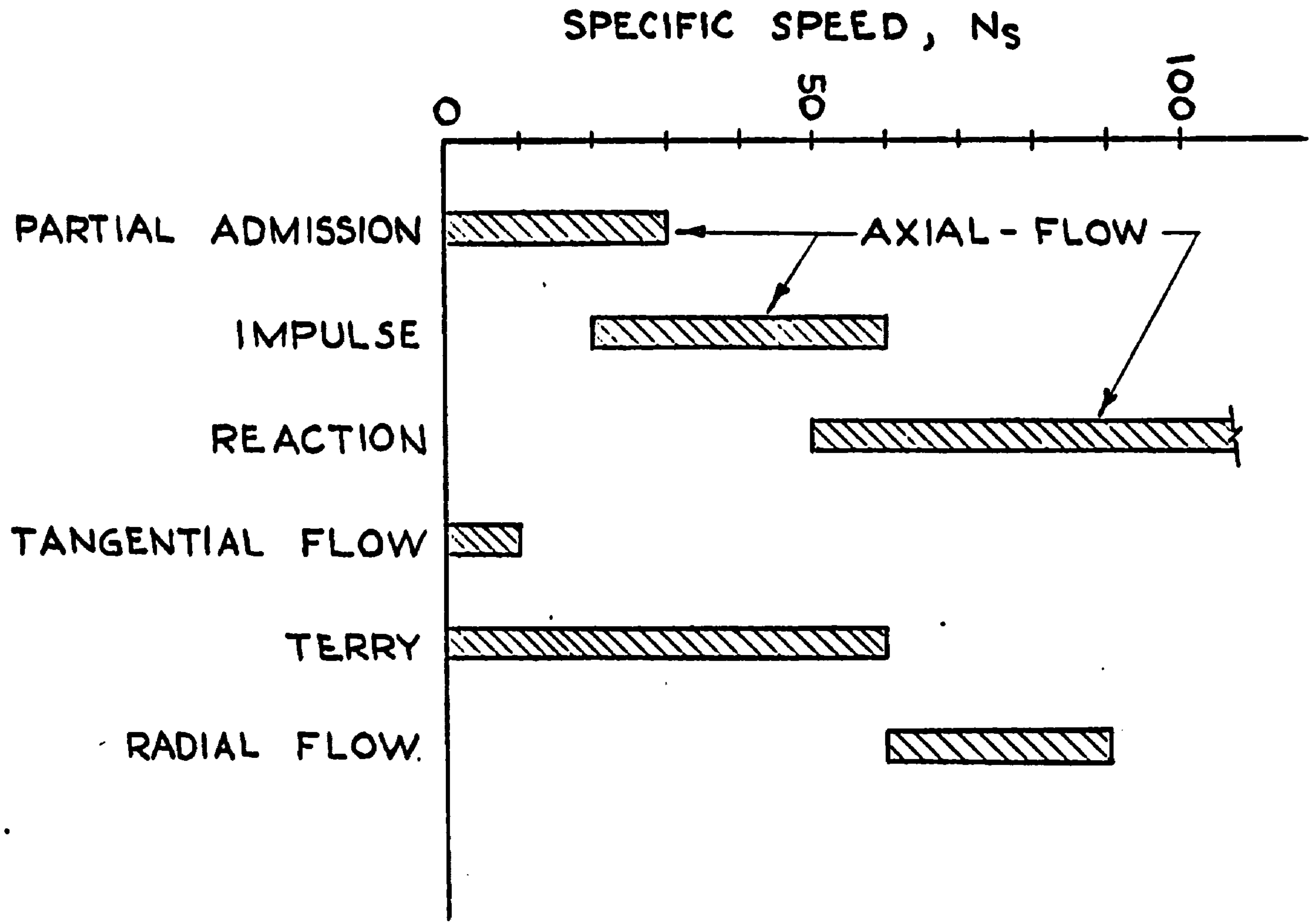

Figure 5.1

Application Regimes of Various Turbine Types

Turbine Design Thermodynamic Parameters

Turbine designs using high and low pressure steam and slightly superheated mercury are evaluated in this section. Cycle comparisons are given in chapter six. The chosen working fluid conditions are as shown in table 5.1.

Table 5.1

Working Fluid Conditions

	Inlet Pressure, psia	Inlet Temperature, °R	Condensing Pressure, psia
A. HIGH PRESSURE SATURATED STEAM	800	518	8
B. HIGH PRESSURE SUPERHEATED STEAM	800	740	3
C. LOW PRESSURE SUPERHEATED STEAM	80	1200	1
D. SUPERHEATED MERCURY	379.4	1800	3.23

A. High Pressure Saturated Steam

The parameters for a turbine design using high pressure saturated steam as a working fluid are

Steam Pressure	800 psia
Steam Temperature	518°F
Turbine Type	Axial Flow
Condensing Pressure	8 psia
Turbine-Alternator Speed	24000 rpm
Turbine Power Output	10.71 hp

Figure 5.2 illustrates the assumed isentropic and actual expansion processes for the turbine. The turbine isentropic expansion head is given by

$$H = J\ (h_1 - h_3)$$
$$= 778\ (1198.6 - 890)$$
$$= 240000 \text{ ft lb/lb}$$

The steam quality at state 3' may be assumed and the assumption checked later in the analysis. Assume that

$$x_{3'} = 90.0\%$$

Therefore

$$v_3 = v_f + x\ v_{fg}$$
$$\approx x\ v_g$$
$$= (0.900)(47.34)$$
$$= 42.6 \text{ ft}^3/\text{lb}$$

where v_g is the specific volume of saturated vapor at 8 psia. The specific density is

$$\rho = 1/v$$
$$= 1/42.6$$
$$= 0.0235 \text{ lb/ft}^3$$

Assume the turbine thermodynamic efficiency, η, to be 60 per cent. The turbine specific speed relationship may be written as

$$N_s = \frac{N(hp)^{0.5}}{H^{1.25}} \left(\frac{550}{\eta\ \rho}\right)^{0.5}$$

Therefore

$$N_s = \frac{24000(10.71)^{0.5}}{(240000)^{1.25}} \left[\frac{550}{(0.60)(0.0235)}\right]^{0.5}$$

$$N_s = 2.79$$

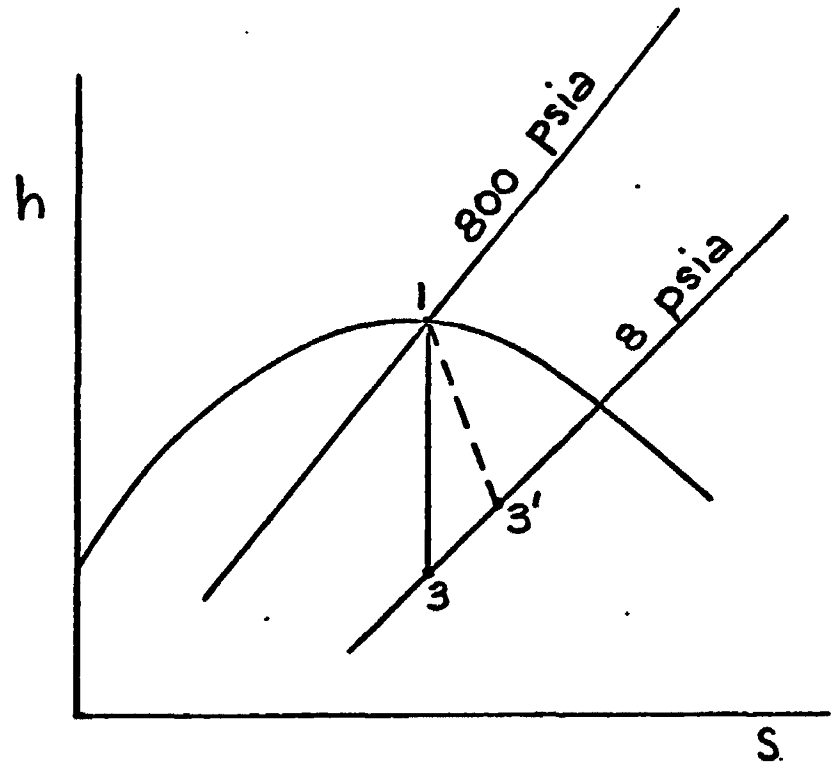

Turbine Expansion Process-
Alternative A
Figure 5.2

Using this value of the turbine specific speed on figure 5.3, (which is based on figure 14 of reference 5) we obtain

$\eta = 57.7\%$ for multi-stage, re-entry type

where

$$\left(\frac{P}{P}\right)_{max} = 100:1$$

In the present case

$$\left(\frac{P}{P}\right)_{max} = 800/8$$

$$= 100:1$$

If we re-calculate N_s using a turbine efficiency η, equal to 57% we get

$$N_s = 2.83$$

and from figure 5.3

$$\eta = 58\%$$

$$D_s = 8 \quad \text{(from figure 14, reference 5)}$$

Thus assume that the estimate for η, (57%), is close enough. Also the optimum number of stages for a single disk turbine is shown to be six by figure 14, reference 5. The turbine diameter, D, may now be determined from the relationship

$$D = \frac{D_s V_{3'}^{0.5}}{H_{ad}^{0.25}}$$

where $V_{3'}$ is the exhaust steam volume flow rate in ft^3/sec. The steam mass flow rate is given by

$$\dot{m} = (hp)\left(\frac{Btu}{hp\ hr}\right)\left(\frac{hr}{sec}\right)\left(\frac{lb}{Btu}\right)\left(\frac{1}{\eta}\right)$$

$$= (10.71)(2545)(1/3600)(1/308.6)(1/0.57)$$

$$= 0.0431 \text{ lb/sec}$$

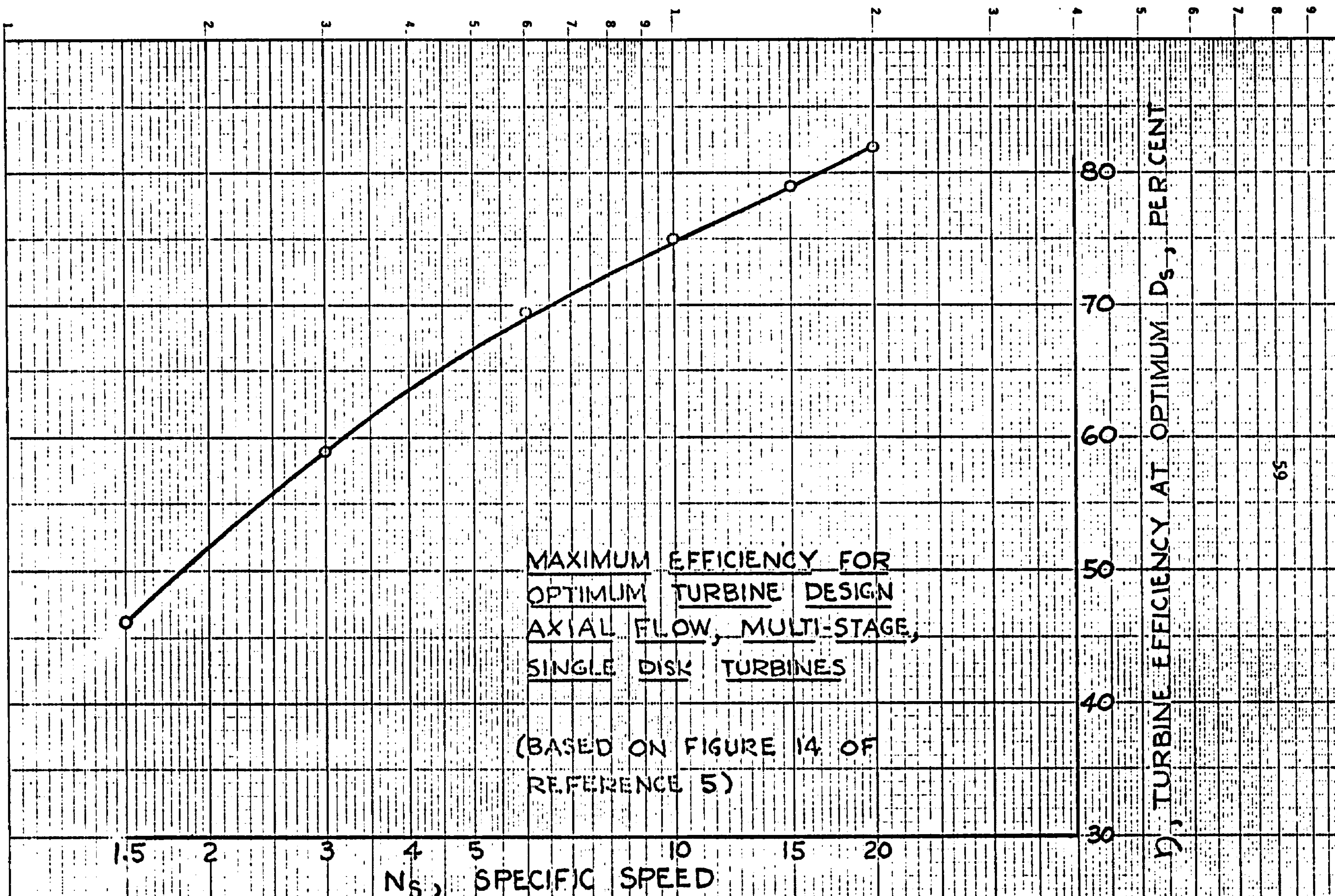
MAXIMUM EFFICIENCY FOR
OPTIMUM TURBINE DESIGN
AXIAL FLOW, MULTI-STAGE,
SINGLE DISK TURBINES
(BASED ON FIGURE 14 OF
REFERENCE 5)
η, TURBINE EFFICIENCY AT OPTIMUM D_s, PERCENT
30
40
50
60
70
80
1.5
2
3
4
5
10
15
20
N_s, SPECIFIC SPEED

Figure 5.3

The actual enthalpy of the steam leaving the turbine may be determined by the relationship

$$\eta = (h_1 - h_{3'})/(h_1 - h_3)$$

Therefore

$$h_{3'} = 1198.6 - (0.57)(308.6)$$

$$h_{3'} = 1022.6 \text{ Btu/lb}$$

The quality of the turbine exhaust steam may be read from the Mollier diagram:

$$x_{3'} = 88.3\%$$

The exhaust steam specific volume may now be determined to be

$$v_{3'} = 41.7 \text{ ft}^3/\text{lb}$$

so that the exhaust steam volume flow rate is given by

$$\begin{aligned} V_{3'} &= \dot{m}\, v_{3'} \\ &= (0.0431)(41.7) \\ &= 1.80 \text{ ft}^3/\text{sec} \end{aligned}$$

The turbine diameter is given by

$$D = \frac{(8)(1.80)^{0.5}}{(240000)^{0.25}}$$

$$= 0.48 \text{ ft}$$

or

$$D = 5.76 \text{ in.}$$

B. High Pressure Superheated Steam

The analysis for this alternate is similar to that for alternative "A" above and is included in the appendix. For this alternative we get for a turbine speed of 24000 rpm

$$\eta = 60\%$$

Exit quality = 98.2%

N_s = 3.06

D_s = 7.2

D = 6.76 inches

Number of stages = 4 (Multi-staged re-entry type turbine)

However, since for this case $(P/P)_{max}$ is equal to 800/3 or 267:1 the results are not entirely accurate.

C. Low Pressure Superheated Steam

The analysis for this alternative is also included in the appendix. The analysis provides the following values

η = 0.68

Exit quality = Superheated

N_s = 5.39

D_s = 6.0

D = 10.13 inches

Number of stages = 4

D. Superheated Mercury

The analysis (included in the appendix) for the turbine using superheated mercury yields the following results for a multi-stage, single disk turbine

η = 0.77

Exit quality = 85%

N_s = 14.62

D_s = 3.3

D = 4.92 inches

Number of stages = 2

$(P/P)_{max}$ = 117:1

Comparison of Turbine Designs

The designs for five turbine alternatives are compared in table 5.2. The results indicate that the turbine design based on superheated mercury as a working substance is about 9 per cent more efficient than the most efficient steam turbine design, (low pressure superheated steam).

In chapter six the influence of the turbine efficiency on the over-all thermodynamic cycle efficiency will be determined.

Table 5.2

Comparison of Turbine Designs

	A. High Pressure Saturated Steam (800 psia, 518°F)	B. High Pressure Superheated Steam (800 psia, 740°F)	C. Low Pressure Superheated Steam	D1. Superheated Mercury, single-stage	D2. Superheated Mercury, Multi-stage
Turbine Efficiency	0.57	0.60	0.68	0.67	0.77
Number of Turbine Stages	6	4	4	1	3
Turbine Diameter, in.	5.76	6.76	10.1	6.25	4.92
Exhaust Quality, %	88.3	98.2	super-heated	89	85
Specific Speed, N_s	2.83	3.1	5.39	14.6	14.6
$(P/P)_{max}$	$\frac{100}{1}$	$\frac{267}{1}$	$\frac{80}{1}$	$\frac{117}{1}$	$\frac{117}{1}$
Specific Diameter, D_s	8	7.2	6	4.2	3.3
Turbine Blade Height, in.	-	-	-	0.46	-

CHAPTER VI

CYCLE THERMODYNAMICS

Introduction

Even though the turbine design analysis has indicated the small mercury turbine to be more efficient than the small steam turbine it does not necessarily follow that the mercury cycle thermodynamic efficiency will be greater than the steam cycle efficiency. This is due to the large influence of the cycle heat rejection temperature upon the cycle efficiency. The combined influence of turbine efficiency and heat rejection temperature upon the cycle efficiency is examined in this chapter.

Turbine Power Summary

The basis for the design turbine power output is indicated by table 6.1

Table 6.1

Turbine Power Summary

Net Electrical Output	5.0 kw	
Electrical Controls	0.1 kw	
Parasitic Load	0.5 kw	
Alternator Output	5.6 kw	
Alternator Input	7.0 kw	
Pumps	0.2 kw	
Bearings and Seals Power Consumption	0.8 kw	
Gross Turbine Output	8.0 kw	(10.71 Hp)

Cycle Arrangement for Steam Cycles

Figure 6.1 is a schematic illustration of the cycle arrangement used as the basis for the analysis of the steam cycle alternatives. The heat interchanger is included only in the cycle for alternative C. Table 6.2 provides a listing of the steam properties at various points in each of the cycles. The thermodynamic analysis for each cycle is given in outline form in the following.

A. High Pressure Saturated Steam Cycle

Turbine efficiency.

$$\eta_t = 0.57$$

Turbine work per pound.

$$w_T = \eta_T (h_1 - h_3)$$
$$= (0.57)(1199 - 890)$$
$$= 176 \text{ Btu/lb}$$

Steam flow rate.

$$\dot{m} = (10.71 \text{ hp})(2545 \text{ Btu/hp-hr})(1 \text{ lb}/176 \text{ Btu})$$
$$= 155 \text{ lb/hr}$$

Turbine work.

$$W_T = (10.71 \text{ hp})(2545 \text{ Btu/hp-hr})$$
$$= 27{,}300 \text{ Btu/hr}$$

Pump work.

$$W_P = (0.2 \text{ kw})(3413 \text{ Btu/kw-hr})$$
$$= 682 \text{ Btu/hr}$$

Heat added.

$$Q_A = \dot{m} (h_1 - h_T)$$
$$= (155)(1199 - 122)$$

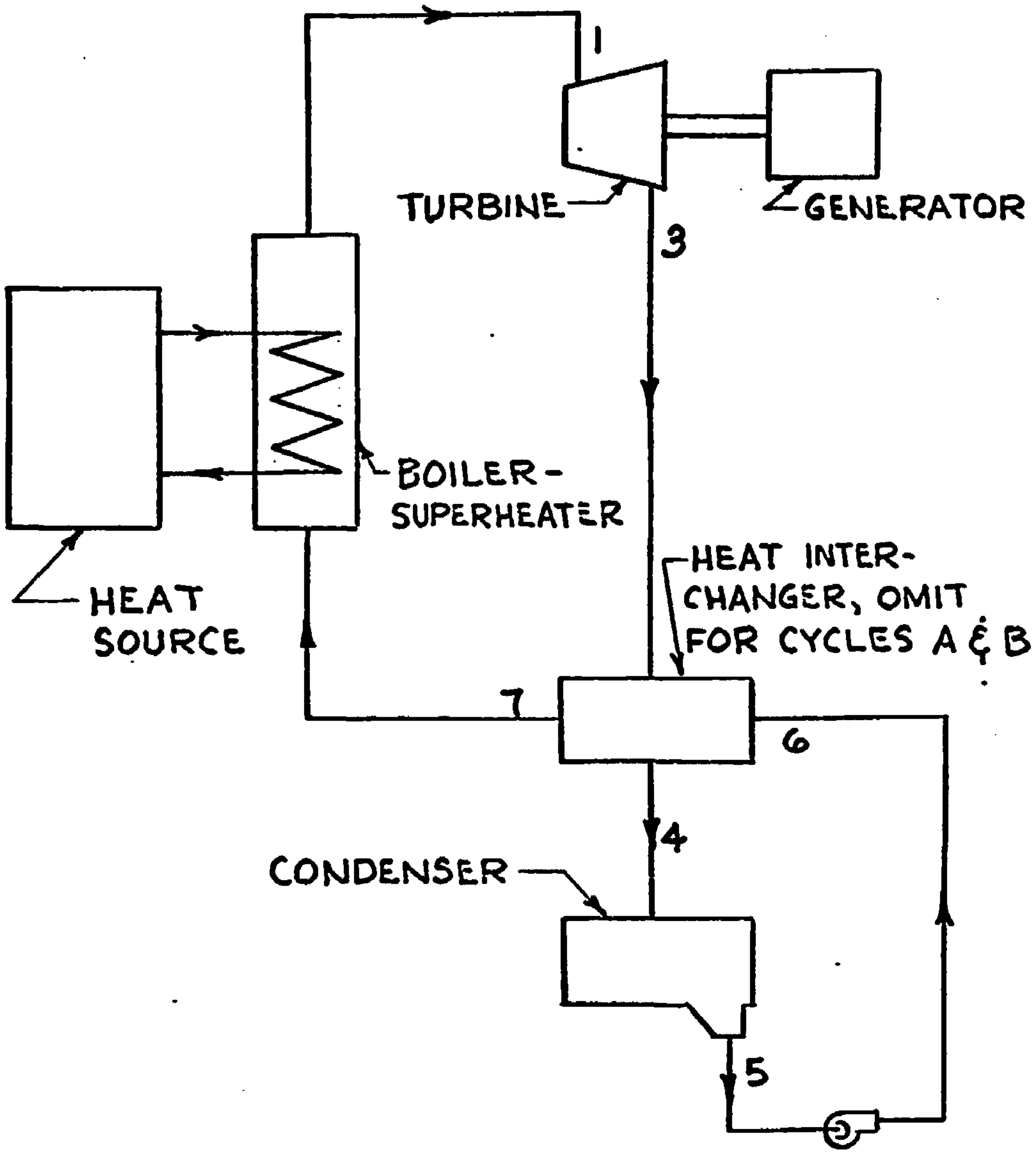

Cycle Arrangement for Steam Cycles
Figure 6.1

Table 6.2

Steam Cycle Properties

State Point Number	Cycle A	Cycle B	Cycle C
1			
Pressure, psia	800	800	80
Temperature, ^{o}F	518	740	1200
Enthalpy, Btu/lb	1199	1363	1636
3 (Isentropic Expansion)			
P	8	3	1
t	183	141	143
h	890	931	1125
4			
P	8	3	1
t	183	141	160
h	890	931	1132
5			
P	8	3	1
t	150	120	95
h	118	88	63
6			
P	850	850	90
t	154	124	98
h	122	92	66
7			
P	850	850	90
t	154	124	254
h	122	92	222

$= 166,800$ Btu/hr

Cycle thermodynamic efficiency.

$$\eta_c = (W_T - W_P)/Q_A$$

$$= (27300 - 682)/166,800$$

$$\eta_c = 0.16$$

B. High Pressure Superheated Steam Cycle

Turbine efficiency.

$$\eta_T = 0.60$$

Turbine work per pound.

$$w_T = (0.60)(1363 - 931)$$

$$= 259 \text{ Btu/lb}$$

Steam flow rate.

$$\dot{m} = (10.71)(2545)(1/259)$$

$$= 105.3 \text{ lb/hr}$$

Heat added.

$$Q_A = (105.3)(1363 - 92)$$

$$= 127,100 \text{ Btu}$$

Cycle thermodynamic efficiency.

$$\eta_c = (27300 - 682)/127100$$

$$= 0.21$$

C. Low Pressure Superheated Steam Cycle

Turbine efficiency.

$$\eta_T = 0.68$$

Turbine work per pound.

$$w_T = 0.68\ (1636 - 1125)$$

$$= 348 \text{ Btu/lb}$$

The steam turbine expansion process for this case is shown in figure 6.2.

Steam flow rate.

$$\dot{m} = (10.71)(2545)(1/348)$$

$$= 78.4 \text{ lb/hr}$$

Steam condition leaving turbine.

$$h_{3'} = h_1 - w_T$$

$$= 1636 - 348$$

$$h_{3'} = 1288 \text{ Btu/lb}$$

$$t_{3'} = 495^{\circ}F \text{ (from Mollier diagram)}$$

Heat interchanger calculations. The steam and condensate states for the heat interchanger are shown in figure 6.3

$$h_7 - h_6 = h_3 - h_4$$

$$h_7 = 66 + (1288 - 1132)$$

$$h_7 = 222 \text{ Btu/lb}$$

$$t_7 = 254\ ^{\circ}F$$

Heat added.

$$Q_A = 78.4\ (1636 - 222)$$

$$Q_A = 111{,}000 \text{ Btu/hr}$$

Pump work.

$$W_P = (\Delta P\dot{m})/J\rho\eta_P)$$

$$= \frac{(90 - 1)(144)(78.4)}{(778)(1/0.01612)(0.10)}$$

$$W_P = 208 \text{ Btu/hr}$$

Cycle thermodynamic efficiency.

$$\eta_c = (27300 - 208)/111000$$

$$\eta_c = 0.244$$

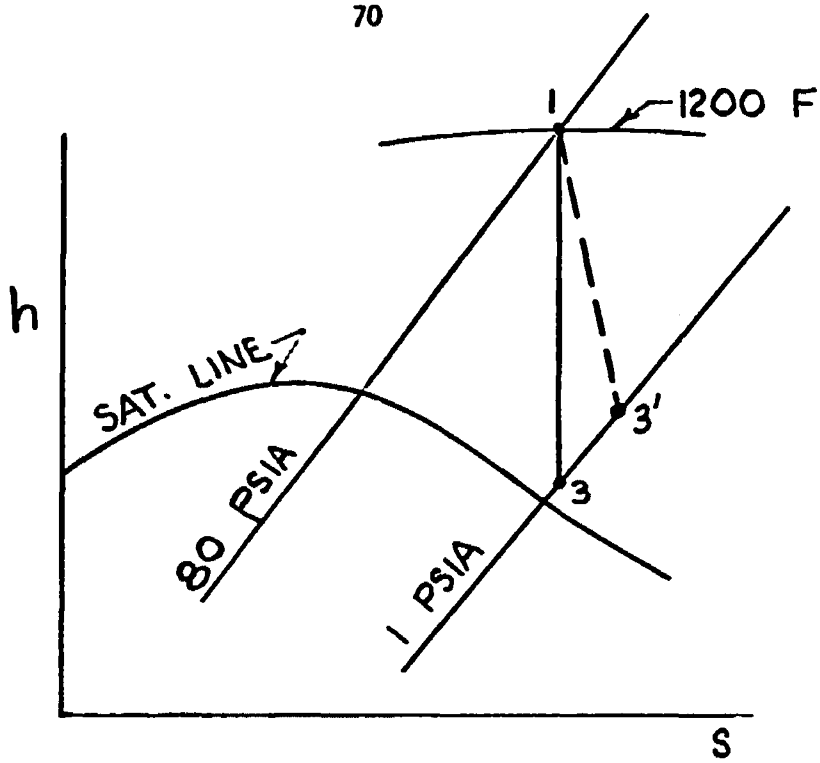

Steam Turbine Expansion Process
Figure 6.2

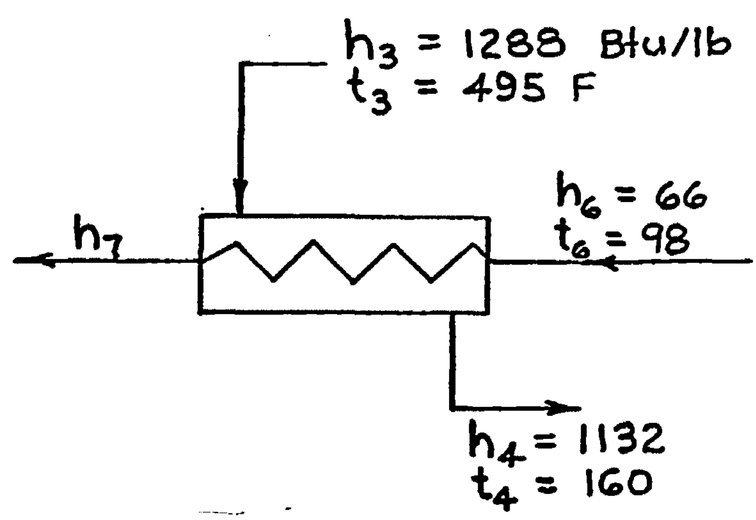

Heat Interchanger Schematic
Figure 6.3

D. Superheated Mercury Cycle

Mercury cycle arrangement. A schematic diagram of the proposed mercury cycle is shown in figure 6.4. State properties for the mercury at various points in the cycle are provided in table 6.3. A value of 77 per cent for the turbine efficiency has been used as the basis for the thermodynamic analysis of the cycle.

Mercury flow rate.

$$w_T = (0.77)(186.9 - 133.9)$$

$$= 40.8 \text{ Btu/lb}$$

$$\dot{m} = (10.71)(2545)(1/40.8)$$

$$= 670 \text{ lb/hr}$$

Heat recovery in alternator. Assume that 50 percent of the alternator energy losses are recovered by the mercury coolant flow stream.

$$Q_{rec.} = (5.6 \text{ kw})(1 - 0.8)(0.5)(3413)$$

$$= 1911 \text{ Btu/hr}$$

$$q_{rec.} = (1911 \text{ Btu/hr})(1 \text{ hr}/670 \text{ lb})$$

$$= 2.9 \text{ Btu/lb}$$

Mercury pump work.

$$w_p = \Delta P / J\rho\eta_p$$

$$= \frac{(447)(144)}{(778)(815)(0.10)}$$

$$= 1.015 \text{ Btu/lb}$$

The specific heat of mercury is approximately 0.032 Btu/lb-$^{\circ}$R. Therefore the temperature rise across the pump is roughly 30°R.

Energy added by heat source.

$$Q_A = \dot{m}\Delta h$$

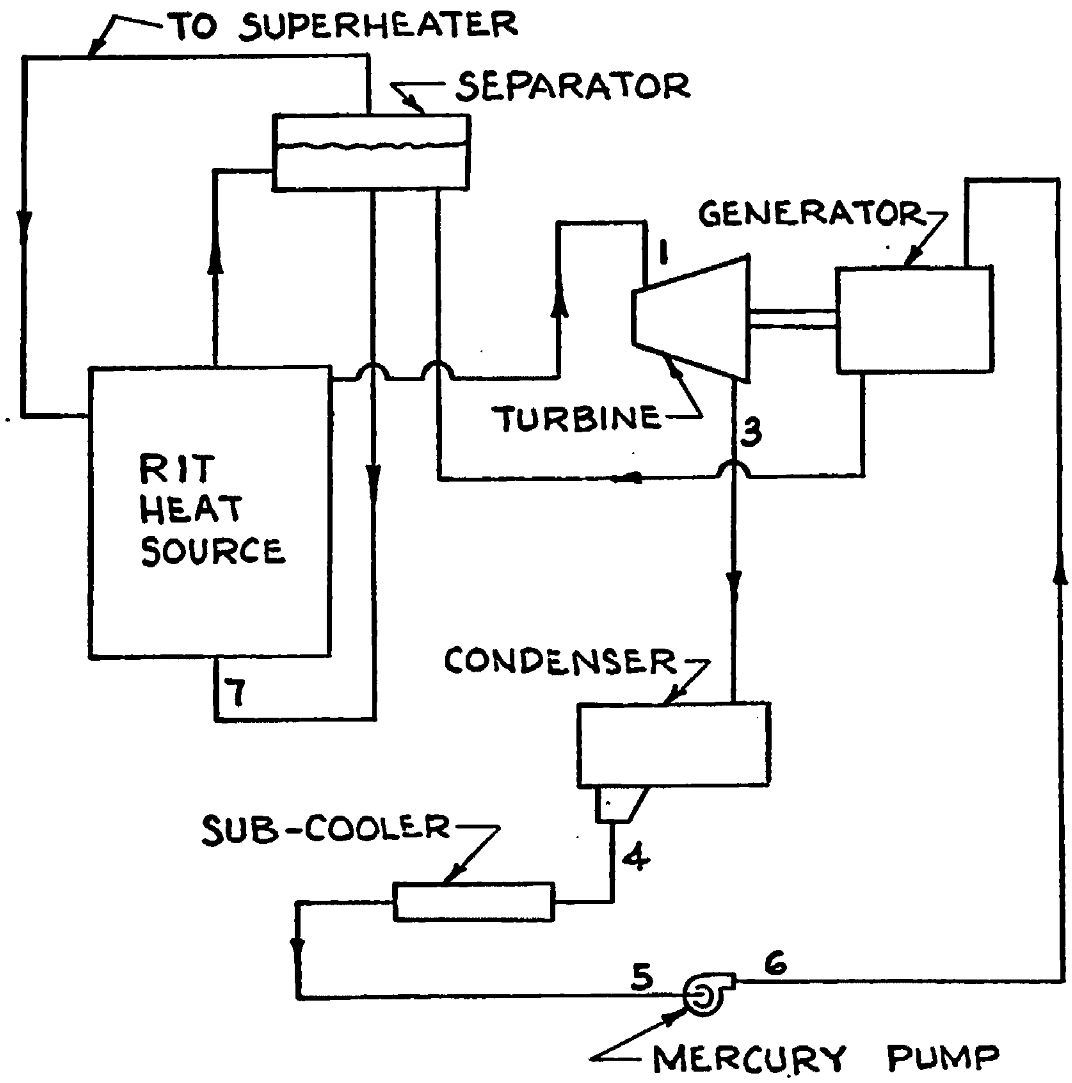

Superheated Mercury Cycle
Figure 6.4

Table 6.3

Mercury State Point Properties

Cycle Point Number	Temperature, ^{o}R	Pressure, psia	Enthalpy, Btu/lb
1	1800*	379.4	186.9
3	1000	3.23	133.9**
4	1000	3.23	39.0
5	940	3.23	37.0
6	970	450.0	38.0
7	1060	440.0	40.9

* 200^{o} Superheat

** Isentropic expansion

$$= (670)(186.9 - 40.9)$$

$$= 97900 \text{ Btu/hr}$$

Turbine work.

$$W_T = (10.71)(2545)$$

$$= 27{,}300 \text{ Btu/hr}$$

Pump work.

$$W_P = (670)(1.02)$$

$$= 684 \text{ Btu/hr}$$

Cycle efficiency.

$$\eta_c = (27{,}300 - 684)/97900$$

$$= 0.272$$

Net cycle efficiency.

$$\eta = \frac{\text{net electrical output}}{Q_A}$$

$$= \frac{(5)(3413)}{97900}$$

$$= 0.174$$

Cycle efficiency if no alternator heat recovered.

$$Q_A = (670)(186.9 - 38.0)$$

$$= 99.700 \text{ Btu/hr}$$

$$\eta_c = (27{,}300 - 684)/99700$$

$$= 0.267$$

Comparison of Cycles

The steam and mercury cycles are compared in table 6.4. Even though the mercury cycle is at a disadvantage for terrestrial applications because of its high heat rejection temperature it nonetheless has the highest thermodynamic efficiency. This results from the higher

Table 6.4

Comparison of Cycles

	A. High Press. Sat. Steam	B. High Press. Superheated Steam	C. Low Press. Superheated Steam	D. Super-Heated Mercury
1. Turbine Inlet Pressure, psia	800	800	80	379.4
2. Condensing Pressure, psia	8	3	1	3.23
3. Condensing Temperature, ^{o}F	183	141	102	540
4. Turbine Efficiency, %	0.57	0.60	0.68	0.77
5. No. of Turbine Stages, (Single Disk)	6	4	4	3
6. Cycle Thermodynamic Efficiency, %	0.16	0.21	0.244	0.272
7. $(P/P)_{max}$	100/1	267/1	80/1	117/1
8. Turbine Inlet Temperature, ^{o}F	518	740	1200	1340
9. Turbine Exhaust Quality, %	88.8	98.2	Superheated	85

turbine efficiency obtainable for the mercury turbine when compared to the steam turbine. The superheated mercury cycle efficiency value of 0.272 is approximately 2.8 per cent greater than the value for the low pressure superheated steam cycle. However the pressure ratio for the mercury turbine (117/1) is somewhat more than the maximum pressure ratio (100/1) upon which the turbine design charts were based. Also the 1340 F turbine inlet temperature chosen for the mercury turbine exceeds the 1200^{o}F chosen for the steam turbine. This connotes more stringent material specifications for the mercury turbine. A rather severe disadvantage for the mercury cycle is that the turbine exhaust quality is 85%. Thus turbine blade erosion may be a problem. But small, high speed, steam turbines in the power range of this design (around 5 kw) have not been produced to date. Conversely mercury turbines have been designed and constructed and performance data is now accumulating. (A less optimistic mercury turbine efficiency would result in a higher turbine exhaust quality--but lower cycle efficiency).

On the basis of the above comments it may be reasoned that the low pressure superheated steam cycle and the superheated mercury cycle may have equal potential design merit. The "designers choice" is that the remainder of this design study will be based on the superheated mercury cycle.

Effect of Turbine Efficiency Upon Cycle Efficiency

The influence of the turbine efficiency on the cycle thermodynamic efficiency is shown by the curve in figure 6.5. The curve is for the mercury power plant cycle. A decrease in turbine efficiency of 5 per cent results in a decrease in cycle efficiency of approximately

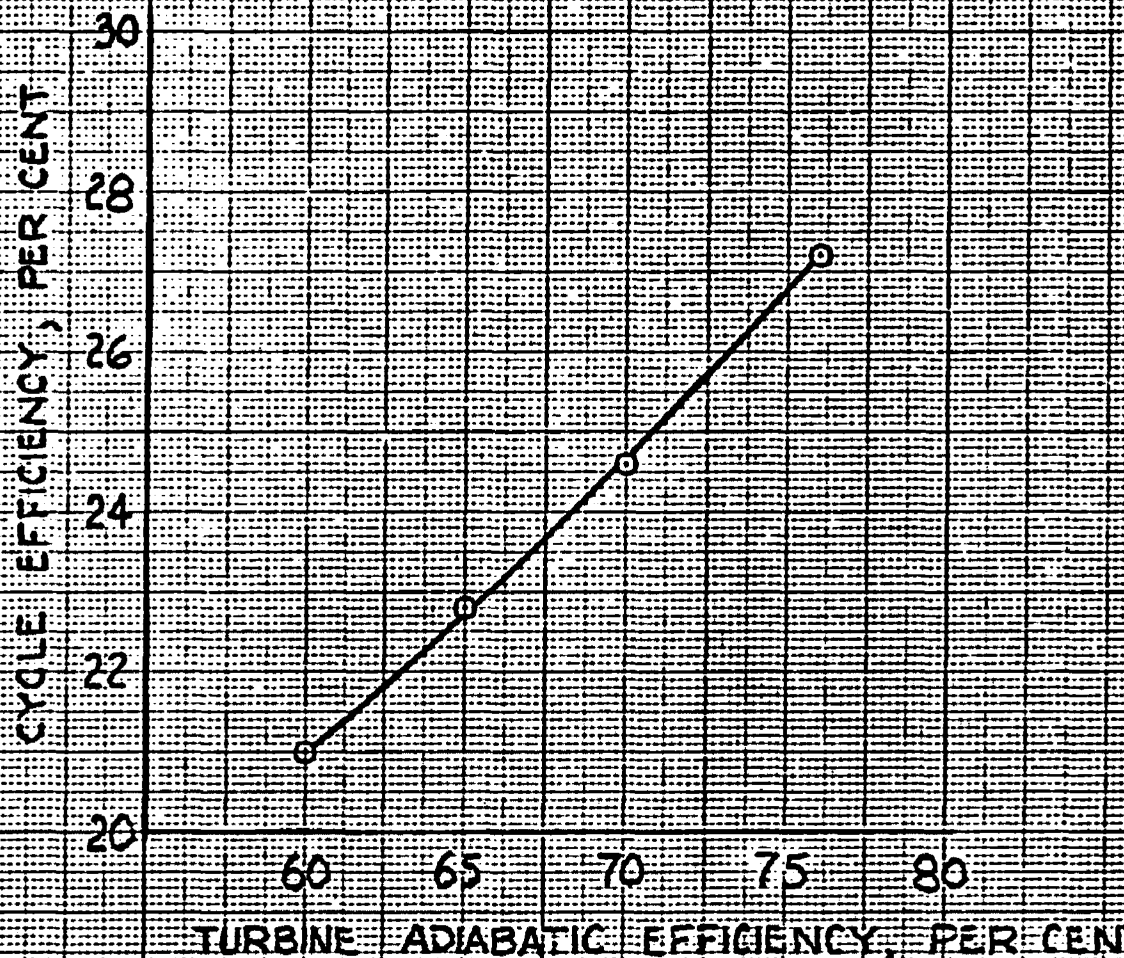

Cycle Efficiency
Figure 6.5

2 per cent. Or stated another way a change in turbine efficiency from 65 to 70 per cent decreases the required energy addition to the cycle from the heat source from 116,200 Btu/hr to 107,700 Btu/hr. The savings in radioisotope cost would be approximately $30,000 on a future cost basis of $10 per thermal watt. The importance of maximizing the turbine efficiency is thus demonstrated.

CHAPTER VII

DESIGN OF THE HEAT-SOURCE BOILER SYSTEM

Introduction

The design alternatives and analysis for the radioisotope heat source-boiler subsystem are contained in this chapter. This design will be based on a conservative value of 60 per cent for the adiabatic turbine efficiency and the analysis will be for the cycle using mercury as the working fluid. The design concept is based on the use of Cobalt-60 as the radioisotope energy source.

Radioisotope Fuel Cost

The energy addition for the cycle which has a turbine with adiabatic efficiency of 60 per cent would be 125,700 Btu/hr. Assume that the heat source energy loss to the surroundings is 10 per cent. The required heat source energy rate is then 138,300 Btu/hr. This converts to 40,600 thermal watts. This is the energy rate required at the end of a one year mission application.

The Cobalt-60 decay factor for one year is

$$F_{decay} = e^{-0.693t/T_{\frac{1}{2}}}$$

where $T_{\frac{1}{2}}$ is the half-life.

$T_{\frac{1}{2}} = 5.24$ years for Cobalt 60.

Therefore the decay factor is equal to

$$e^{-(0.693)(1)/(5.24)} = 0.875$$

and the required heat source power at the beginning of a one year mission becomes

$$\text{Heat source power} = 40600/0.875$$
$$= 46400 \text{ watts}$$

The current cost for Cobalt-60 is estimated to be \$32.50 per thermal watt, (reference 6). Therefore the

$$\text{Fuel Cost} = (46400 \text{ watts})(\$32.50/\text{watt})$$
$$= \$1,509,000$$

and the

$$\frac{\text{Cost}}{\text{kw-hr}} = (1509000)\left(\frac{1 \text{ year}}{8760 \text{ hr}}\right)\left(\frac{1}{5 \text{ kw}}\right)$$
$$= \$34.40/\text{kw-hr}.$$

The "future" cost of Cobalt-60 is estimated to be \$10.00 per thermal watt. The fuel cost on a future basis is therefore

$$\text{Fuel cost} = (46400 \text{ watts})(\$10/\text{watt})$$
$$= \$464000 \quad \text{(future basis)}$$

and the cost per kilowatt-hour becomes

$$\frac{\$464000}{43800 \text{ kw-hr}} = \$10.60/\text{kw/hr}$$

for a one year mission. The figure assumes the fuel has no salvage or "trade-in" value. The above results are for an over-all cycle efficiency of

$$\frac{(5 \text{ kw})(3413 \text{ Btu/kw-hr})}{125700 \text{ Btu/hr}} = 0.136$$

Fuel Cost If Cycle Efficiency Is Increased By One Per Cent

The required heat source energy for a cycle with an overall thermal efficiency of 0.146 would be

$$(5\ \text{kw})\left(\frac{1}{0.146}\right)(1.10)\left(\frac{1}{0.875}\right) = 43.1\ \text{kw}.$$

The fuel cost on the future basis would then be $431000. The per cent reduction in fuel cost is therefore given by

$$\frac{(464000 - 431000)(100)}{(464000)} = 7.1\%$$

Radioisotope Capsule Description

If the power density of the Cobalt fuel is taken as 27 watts per cubic centimeter, (corresponding to 200 curies per gram), then the quantity of radioisotope fuel required will be

$$(46400\ \text{watts})\left(\frac{1\ \text{cc}}{27\ \text{watts}}\right) = 1720\ \text{cc}.$$

The design fuel form is to be strips having the following dimensions, (reference 10):

Width, inches	0.80
Thickness, inches	0.0625
Length, inches	10.0

For Nickel coated strips the dimensions are:

Width, inches	0.84
Thickness, inches	0.1025
Length, inches	10.04

The dimensions of the Co-60 capsules having two strips per capsule will be taken as:

Width, inches	0.88
Thickness, inches	0.245
Length, inches	10.20

Number of Cobalt-60 Capsules

The quantity of fuel capsules required is determined as follows:

$$(2)(0.80)(0.0625)(10.0) = 1 \text{ in}^3 \text{ fuel/capsule}$$

$$(1 \frac{\text{cu in.}}{\text{capsule}})(\frac{2.54 \text{ cm}}{\text{in}})^3 = 16.39 \frac{\text{c.c.}}{\text{capsule}}$$

$$(1720 \text{ c.c.})(\frac{1 \text{ capsule}}{16.39 \text{ c.c.}}) = 105 \text{ capsules}$$

The heat source will be designed to be two capsules in height, (i.e. 20.4 inches) and the diameter of the fuel capsule ring is therefore given by the following calculation:

$$(53 \text{ capsules})(0.88 \frac{\text{in.}}{\text{capsule}}) = 46.7 \text{ inches}$$

$$D = 46.7/\pi$$

$$= 14.85 \text{ in.}$$

The geometric arrangement for the heat source is indicated in figure 7.1.

Boiler Tube Heat Transfer Calculations

The boiling heat transfer coefficient may be obtained from figure 7.2, which is taken from reference 16.

From the curve of figure 7.2, at ΔT equal to $60^{\circ}F$, the value of the boiling heat transfer coefficient, h_i, is 170 Btu/hr $ft^2\ {}^{\circ}F$. The temperature difference, ΔT, is the metal surface temperature minus the liquid temperature. The boiler tubes are tentatively selected to be nominal 1/8 inch diameter, schedule 80, carbon steel pipe with an OD of 0.405 inches and an ID of 0.215 inches. The required tube length is estimated as follows:

$$Q_B = h_i A_i \, \Delta T$$

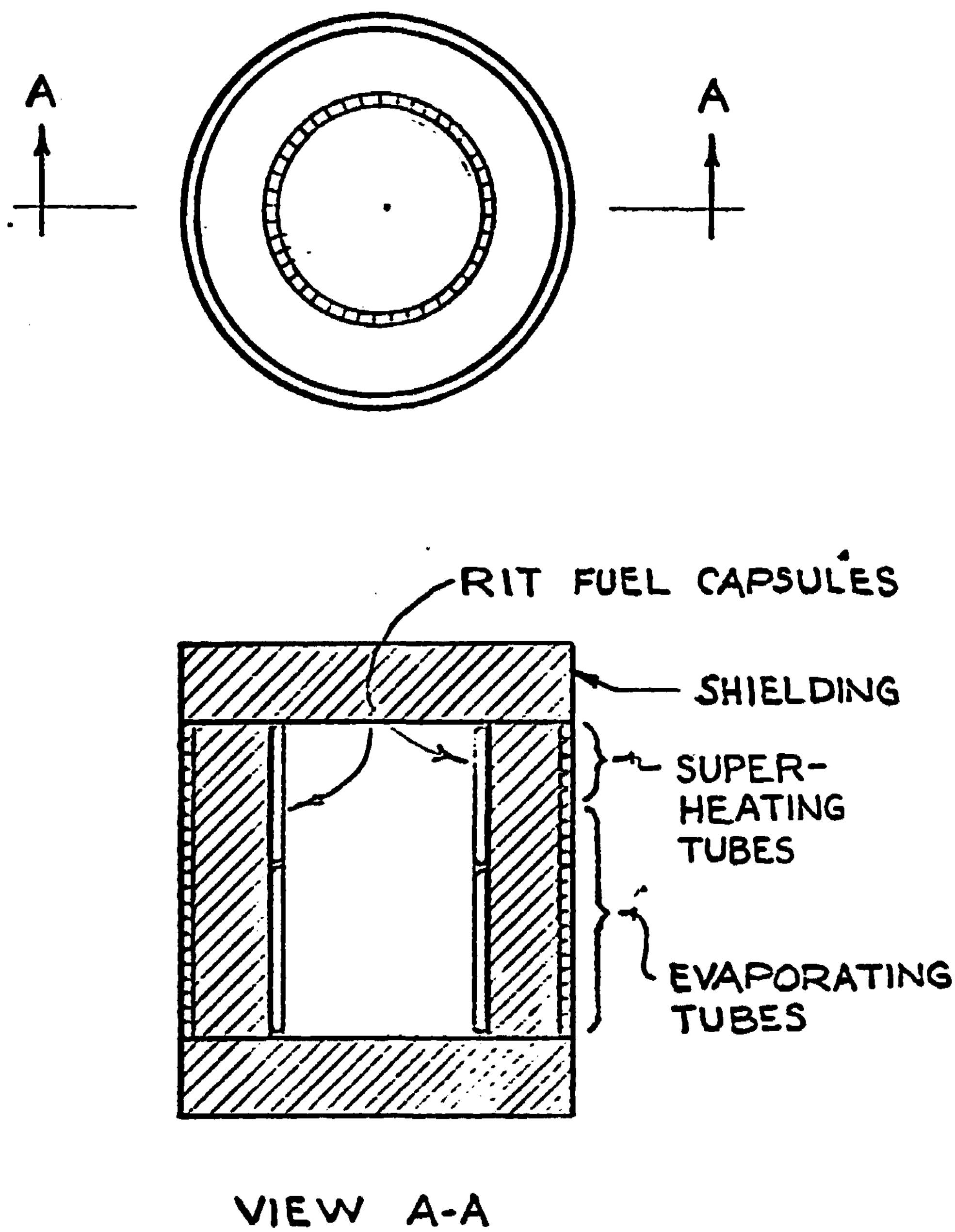

Heat Source Design
Alternative No. 1
Figure 7.1

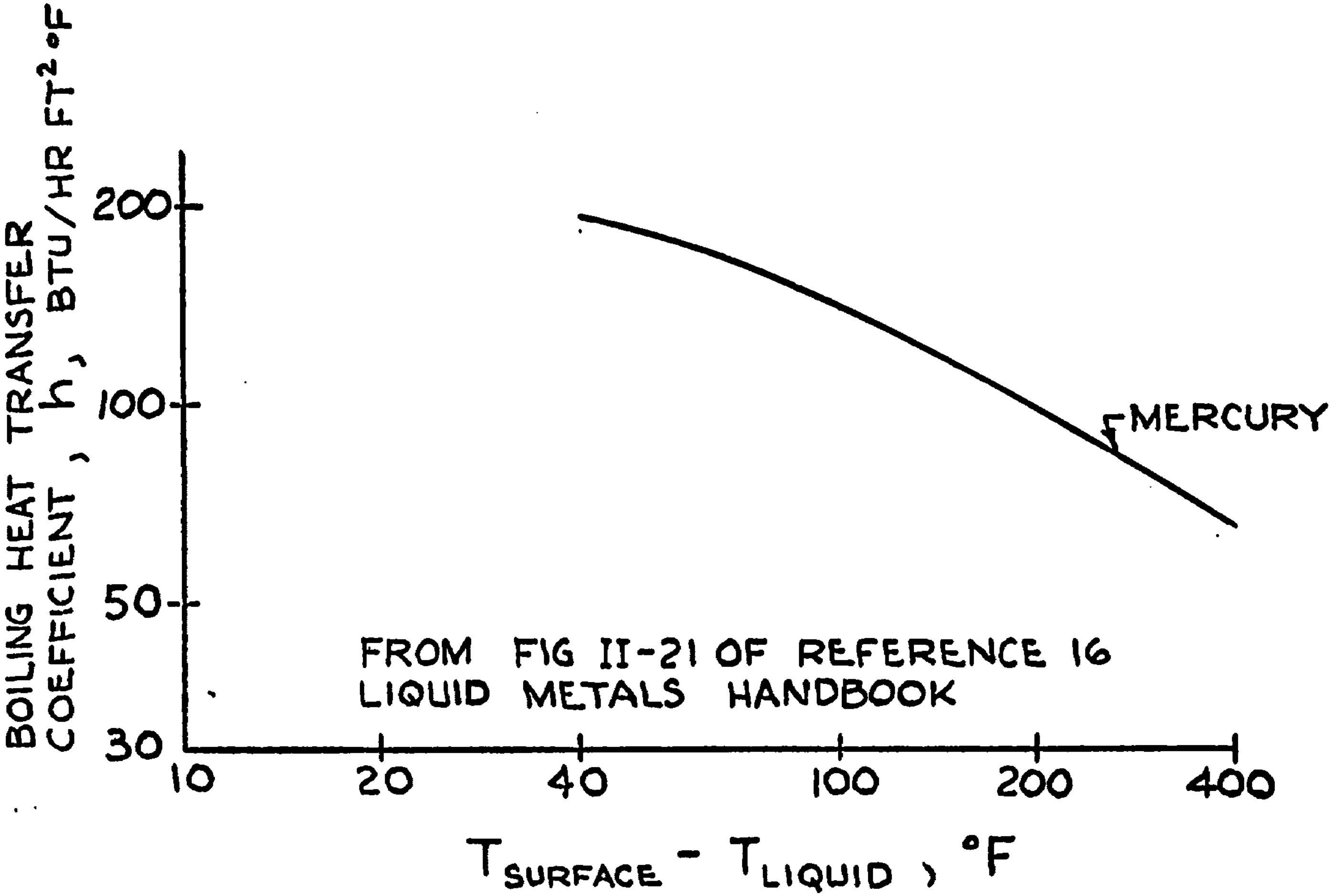

Experimental Boiling Heat Transfer Coefficient

Figure 7.2

$$A_i = \frac{125700}{(170)(60)} = 12.3 \text{ ft}^2$$

$$A_i/\text{tube} = \left(\frac{0.215}{12}\right)(\pi)(1)$$

$$= 0.0563 \text{ ft}^2/\text{ft}$$

$$\text{Tube length} = 12.3/0.0563$$

$$= 219 \text{ ft}$$

If the shielding thickness is taken as 4 inches then the boiler diameter at the heating tube surface will be approximately

$$D = 15 \text{ in.} + 8 \text{ in.} = 23.0 \text{ inches.}$$

Let each tube circle the boiler four times. The required number of tubes, (N), is therefore

$$N = \frac{(219)(12)}{(4)(\pi)(23)}$$

$$= 9 \text{ tubes}$$

The total tube height, H, is given by

$$H = (4)(9)(0.405)$$

$$\cong 15.0 \text{ inches}$$

The remainder of the heat source height, (about six inches), may be utilized for the superheating tube surface.

Forced Convection Heat Transfer Coefficient

Since the determination of the heat transfer coefficient for the boiling liquid mercury is a matter of some uncertainty it will be informative to determine the forced convection heat transfer coefficient to non-boiling liquid mercury. The Lubarsky and Kaufman equation (reference 23, page 45) for liquid metals in forced convection at turbulent flow inside tubes is

$$\frac{hD}{k} = 0.625 \left(\frac{DV}{\alpha}\right)^{0.4}$$

Let the flow velocity, V, be equal to 1 ft/sec or 3600 ft/hr. Also

$D = 0.018$ ft

$\alpha \approx 310 \times 10^{-3}$ ft^2/hr

$k = 8.1$ Btu/hr ft ^{o}F

Therefore

$$h = \left(\frac{8.1}{0.018}\right)(0.625)\left[\frac{(0.018)(3600)}{(310)(10)^{-3}}\right]^{-0.4}$$

$$h = 2380 \text{ Btu/hr ft}^2 \text{ F.}$$

This value of the heat transfer coefficient is much larger than the boiling coefficient used above to determine the heat transfer surface needed. The free convection coefficient can be estimated to be one-half the forced convection coefficient.

Heat Source Alternatives

The intent thus far in the design program has been to employ a "direct" cooled heat source as illustrated in figure 7.1. However it now becomes evident that there may be boiler stability problems with this design concept. The problem has to do with the means to be employed in order to utilize the radioisotope heat source as energy source for both the evaporating and superheating components of the mercury vapor generator whenever natural circulation is depended on as the transport mechanism for the working fluid. Thus it is expedient to consider additional alternatives for the arrangement of the mercury vapor generator. The following alternatives may be considered:

1. A single heat source component used for both evaporating and superheating the mercury fluid, figure 7.1.
2. A "once-through" boiler design, figure 7.3a.

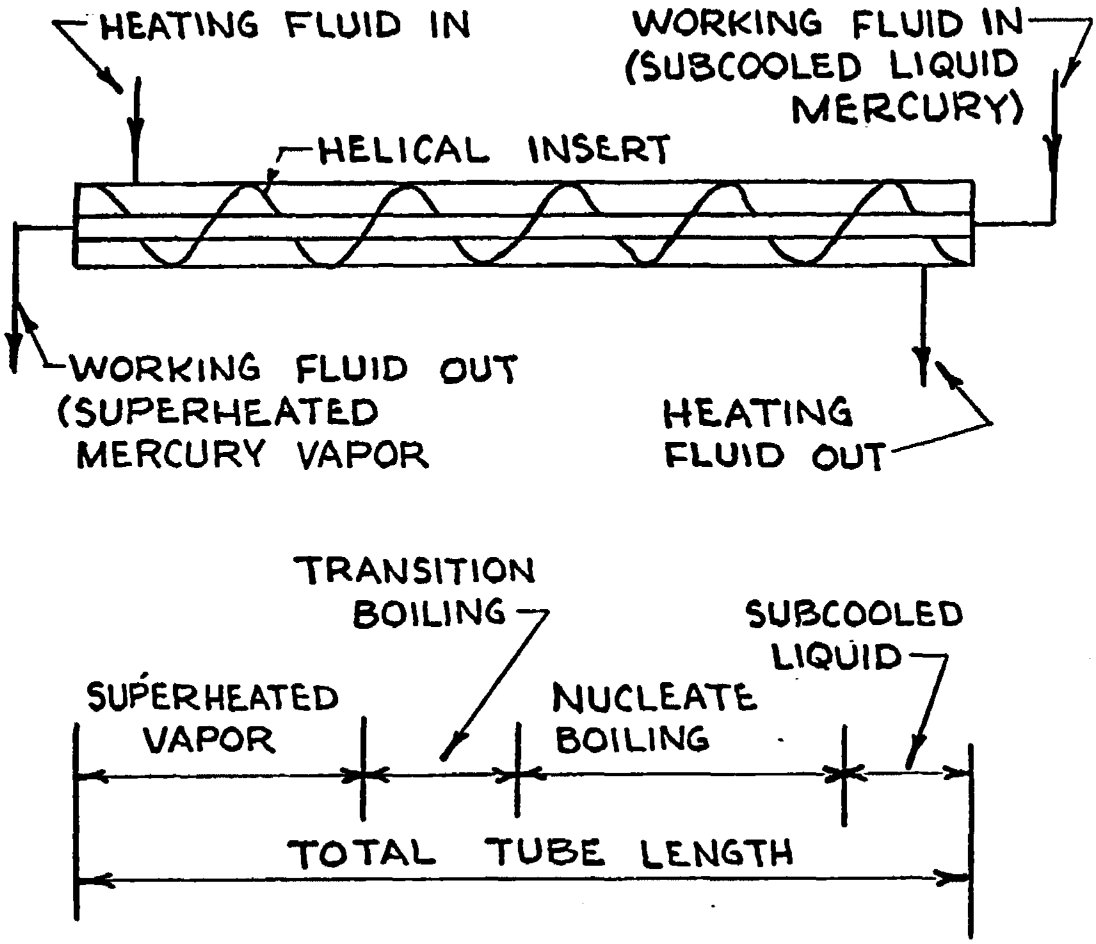

<u>Schematic</u> <u>Illustration</u>
<u>Once</u> - <u>Through</u> <u>Boiler</u>
Figure 7.3a

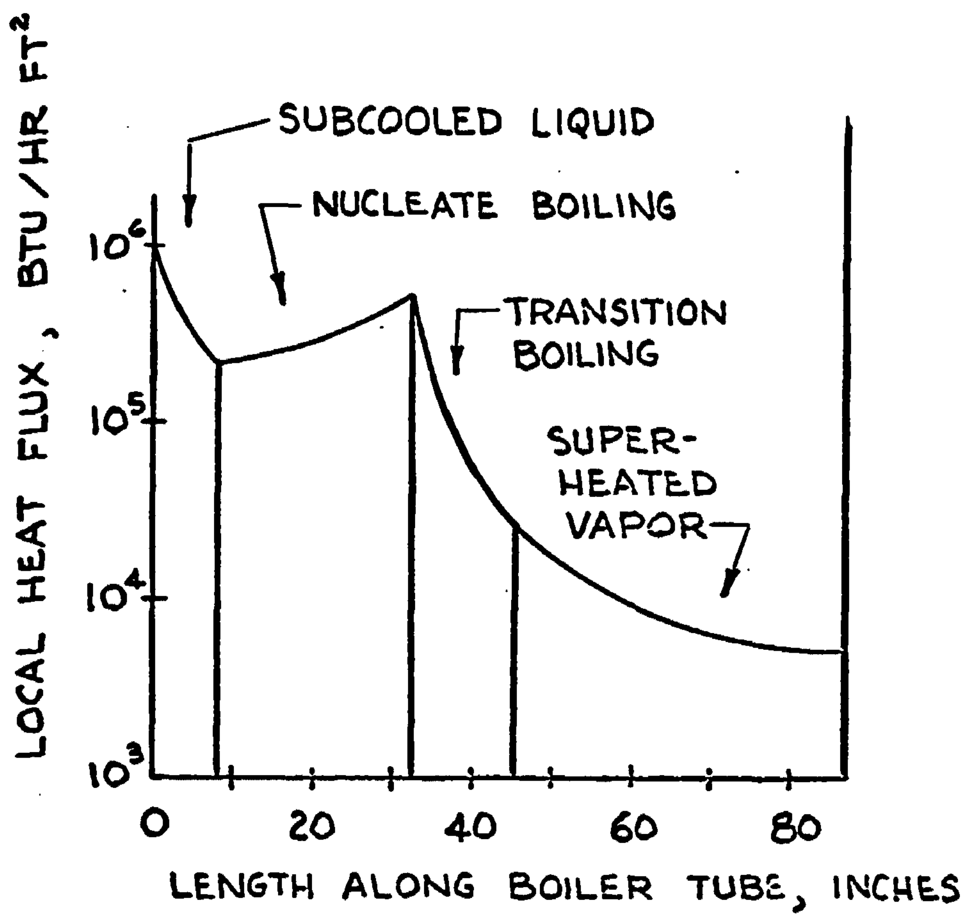

Typical Heat Flux Distribution in a Liquid-Heated, Counter-Flow Boiler Tube

(FROM REFERENCE 24, FOR POTASSIUM)

Figure 7.3 b

3. A two fluid system with the heat source indirectly cooled, figure 7.4 and,
4. Use two separate heat source components, one for the evaporating section and one for the superheating section, figure 7.5.

The fourth alternative is chosen primarily because of simplicity in the application of design principles. Increased development and test time is anticipated to evolve satisfactory "once-through" boiler design concepts. The two fluid system has the disadvantage of requiring liquid metal-to-liquid metal heat exchangers and thus increased design complexity.

Alternative number 2, a "once-through" boiler design concept is illustrated schematically in figure 7.3. Reference 24 provides thermal design procedures for once-through boilers employing counterflow of two heat exchange fluids. The procedure of reference 24 considers nonuniform axial distribution of heat flux wherein four distinct heat transfer regions are identified: the superheat, transition, nucleate and subcooled regions. The design procedure is based on calculating in sequence the pressure drop and length of the four heat transfer regions. Contained in the reference are results of an experimental test of a single tube once-through mercury boiler.

A major disadvantage of the fourth alternative would be the additional shielding mass required. Even so the next iteration for the heat source design will be based on the concept of utilizing separate heat source components for mercury evaporation and for mercury superheating.

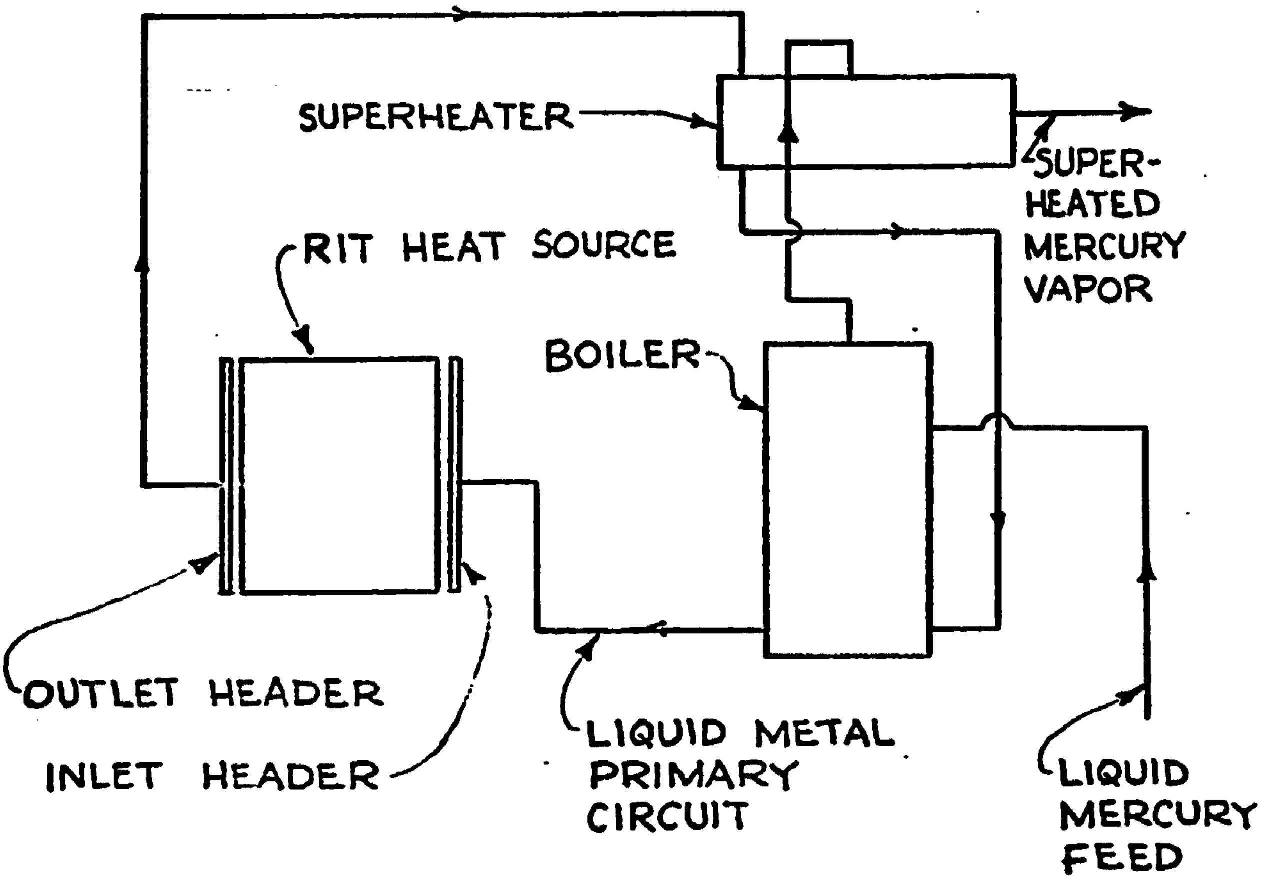

Heat Source Cycle Arrangement
Alternative No. 3

Figure 7-4

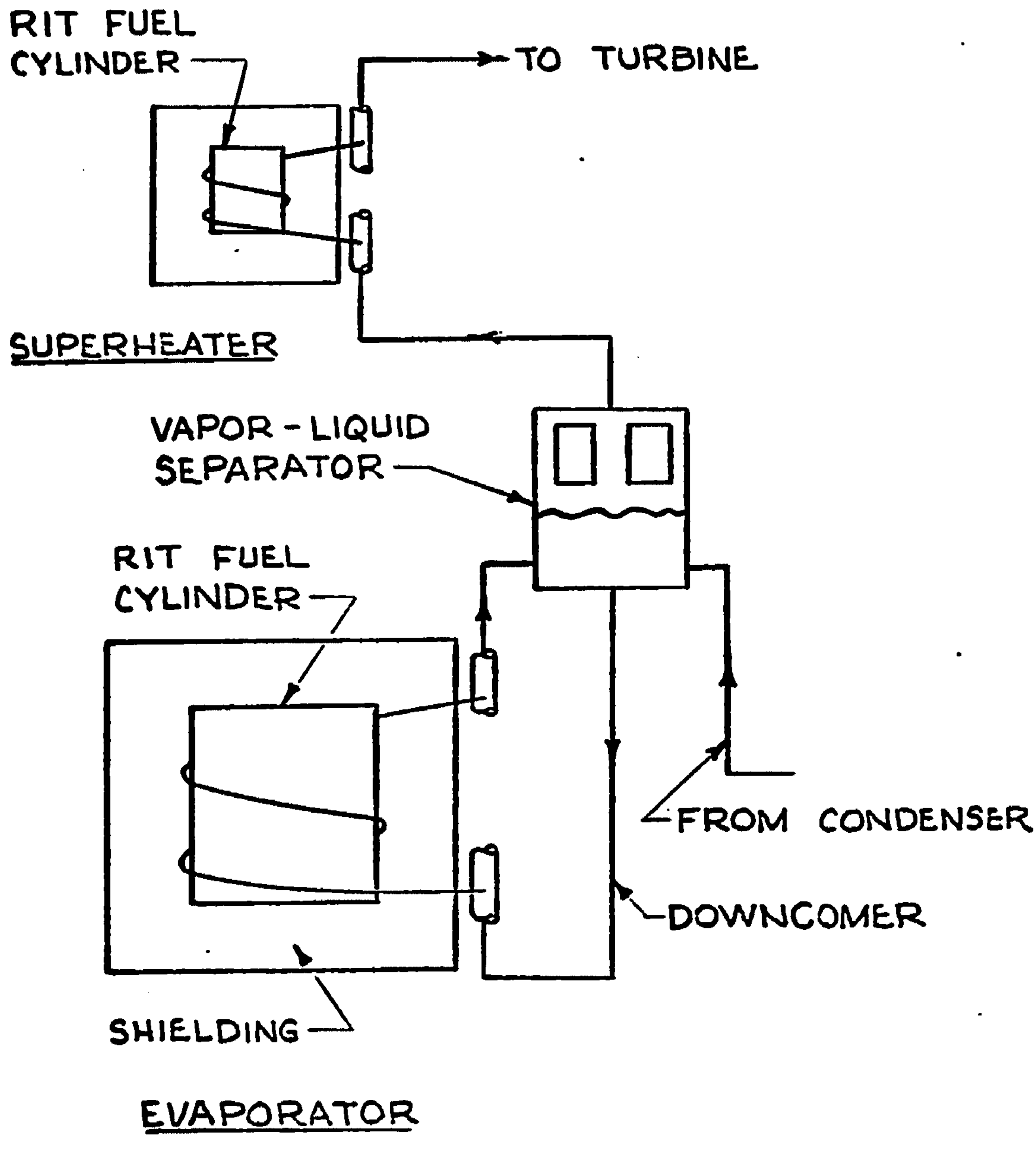

Heat Source - Boiler Design
Alternative No. Four
Figure 7.5

Re-Design of Evaporating Section of Boiler

Revise the design of the fuel strips so that the dimensions are as follows:

Width, inches	0.80
Thickness, inches	0.0625
Length, inches	9.0

For nickel coated strips the dimensions are:

Width, inches	0.84
Thickness, inches	0.1025
Length, inches	9.04

The dimensions of the Co-60 capsules containing two strips per capsule will be taken as

Width, inches	0.88
Thickness, inches	0.245
Length, inches	9.20

Number of Cobalt-60 Capsules

The quantity of fuel capsules required is determined as follows:

$$(2)(0.80)(0.0625)(9.0) = 0.9 \text{ in}^3 \text{ fuel/capsule}$$

$$(0.9 \frac{\text{in}^3}{\text{capsule}})(2.54 \frac{\text{cm}}{\text{in}})^3 = 14.78 \frac{\text{c.c.}}{\text{capsule}}$$

The enthalpy of the saturated mercury vapor at 379.4 psia is 182.25 Btu/lb. The energy required for evaporation is

$$Q_B = (857)(182.3 - 40.2)$$

$$= 121{,}900 \text{ Btu/hr} \qquad (\eta_T = 0.60)$$

The required fuel quantity is given by

$$(\frac{121{,}900}{3.41})(\frac{1 \text{ c.c.}}{27 \text{ watts}}) = 1322 \text{ c.c.}$$

Including an allowance for heat loss and fuel radiation decay the required fuel quantity is therefore

$$\frac{(1322)}{(0.9)(0.875)} = 1680 \text{ c.c.}$$

or

$$N_B = (1680 \text{ c.c.})(1 \text{ capsule}/14.78 \text{ c.c.})$$
$$= 114 \text{ capsules}$$

Evaporator Heat Source Dimensions

If the heat source is designed to be two capsules in height, (i.e., 18.4 inches), the diameter of the fuel ring is then given by

$$(57 \text{ capsules})(0.88 \frac{\text{in.}}{\text{capsule}}) = 50.2 \text{ in.}$$

$$D = \frac{50.2}{\pi} = 16.0 \text{ inches}$$

Superheater Heat Source

The energy transfer rate for the superheater is

$$Q_{S.H.} = \dot{m} \, (\Delta h)$$
$$= (857)(186.9 - 182.3)$$
$$= 3940 \text{ Btu/hr.}$$

Allowing for a 10 per cent heat loss to the surroundings and for the exponential decay of the radioisotope the superheater energy source must provide

$$Q_{S.H.} = \frac{3940}{(0.9)(0.875)}$$
$$= 5000 \text{ Btu/hr}$$

The number of capsules required is therefore (one strip per capsule)

$$N_{S.H.} = (5000 \frac{\text{Btu}}{\text{hr}})(\frac{\text{watt-hr}}{3.41 \text{ Btu}})(\frac{1 \text{ c.c.}}{27 \text{ watts}})(\frac{\text{capsule}}{7.39 \text{ c.c.}})$$

$= 7.36$ capsules

or, say, 8 capsules. The diameter of the capsule ring is

$$D = (8)(0.88)/\pi$$

$$= 2.24 \text{ in.}$$

Heat Transfer-Superheater

The heat transfer coefficient for the superheated mercury vapor will be determined by the following equation, (Chapter 7, reference 17):

$$\frac{h_c L}{k_f} = 0.13 \left[\frac{L^3 \rho_f^2 g \beta_f \Delta t}{\mu_f^2} \quad \frac{c_p \mu}{k}_f \right]^{1/3}$$

where h_c is the natural convection heat transfer coefficient and L is the height of the vertical surface.

Since the physical properties of mercury vapor are not available for the temperatures of interest use the properties of carbon dioxide. At $1500^{\circ}F$

$$\mu = 0.103 \ lb_M/ft\ hr$$

$$k = 0.0420 \ Btu/hr\ ft\ ^{\circ}F$$

$$\rho = 0.0308 \ lb_M/ft^3$$

$$c_p = 0.289 \ Btu/lb_m\ ^{\circ}F$$

$$v = 0.0308 \ lb_M/ft^3$$

The volumetric expansion coefficient is given by

$$\beta \equiv \frac{1}{v} \left(\frac{\partial v}{\partial T}\right)_P .$$

For carbon dioxide at $1500\ ^{\circ}F$ and at 360 psia

$$\beta = \frac{1}{1.329} \left(\frac{1.397 - 1.261}{1600 - 1400}\right)$$

$$\beta = 0.000511\ ^{\circ}F^{-1}$$

Let $L = 9$ inches or 0.75 feet. Also take $\Delta t = 50\ ^{o}F$. The density of carbon dioxide at 1500 ^{o}F is equal to

$$\rho = \frac{1}{v} = \frac{1}{0.0308} = 32.4\ \frac{ft^3}{lb_m}$$

Thus

$$h_c = \frac{0.0420}{0.75}\ (0.13)\ \left[\frac{(0.75)^3(32.4)^2(32.2)(4.17)(10)^8(5.11)(50)}{(10)^4(0.103)^2}\right.$$

$$\left. \times\ \frac{(0.0298)(0.103)}{(0.042)}\right]^{1/3}$$

$$h_c = 154\ \frac{Btu}{hr\ ft^2\ ^{o}F}$$

McAdams, (Chapter 1 of reference 17), gives the approximate range of values of h_m for superheating steam as 5 to 20 Btu/hr $ft^2\ ^{o}F$. A conservative value of 15 Btu/hr ft^2 F will be chosen for the natural convection coefficient of superheated mercury.

Assume the superheater pipe coil to be 12 inches across and to consist of thirteen coils of nominal 3/8 inch schedule 80 pipe. The internal surface area is 0.1108 ft^2/ft of pipe. The total superheater tube surface area required is

$$A_{S.H.} = \pi\ D(\text{No. of turns})\ (\frac{A_i}{ft})$$

$$= \pi\ (\frac{12}{12})\ (13)\ (0.1108)$$

$$= 4.52\ ft^2$$

The required temperature difference between the tube wall surface and the mercury vapor is given by

$$\Delta t = \frac{Q_{S.H.}}{h_i\ A_i}$$

$$= \frac{3940}{(15)(4.52)}$$

$$= 58^{o}F$$

Superheater Pressure Loss Calculation

The pressure drop for the superheated mercury may be determined from the following:

$$\Delta P = f \frac{L}{D_e} \frac{\rho V^2}{2g_c}$$

where f is the Darcy-Weisbach friction factor and

$$g_c = 4.17 \times 10^8 \ lb_m \ ft/lb_f \ hr^2.$$

The friction factor, f, may be given by, (reference 17, Chapter 6):

$$f = \frac{0.184}{\left(\frac{D_e V \rho}{\mu}\right)^{0.2}}$$

The average mercury vapor density is

$$\rho = \frac{1}{\frac{v_i + v_f}{2}} = \frac{1}{\frac{0.2258 + 0.2540}{2}}$$

$$\rho = 4.17 \ lb/ft^3$$

The flow velocity is given by

$$V = \frac{\dot{m} \ v}{A_i}$$

$$V = \frac{(857)(0.2399)}{0.0009}$$

$$V = 228{,}000 \ ft/hr$$

Also

$$D_e = 0.423/12 = 0.0352 \ ft.$$

$$\mu = 3.320 \times 10^{-5} \ \frac{lb_m}{ft \ sec}$$

or

$$\mu = 0.1195 \frac{lb_m}{ft\ hr} .$$

Therefore

$$f = \frac{0.184}{\left[\frac{(0.0352)(228000)(4.17)}{(0.1195)}\right]^{0.2}}$$

$$f = 0.015$$

and

$$\Delta P = (0.015)\frac{(40.8)}{(0.0352)} \frac{(4.17)(2.28)^2(10^5)^2}{(2)(4.17)(10^8)}$$

$$\Delta P = 4530 \text{ psf or } 31.5 \text{ psi.}$$

If the tube length is halved (by providing two parallel tube circuits) the superheater pressure drop becomes approximately 4 psi. This magnitude of pressure drop is assumed to be satisfactory for conceptual design purposes.

Evaporator Flow Calculations and Pressure Drop

Flow and pressure loss calculations are included in the appendix. The analysis indicates that an acceptable flow condition results under the following conditions:

Recirculation Ratio	9 lb liquid/lb vapor
Evaporating Tube Entering Velocity	1.4 ft/sec
Entering Temperature	1542 ^{o}R
No. of Degrees of Subcooling	60.3
No. of Tube Circuits	18
Evaporating Tube Pressure Loss	7 psi
Evaporating Tube Size	1/8", Sch 80

Heat Source Temperature Analysis

Assuming A Flat Slab Model

The derivation for the case wherein the cylindrical shield is assumed to be adequately modeled by a flat slab is based on the schematic illustration of figure 7.6.

The heat energy entering an infinitesimal thickness dx is given by

$$q_x = - k\ A\ dt/dx$$

and that leaving is given by

$$Q_{x+dx} = q_x + (dq_x/dx)dx = -k\ A\ dt/dx - k\ A(d^2t/dx^2)dx$$

The heat generated in dx is thus

$$dq_x = q_{x+dx} - q_x = - k\ A(d^2t/dx^2)dx$$

Also

$$dq_x = q'''\ A\ dx$$

Therefore

$$-k\ A(d^2t/dx^2)dx = q'''\ A\ dx$$

or

$$d^2t/dx^2 = - q'''/k = - q_1'''e^{-\mu x}/k$$

The heat generation per unit volume due to attenuation of the gamma rays is given by

$$q''' = \mu\ I$$
$$= \mu\ I_1\ e^{-\mu x}$$

where μ is the gamma ray attenuation coefficient and I is the intensity of the gamma radiation. Thus the temperature differential equation may be written

$$d^2t/dx^2 = - \mu\ I_1\ e^{-\mu x}/k$$

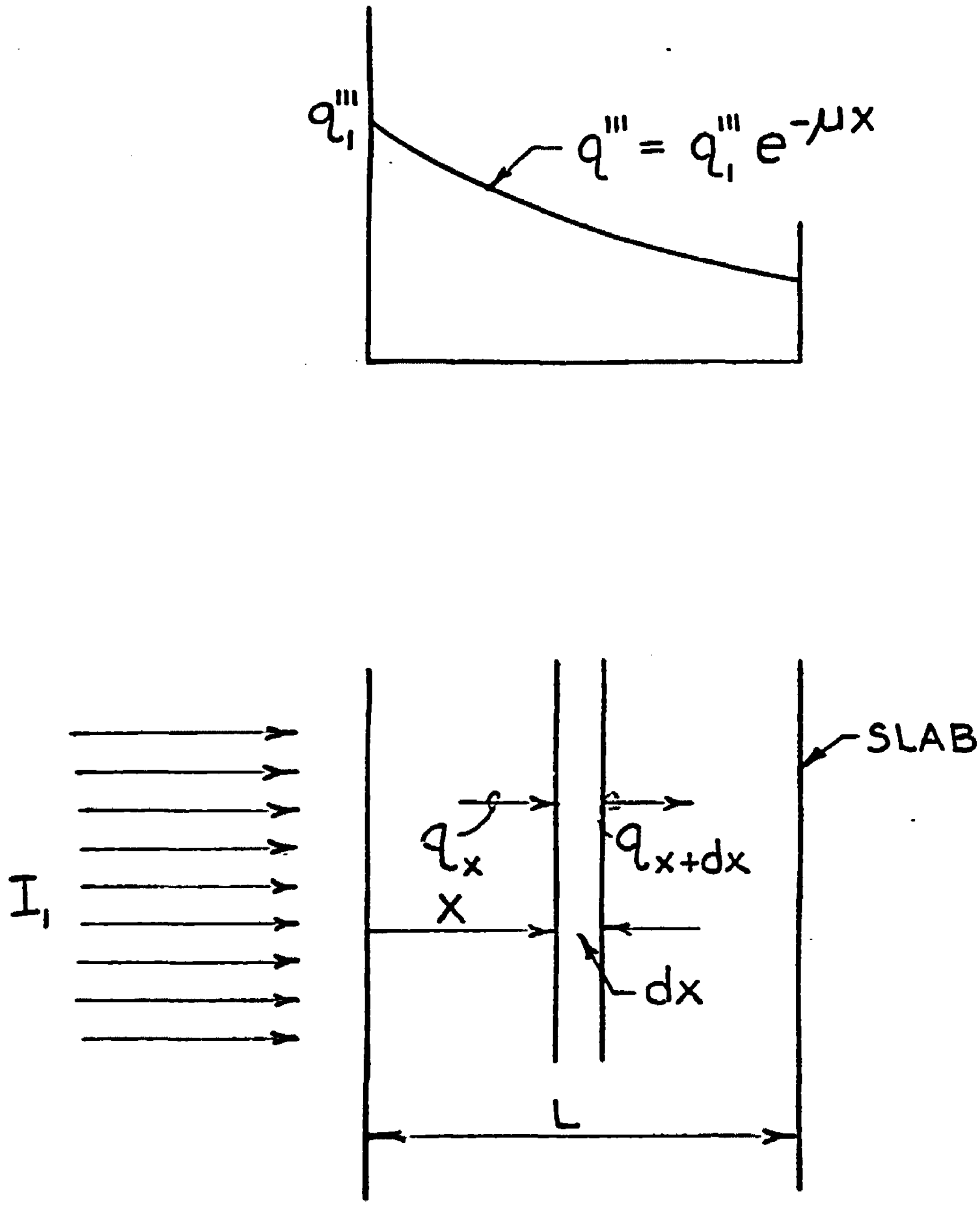

Flat Slab Model - Temperature Analysis
Figure 7.6

Integrating once we obtain

$$dt/dx = I_1 \, e^{-\mu x}/k + C_1$$

A second integration results in

$$t = - I_1 \, e^{-\mu x}/\mu k + C_1 \, x + C_2$$

where C_1 and C_2 are constants of integration. Appropriate boundary conditions are

$$dt/dx = 0 \text{ at } x = 0$$

$$t = t_M \quad \text{at } x = L$$

Using the first boundary condition results in

$$C_1 = - I_1/k$$

Substituting the solution into the second boundary condition gives

$$t_M = - I_1 \, e^{-\mu L}/\mu - I_1 L/k + C_2$$

or

$$C_2 = t_M + I_1 \, (e^{-\mu L}/\mu + L/k)$$

Thus the solution may be written

$$t - t_M = \frac{I_1}{k}(L - x + \frac{e^{-\mu L}}{\mu} - \frac{e^{-\mu x}}{\mu})$$

If tungsten is chosen as the shield material the thermal conductivity for the temperature level of interest here is approximately

$$k = 65.1 \text{ Btu/hr ft } ^{o}F$$

Values for the ratio μ/ρ, (where ρ is the density), for tungsten are as follows:

Photon Strength, Mev	μ/ρ, cm^2/gm
0.5	0.1310
1	0.0655
2	0.0432
3	0.0400
6	0.0418

The predominant gamma radiation for the cobalt-60 radioisotope consists of an equal number of 1.33 and 1.17 Mev photons. This select μ/ρ equal to 0.05. The density of tungsten is 19.3 gm/cm^3 or 1170 lb/ft^3. Therefore

$$\begin{aligned} \mu &= (\mu/\rho)(\rho) \\ &= (0.05)(19.3) \\ &= 0.965 \text{ cm}^{-1} \\ &= 29.4 \text{ ft}^{-1} \end{aligned}$$

The surface area of the inner surface of the radiation shield is approximately

$$\begin{aligned} A &= \pi D L \\ &= (\pi)(16/12)(18.4/12) \\ &= 6.42 \text{ ft}^2 \end{aligned}$$

If the self-attenuation of the fuel is neglected the intensity of the energy flux at the inner surface is given by

$$I_1 = \frac{(125700)(1.1)}{(9.857)(6.42)} = 24600 \frac{\text{Btu}}{\text{hr ft}^2}$$

The energy flux at the outer surface of the shield is

$$\begin{aligned} q_{x=L} &= - k A \frac{dt}{dx}\bigg|_{x=L} \\ &= - A I_1 (e^{-\mu L} - 1) \end{aligned}$$

$$= -(6.42)(24600)\left[e^{-(29.4)(0.333)} - 1\right]$$

$$\approx 158{,}000 \text{ Btu/hr}$$

if the shield thickness is taken to be four inches. This result indicates that virtually all of the gamma radiation is attenuated by four inches of tungsten shielding and converted to thermal energy.

The temperature drop across the shield is given by

$$(t-t_M)_{x=0} = \frac{I_1}{k}\left[L + \frac{e^{-\mu L}}{\mu} - \frac{1}{\mu}\right]$$

$$= \frac{24600}{65.1}\left[0.333 + \frac{0.000055}{29.4} - \frac{1}{29.4}\right]$$

$$= 113^{\circ}\text{F}$$

This is the value of the temperature drop across the tungsten which serves as both radiation shield and thermal conductor.

The total heat flow to the outer surface must be equal to the total heat generated in the slab, which is given by

$$q_g = \int_0^L q''' \, A \, dx = \int_0^L \mu \, I_1 \, A \, e^{-\mu x} \, dx$$

$$= I_1 A \left(1 - e^{-\mu L}\right) \equiv q_{x=L}$$

or

$$q_g = 158{,}000 \text{ Btu/hr}$$

An alternate thermal conductor-radiation conductor would be lead or depleted uranium.

Thermal Analysis for Lead

The pertinent properties for lead are

$\rho = 11.34 \text{ gm/cm}^3 = 708.4 \text{ lb/ft}^3$.

$k = 17.2 \text{ Btu/ft hr }^{\circ}\text{F}$

$$\mu = 0.468 \text{ cm}^{-1} = 14.29 \text{ ft}^{-1}$$

The temperature drop for a 4 inch thick lead shield would be

$$(t - t_M)_{x=0} = \frac{I_1}{k}\left[L - x + \frac{e^{-\mu L}}{\mu} - \frac{e^{-\mu x}}{\mu}\right]$$

$$= 377^{\circ}\text{F}$$

This relatively high temperature drop across the lead shield would produce a high fuel temperature. The gamma radiation absorbed by the lead is

$$q_g = A\, I_1\, (1 - e^{-\mu L})$$

$$= 156{,}900 \text{ Btu/hr.}$$

Thus approximately 1,100 Btu/hr of the gamma ray energy would escape the lead shield.

Values for uranium would be roughly the same as for lead.

The tungsten material is therefore the better material for the combined function of gamma ray attenuation and thermal energy conduction. However, tungsten is expensive: tungsten fabricated as rolled sheet costs approximately 25 dollars per pound. Tungsten powder of 99+ per cent purity costs \$3.80 per pound. (Reference 4).

Heat Source Temperature Analysis-Cylindrical Model

A more accurate approximation to the solution of the problem of obtaining the temperature distribution in the heat source component may be obtained by considering only the tungsten shield and by assuming one-dimensional, steady-state, radial heat flow. Figure 7.7 shows the radius notation used in the following derivations.

The heat conducted at the surface at radius r is given by

$$q_r = - k\, A \frac{dt}{dr}$$

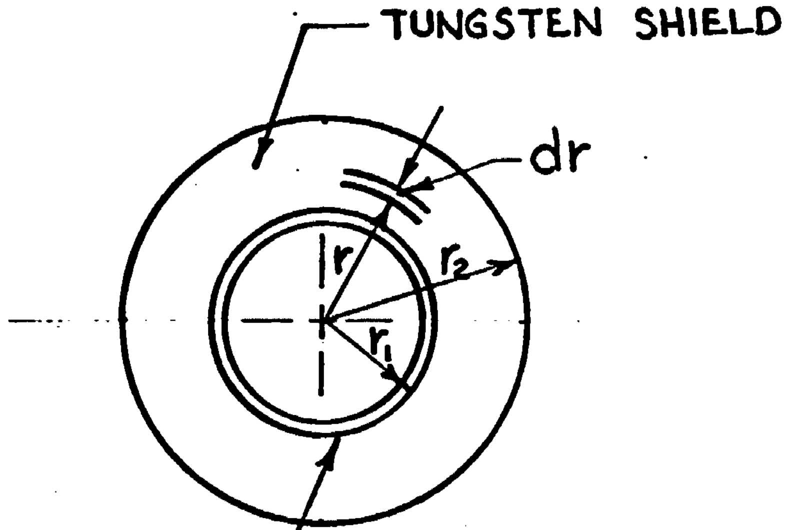

Cross Section, Cylindrical Heat Flow Model
Figure 7.7

The heat conducted out of the volume element at the surface r + dr is

$$q_{r + dr} = q_r + (\frac{dq_r}{dr})\, dr$$

$$= -k2\pi r\, L\, \frac{dt}{dr} + (-2k\pi r\, L\, \frac{dt^2}{dr^2} - 2k\pi\, L\, \frac{dt}{dr})dr$$

Since the thermal energy leaving the volume element minus the energy conducted into the volume element is equal to the energy generated within the element we may write

$$q_{r + dr} - q_r = q''' \, A\, dr$$

where

$$A = 2\pi r L.$$

The gamma ray flux at the inner surface of the volume element may be given by

$$I = \frac{r_1}{r}\, I_1\, e^{-\mu(r - r_1)}$$

where I_1 is the gamma ray intensity at the inner surface of the shield, located at $r = r_1$. The attenuation of the gamma rays per unit volume of the shield is given by

$$q''' = -\lim_{\Delta r \to 0} \frac{A(\frac{r_1}{r})I_1 e^{-\mu(r-r_1)}\Big|_{r+\Delta r} - A(\frac{r_1}{r})I_1 e^{-\mu(r-r_1)}\Big|_r}{A\Delta r}$$

$$= -\lim_{\Delta r \to 0} \frac{2\pi r\, (\frac{r_1}{r})I_1 e^{-\mu(r-r_1)}\Big|_{r+\Delta r} - 2\pi r(\frac{r_1}{r})I_1 e^{-\mu(r-r_1)}\Big|_r}{2\pi r\Delta r}$$

$$= -\left[\frac{1}{r}\frac{d}{dr}\, (r\cdot\frac{r_1}{r}\, I_1 e^{-\mu(r-r_1)})\right]$$

$$q''' = +\mu\, \frac{r_1}{r}\, I_1 e^{-\mu(r-r_1)}$$

Thus

$$(-2k\pi rL \frac{d^2t}{dr^2} - 2k\pi L \frac{dt}{dr})dr$$

$$= + \frac{\mu r_1 I_1}{r} e^{-\mu(r-r_1)} dr \cdot 2\pi rL$$

or

$$r \frac{d^2t}{dr^2} + \frac{dt}{dr} + \frac{\mu r_1 I_1}{k} e^{-\mu(r-r_1)} = 0$$

The latter equation may also be written as

$$\frac{d}{dt} (r \frac{dt}{dr}) = - \frac{\mu r_1 I_1 e^{-\mu(r-r_1)}}{k}$$

With the boundary conditions taken to be

$$\frac{dt}{dr} = 0 \text{ at } r = r_1$$

$$t = t_M \text{ at } r = r_2$$

Integrating the differential equation once we get

$$r \frac{dt}{dr} = \frac{r_1 I_1}{k} \int_0^r e^{-\mu(r-r_1)} (- \mu dr) + A_1$$

$$= \frac{r_1 I_1}{k} (e^{-\mu(r-r_1)}) + A_1$$

and

$$\frac{dt}{dr} = \frac{r_1 I_1}{rk} e^{-\mu(r-r_1)} + \frac{A_1}{r}$$

Substituting this equation into the boundary condition

$$\left.\frac{dt}{dr}\right|_{r=r_1} = 0$$

we get

$$A_1 = - \frac{r_1 I_1}{k} .$$

Therefore

$$\frac{dt}{dr} = \frac{r_1 I_1 e^{-\mu(r-r_1)}}{rk} - \frac{r_1 I_1}{rk}$$

Integrating again results in

$$t = \frac{r_1 I_1}{k}\left\{e^{\mu r_1}\int_0^r \frac{e^{-\mu r}}{r}\,dr - \ln r\right\} + A_2 \qquad (1)$$

Using as a boundary condition

$$t = t_M \text{ at } r = r_2$$

we get

$$t_M = \frac{r_1 I_1}{k}\left\{e^{\mu r_1}\int_0^{r_2} \frac{e^{-\mu r}}{r}\,dr - \ln r_2\right\} + A_2 \qquad (2)$$

Substract equation (1) from equation (2)

$$t_M - t = \frac{r_1 I_1}{k}\, e^{\mu r_1}\left[\int_0^{r_2} \frac{e^{-\mu r}}{r}\,dr - \int_0^{r} \frac{e^{-\mu r}}{r}\,dr\right] + \frac{r_1 I_1}{k}\left(\ln \frac{r}{r_2}\right)$$

or

$$t_M - t = \frac{r_1 I_1}{k}\, e^{\mu r_1}\left[\int_0^{r_2} \frac{e^{-\mu r}}{r}\,dr\right] + \frac{r_1 I_1}{k}\ln \frac{r}{r_2}$$

In order to use the exponential integral graphs in reference 22

let $x = \mu r$

then $dx = \mu dr$

so that

$$\int_r^{r_2} \frac{e^{-\mu r}}{r}\,dr \equiv \int_{\mu r}^{\mu r_2} \frac{e^{-x}}{x}\,dx$$

Also

$$\int_{\mu r}^{\mu r_2} \frac{e^{-x}}{x}\,dx = \int_{\mu r}^{\infty} \frac{e^{-x}}{x}\,dx - \int_{\mu r_2}^{\infty} \frac{e^{-x}}{x}\,dx$$

Therefore

$$t_M - t = \frac{r_1 I_1}{k} e^{\mu r_1} \left[\int_{\mu r}^{\infty} \frac{e^{-x}}{x} dx - \int_{\mu r_2}^{\infty} \frac{e^{-x}}{x} dx \right] + \frac{r_1 I_1}{k} \ln \frac{r}{r_2}$$

The temperature drop across the tungsten shield is therefore given by

$$t_1 - t_M = - \frac{r_1 I_1}{k} e^{\mu r_1} \left[\int_{\mu r_1}^{\infty} \frac{e^{-x}}{x} dx - \int_{\mu r_2}^{\infty} \frac{e^{-x}}{x} dx \right] + \frac{r_1 I_1}{k} \ln \frac{r_2}{r}$$

For

$$r_1 = 0.625, \quad \mu r_1 = 18.39$$

$$r_2 = 0.959, \quad \mu r_2 = 28.2$$

The exponential integral graph on page 377 of reference 22 provides the value

$$\int_{18.39}^{\infty} \frac{e^{-x}}{x} dx = (5.4)(10^{-10})$$

and the graph on page 379 of the same reference shows

$$\int_{28.2}^{\infty} \frac{e^{-x}}{x} dx = (1.9)(10^{-14})$$

Thus for tungsten, (μ = 29.4), and for I_1 = 24,600 Btu/hr ft^2

$$t_1 - t_M = - \frac{(0.625)(24600)}{65.1} e^{(29.4)(0.625)} \left[(5.4)(10^{-10}) - (1.9)(10^{-14}) \right]$$

$$+ \frac{(0.625)(24600)}{65.1} \ln \frac{0.959}{0.625}$$

or

$$t_1 - t_M = 100.5 - 12.7 = 87.8^{\circ}F$$

This result neglects the build-up factor associated with gamma ray attenuation. Values of the temperature at various radius positions are shown in the following table.

Radius Position	Δt	$\Delta t/\Delta t_{max}$
r_1	87.8	1.00
r_1 + 1"	70.2	0.80
r_1 + 2"	45.1	0.514
r_1 + 3"	21.4	0.244
r_1 + 4"	0.0	0.0

Other calculational methods which provide estimates of the temperature drop across the radiation shield are included in the appendix. The results of the various assumed calculational models are summarized in the following section.

Comparison of Values for the Temperature Drop Across the Tungsten Shield

The values obtained for the temperature drop across the tungsten shield by means of the various models used above are summarized as follows:

	Assumed heat transfer model	Δt, ^oF
1.	One dimensional, cylindrical, heat generation in the shield	87.8
2.	Same as 1 except use $(r_1/r)^{20}$ in place of $e^{-\mu(r-r_1)}$	85.4
3.	One dimensional, cylindrical, all energy incident as thermal energy on the inside surface of the shield	102
4.	One dimensional flat slab, heat generation in the shield	113

Therefore, comparing the above values, it is determined that conservative values for the temperatures in the heat source will be obtained if the temperature analysis is based on one dimensional, flat slab, heat transfer configurations. The "detailed analysis" contained in the appendix is based on a one dimensional flat slab model. This analysis provides the following values for the temperature drops across the various materials:

Material	Δt, °F
Fuel	0.8
Fuel Cladding	0.3
Capsule Wall	3.6
Shielding	113.0
Pipe Wall	10.1
Δt total	127.8°F

Comparing the value of the temperature drop for the one dimensional cylindrical model with all energy incident as thermal energy on the inside surface of the shield, (102°F), with the more accurate value obtained by accounting for heat generation in the shield, (87.8°F), indicates that useful test results applicable for radioisotope (cobalt-60) fueled heat sources may be obtained from heat source models or prototypes which utilize electric resistance heating as an energy source. Thus the heat source-boiler system may be constructed and tested in normal open facilities. That is, "hot-lab" facilities would not be required for such tests.

The conceptual design proposed for the heat source-boiler component is shown schematically in figure 7.8.

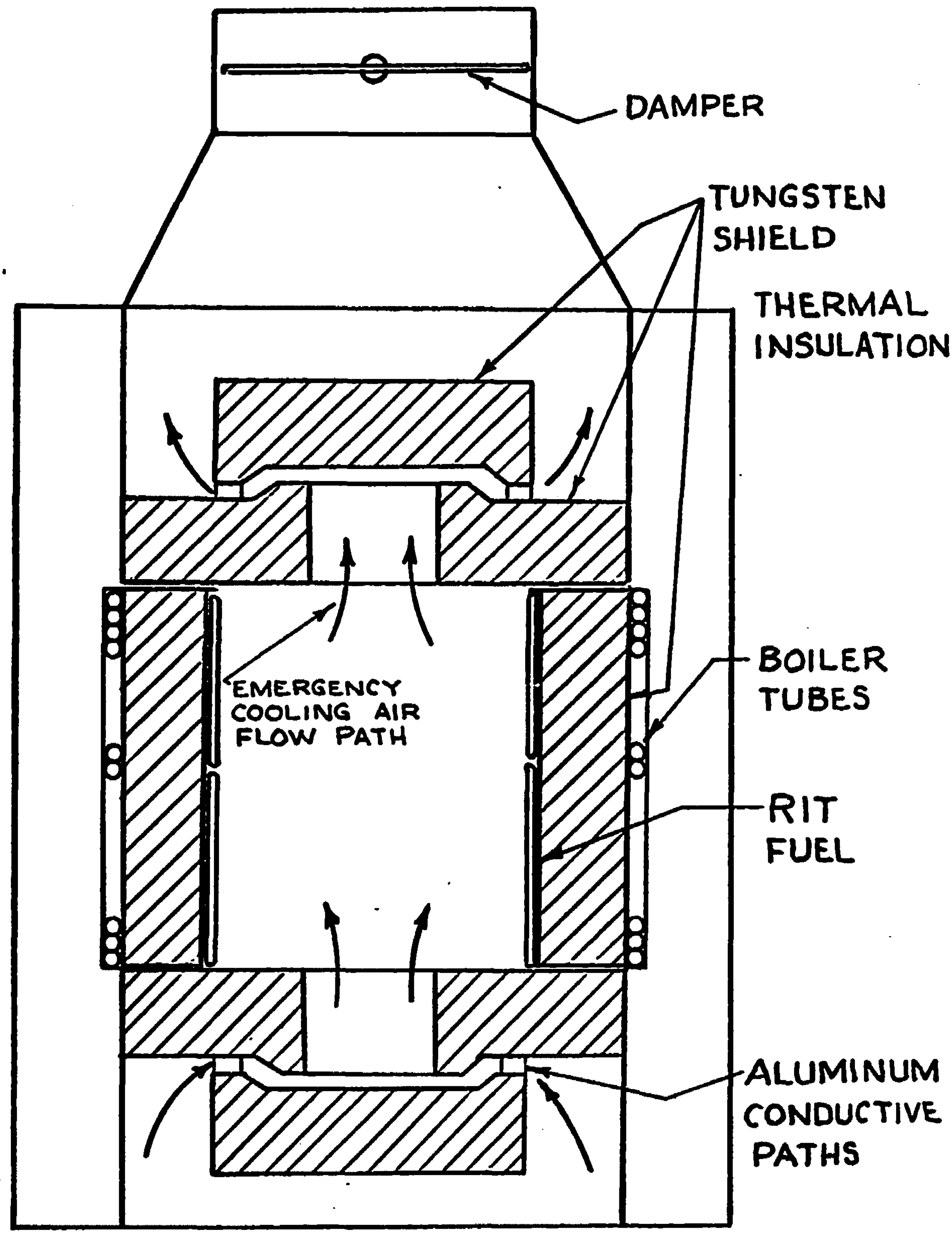

Cross Section of RIT Heat Source - Boiler
Figure 7.8

Estimate of Radioisotope Fuel

Operating Temperature, (Boiler)

The fuel temperature under design operating conditions may be estimated on the basis of the following:

Item	Δt, ^{o}R
Boiling mercury resistance	60.0
Thermal conductive resistances, (Solid Materials)	128.0
*Thermal contact resistance between boiler tubes and shield	200.0
Mercury temperature	1600
Estimated Fuel Temperature	1988^{o}R

The melting point for cobalt-60 metal is 3160^{o}R, reference 27.

*See for example table 9.12, page 414 of reference 23.

CHAPTER VIII

A LATER DESIGN PHASE: PRELIMINARY DESIGN

Introduction

The intent of this chapter is to outline the design work which must be accomplished by the preliminary design phase of a design program. The aim of a preliminary design phase is to optimize the design of the various sub-systems, and then to optimize the performance of the power system by choosing the best values of the system operating parameters. Only then may the proposed power system design concept be compared with other alternative systems. (One alternative power system which appears to have equal merit to the design concept herein proposed is a system which uses steam as working fluid. A second promising system alternative is one using a once-through boiler and mercury as the working fluid.)

Heat Source-Boiler Component

The preliminary design phase must determine the optimum dimensions for the heat source-boiler. This will be largely determined by finding that configuration which results in the minimum acceptable shield mass requirement. By using fewer fuel capsules, that is, by putting more RIT fuel in each capsule, it may be expected that the diameter of the heat source (and thus the mass of shielding) may be decreased. A more detailed comparison of the relative merits of tungsten, lead, and depleted uranium shields is needed. Alternative methods of providing an acceptable thermal bond between the boiler tubes and the radiation shield must be evaluated.

Condenser and Condensate Pump

The mercury pump must be carefully analyzed in order to determine the influence of pump type and physical location of the pump, with respect to the mercury condenser, on the operating characteristics and cavitation tendency of the pump. The pump cavitation limitations will determine the lower permissible limit of the condensing pressure and temperature.

Mercury Turbine

Alternate turbine designs based on various working fluid pressures and temperatures must be compared in order to select the optimum turbine design and best working fluid conditions. Also to be more carefully considered are the relative merits of single disk versus multiple disk turbine designs.

Prototype Power System

After the optimum paper designs for the various sub-systems have been produced the paper designs may be converted into hardware and a prototype system produced. The initial system prototype would utilize electric resistance heating in the heat source. Initial testing would aim to demonstrate compatibility of the various sub-systems in the system. Later system test programs would be designed to verify heat transfer performance of the heat source-boiler and heat source-superheater and also to verify the thermodynamic performance of the cycle in regard to thermal efficiency. Later long-term tests would be required in order to demonstrate system reliability. Finally, testing using the cobalt-60 radioisotope fuel would be required in order to verify the efficacy of the radiation shielding.

Fuel Capsules

The procedures and facilities that will be required for replacing the fuel elements (or the complete heat source component) must be determined. Integrity of the fuel capsules for a suitable period of time in relevant environments must be demonstrated.

Costs

An order-of-magnitude estimate for the design program through the construction and testing of a full-scale prototype, but excluding radioisotope costs, is $1,500,000.

CHAPTER IX

RELIABILITY CONSIDERATIONS

Elementary Theory

"Reliability" is the probability that a device will satisfactorily perform the function for which it was designed for a specified time when operating under specified conditions. Thus reliability is a probability.

The reliability of components which undergo "constant-hazard-rate" failures may be expressed by

$$r = \frac{x}{X} = e^{-t/t_m}$$

where x is the number of units which will still be operating in time t, if X units are in operation having a mean time to failure of t_m.

The "failure rate" is the number of failures per unit time expressed as a percentage of the total number of components involved. Thus

$$F = \frac{1}{N} \lim \frac{\Delta f}{\Delta t} = \frac{1}{N} \frac{df}{dt}$$

where

F = failure rate

f = number of failures

N = population during the time interval dt.

For a system with n components in series, the relationship between system reliability and component reliability may be given by

$$R_{system} = r^n$$

where

n = the number of components in the system operating in series

and

r = the individual component reliability

The reliability of a system may be increased by adding redundant components. Consider the two methods of providing component redundancy illustrated in figures 9.1a and 9.1b.

For the parallel redundant system

$$R = 1 - (1 - r^n)^p .$$

For the series-parallel redundant system

$$R = \left[1 - (1 - r)^p\right]^n .$$

Thus for the same number of components the series-parallel arrangement is more reliable than the parallel arrangement.

Power System Reliability

The power system which is the subject of this design study may be considered as being composed of the following components:

1. Turbine
2. Alternator
3. Power Conditioning Package
4. Turbine-alternator bearings
5. Mercury pump
6. Turbine control system
7. Bearing coolant pump

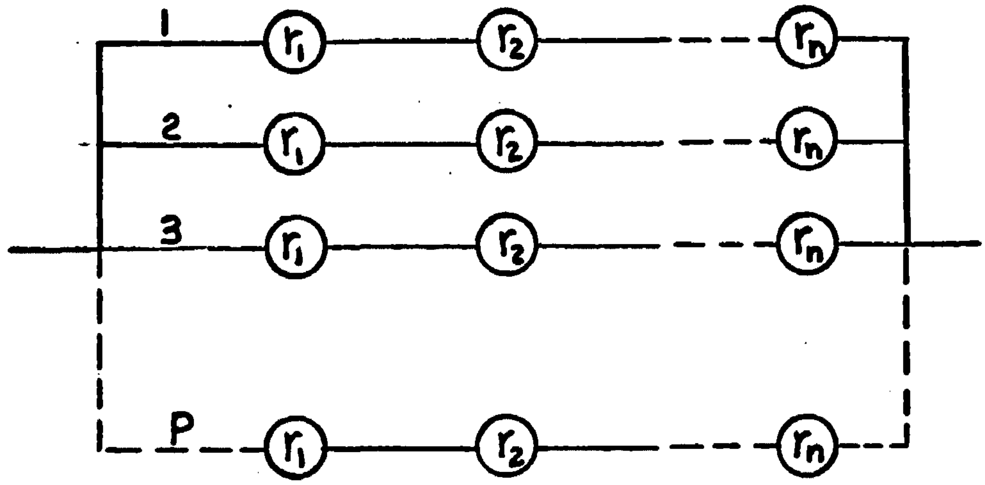

Parallel Redundant System
Figure 9.1 a

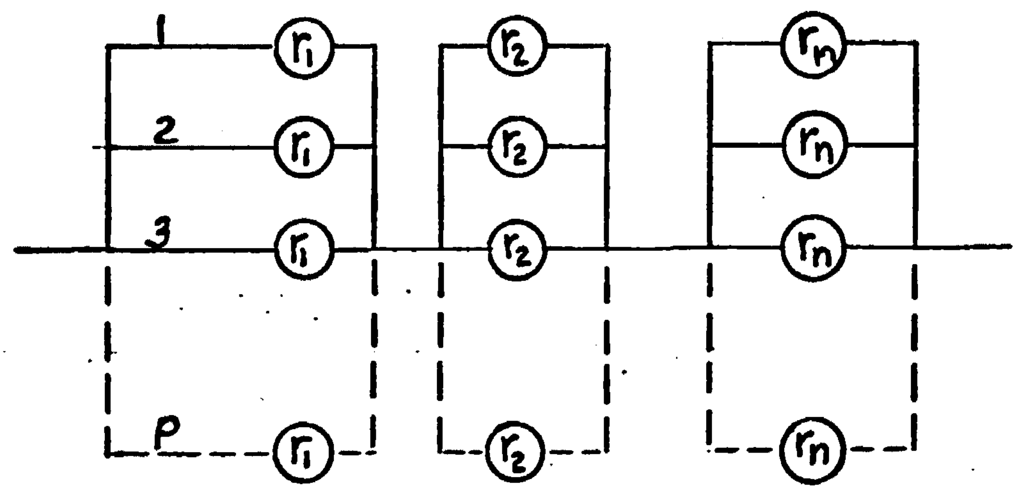

Series - Parallel Redundant System
Figure 9.1 b

(Heat exchangers,condensers, and the heat source system will be considered to be constructed with a very high reliability and thus are excluded from the reliability analysis.)

The power system reliability is given by

$$\begin{aligned} R_{system} &= r^n \\ &= (0.95)^7 \\ &= 0.698 \end{aligned}$$

if each component reliability is 0.95. This estimated value of the system reliability is unacceptably low and component redundancy must be resorted to since efforts to increase component reliability above the assumed 0.95 value would be prohibitively expensive. Due to the nature of the proposed power system (turbine, alternator, bearings integrally arranged) it would be difficult or impossible to use the true series parallel arrangement illustrated above. For the parallel redundant scheme

$$\begin{aligned} R &= 1 - (1 - r^n)^p \\ &= 1 - (1 - 0.95^7)^2 \\ &= 1 - 0.0911 \\ &= 0.9089 \end{aligned}$$

where there is one redundant set of components, $(m = 2)$.

Also, consider the system arrangement shown in figure 9.2. . For the parallel redundant portion of the system

$$\begin{aligned} R_1 &= 1 - \left[1 - r^n\right]^p \\ &= 1 - \left[1 - 0.95^4\right]^2 \\ &= 1 - 0.0346 \end{aligned}$$

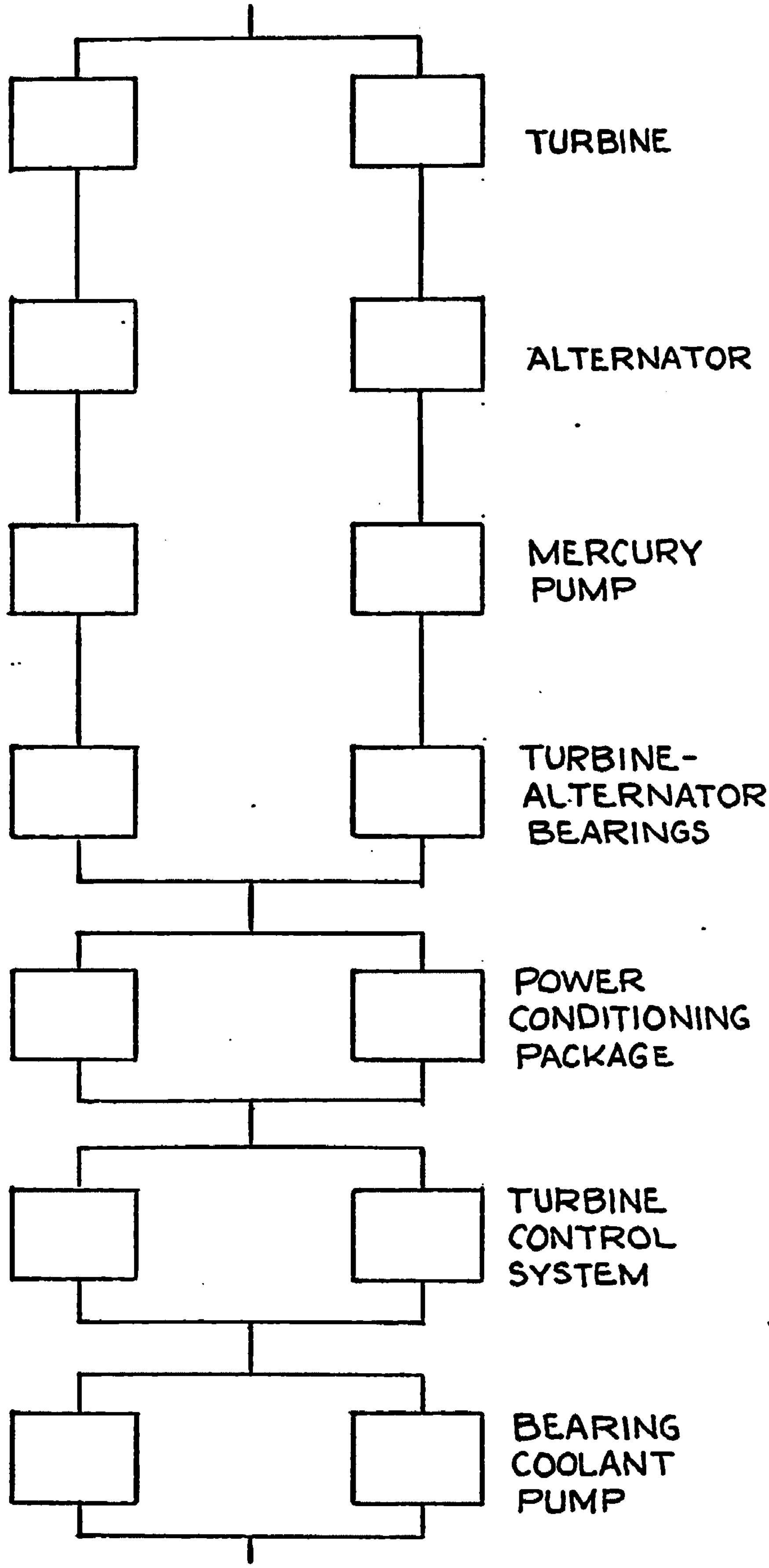

System Arrangement for Redundancy

Figure 9.2

$$= 0.9654$$

For the series-parallel redundant portion of the system

$$R_2 = \left[1 - (1 - r)^p\right]^n$$

$$= \left[1 - (1 - 0.95)^2\right]^3$$

$$= 0.9925$$

Therefore for the system

$$R = R_1 R_2$$

$$= (0.9654)(0.9925)$$

$$R = 0.958$$

Therefore the latter system arrangement is the most desirable one for the design scheme.

Component Reliability

For a component reliability of 0.95 the mean time to failure for the component must be as follows

$$r = e^{-t/t_m}$$

or

$$t_m = -\frac{t}{\ln r}$$

let t = 8760 hours, (one year) then

$$t_m = -\frac{8760}{\ln 0.95} = 171{,}000 \text{ hours.}$$

This represents a very high value for the mean time to failure. A design based on a more reasonable value of t_m would have a higher probability of successful development.

The system reliability estimate for a component reliability of

0.80 would be

$$R_1 = 1 - \left[1 - r^n\right]^p$$

$$= 1 - \left[1 - 0.80^4\right]^2$$

$$= 1 - 0.348$$

$$= 0.652$$

$$R_2 = \left[1 - (1 - r)^p\right]^n$$

$$= \left[1 - (1 - 0.80)^2\right]$$

$$= 0.885$$

$$R = R_1R_2$$

$$= (0.652)(0.885)$$

$$R = 0.577$$

For a component reliability of 0.80 the mean time to failure must be for 8760 hours of operation:

$$t_m = - \frac{t}{\ell n\ r}$$

$$= \frac{8760}{\ell n\ 0.80}$$

$$= 38{,}300 \text{ hours}$$

The component reliability should therefore be at least equal to 0.80. Since the attainment of a very high power system reliability is likely to be very costly it will be more logical to accept a compromise system reliability which when combined with an emergency storage battery system of proper capacity will result in adequate safety of any dependent personnel. For example, for a manned underseas station, the battery system should have capacity to power emergency lighting and the life-support system for a period of time sufficient to permit accomplishment of emergency evacuation.

The reliability of the power system may also be increased by employing the "derating" technique. That is, where otherwise practical component parts may be designed to operate at only partial full-load capacity.

Reference 28 is the basic reference for the material in this chapter.

CHAPTER X

DESIGN CONCEPT SUMMARY

System Description

The system concept proposed by this conceptual design study is a direct, single fluid, Rankine cycle using mercury as the working fluid. Tungsten radiation shields are directly cooled by the mercury evaporator and superheater tubes. The analysis has shown that even though the mercury fluid is handicapped by a high heat rejection temperature the cycle thermodynamic efficiency may still be comparable to that of a power system using water as the working fluid. This results from the fact that the small mercury turbine has a higher adiabatic efficiency than the small steam turbine. The proposed power system is shown schematically in figure 10.1.

Component Description

A partial specification listing for the major system components is contained in this section.

Turbine-Generator

Turbine output	10.71 hp
Working fluid	mercury
Inlet temperature	$1800^{o}R$
Inlet pressure	379.4 psia

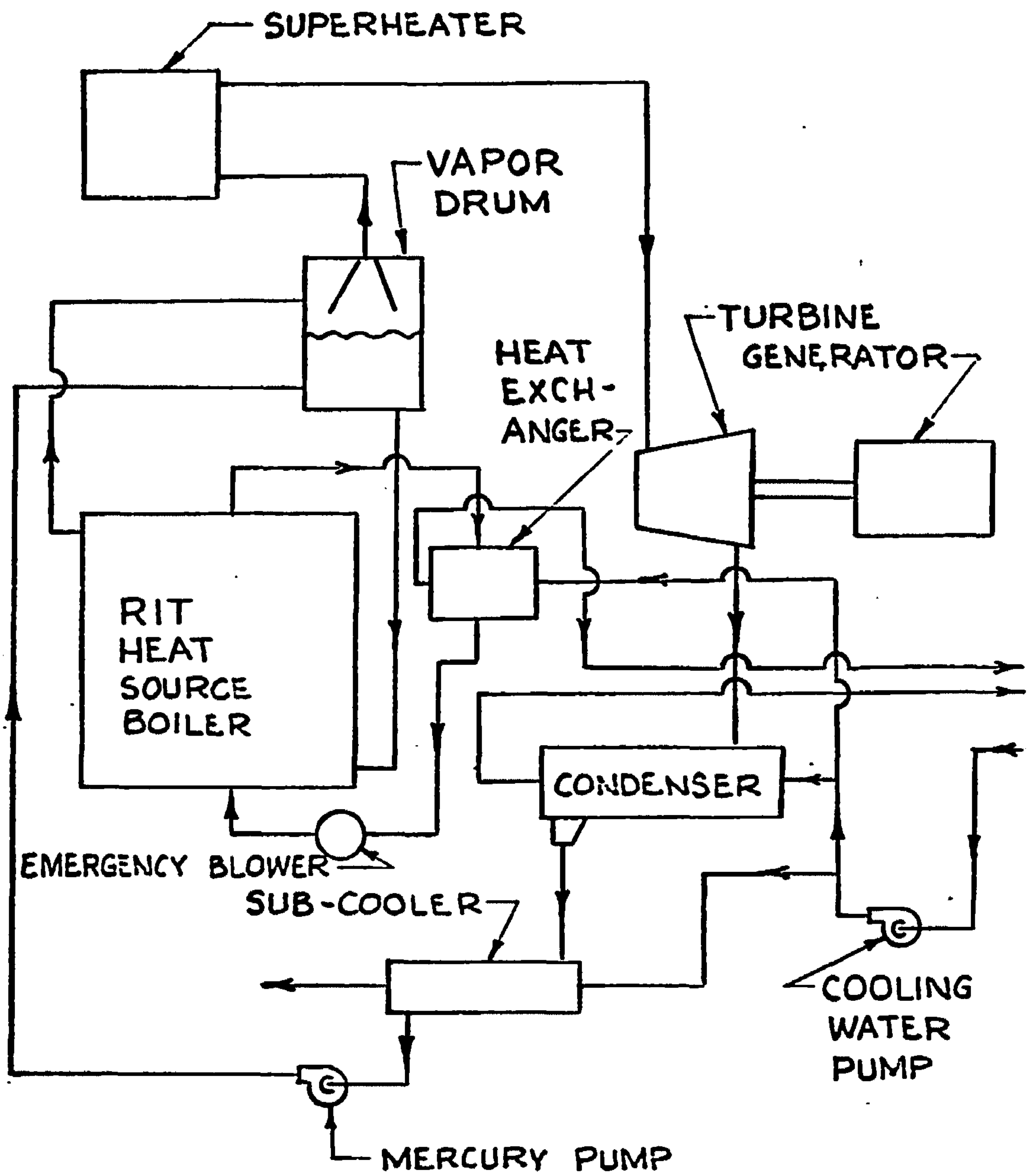

Design Concept
Direct Cycle Power System
Figure 10.1

Exhaust temperature	1000°R
Exhaust pressure	3.23 psia
Turbine adiabatic efficiency	0.77
Turbine type	single disk, multi-stage axial flow
Number of stages	3
Turbine diameter	4.92
Net generator output	5 kw
Turbine-generator speed	24000 rpm

Radioisotope-Fuel

Radioisotope type	Cobalt-60
Power density	27 watts/cc
Number of capsules	114 (boiler) 8 (superheater)
Fuel per capsule	14.78 c.c. (boiler) 7.39 c.c. (superheater)
Half-life of RIT	5.24 years
Fuel form	encapsulated metal strips
Estimated fuel operating temperature, boiler	1988°R

Heat Source-Boiler

Capsule ring dimensions:	
diameter	16 in.
height	18.4 in.
Shield material	tungsten
Shield thickness	4 inches
Boiler tubes	
size	1/8", Sch. 80
No. of tube circuits	18
tube circuit length	12.6 ft.
Heat transferred	121,900 Btu/hr

Heat Source-Superheater

Capsule ring dimensions:	
diameter	2.24 in.
height	9.2 in.
Shield material	tungsten
Shield thickness	4 in.
Superheater tubes	
size	3/8", Sch. 80
no. of tube circuits	2
tube circuit length	20.4 ft.
Heat transferred	5000 Btu/hr

Condenser

Type	shell and tube counter flow
Heat transferred	71800 Btu/hr
Coolant	liquid mercury

Recommendations for Preliminary Design Phase

The next phase of the design study, that of preliminary design, would be expected to optimize the power system concept herein presented. The following recommendations apply to such later design phase:

1. Examine the effect on the cycle efficiency of using a lower mercury pressure with increased degrees of superheat (maintaining the same mercury temperature, 1800°R). (Use of the lower pressure mercury would be expected to improve the quality of the turbine exhaust vapor.)
2. The heat source components should be optimized with respect to size and with respect to mass of tungstem shield required.
3. An alternate concept using "once-through" boiler designs should be fully examined.

4. The possibility of two staged direct cycle systems should be examined. For example, the condenser of a topping mercury cycle would serve as the boiler of a steam cycle. This concept would probably require that the power rating of the power system be increased.

BIBLIOGRAPHY

1. Mackay, D.B., "Secondary Power Systems for Space Vehicles", SAE Transactions, vol. 69, (1961), pp. 331-345.

2. Lyon, R.N., Editor, Liquid Metals Handbook, Atomic Energy Commission, Department of the Navy, Washington, D.C., Second Edition, June, 1952.

3. El-Wakil, M.M., Nuclear Power Engineering, McGraw-Hill Book Company, Inc., N.Y., N.Y.

4. Tipton, C.R., Editor, Reactor Handbook, Volume I, Materials, Interscience Publishers, Inc., New York, Second Edition.

5. Balje, O.E., "A Study on Design Criteria and Matching of Turbomachines: Part A - Similarity Relations and Design Criteria of Turbines", Transactions of the ASME, Journal of Engineering for Power, vol. 84, January, 1962.

6. Lynn, Warren C. and Maurice D. Starr, "Terrestrial Radioisotope Fueled Kilowatt Power Systems", Advances in Energy Conversion Engineering, The American Society of Mechanical Engineers, 1967.

7. Boretz, J.E., "Isotope Dynamic Space Power Systems", Advances in Energy Conversion Engineering, The American Society of Mechanical Engineers, 1967.

8. Robinson, R.A., et al, "Brayton-Cycle Radioisotope Heat Source Design Study Phase I (Conceptual Design) Report", ORNL-TM-1691, August 1967, Oak Ridge National Laboratory, Oak Ridge Tennessee.

9. Gouse, S. William, Jr., "Steam-Powered Automobiles Should Come Back", Engineer, (Engineers Joint Council), May/June, 1968, Vol. IX, No. 3.

10. Westinghouse Electric Corporation, "Concept Design for a Manned Underwater Station", Report Number CR 67.017, March, 1967.

11. General Dynamics Corporation, Electric Boat Division, "Conceptual Study of a Manned Underwater Station", Report Number CR 67.019, April 1967.

12. Hagey, G.L., "Navy Radioisotope Power Programs for Terrestrial and Undersea Applications", Advances in Energy Conversion Engineering, The American Society of Mechanical Engineers, 1967.

13. Angelino, G., "Carbon Dioxide Condensation Cycles for Power Production", Paper No. 68-GT-23, The American Society of Mechanical Engineers, 1968.

14. Feher, Ernest G., "The Supercritical Thermodynamic Power Cycle", Advances in Energy Conversion Engineering, The American Society of Mechanical Engineers, 1967.

15. Sternlicht, B., and J.W. Bjerklie, "Comparison of Dynamic and Static Power Conversion Systems for Undersea Missions", Transactions of the American Society of Mechanical Engineers, Journal of Engineering for Power, Vol. 88, 1966.

16. Jackson, C.B., Editor-in-Chief, Liquid Metals Handbook, Sodium-Na K Supplement, TID 5277, Atomic Energy Commision and Department of the Navy, Washington, D.C.

17. McAdams, W.H., Heat Transmission, McGraw-Hill Book Company, Inc., New York, New York, Third Edition.

18. Martinelli, R.C., and D.B. Nelson, "Prediction of Pressure Drop During Forced-Circulation Boiling of Water", Trans. ASME, Vol. 70, p. 695, 1948.

19. Rich, G.E., "The Selection of Power Systems for Advanced Deep Submersibles", ASME Paper No. 67 WA/UNT-10.

20. Savannah River Laboratory Isotropic Power and Heat Sources, Quarterly Progress Report for October-December, 1966, DP-1094, January 1967.

21. Hodgson, J.N., R.G. Geimer, and A.H. Kreeger, "Snap 8 - A Technical Assessment", Advances in Energy Conversion Engineering, The American Society of Mechanical Engineers, 1967.

22. Rockwell, Theodore, Reactor Shielding Design Manual, D. Van Nostrand Company, Inc., Princeton, New Jersey, First Edition.

23. McLain, Stuart and John H. Martens, Reactor Handbook, Volume IV, Engineering, Interscience Publishers, Inc., New York, Second Edition.

24. Peterson, J.R., R.N. Weltman and M.W. Gutstein, "Thermal Design Procedures for Space Rankine Cycle System Boilers", Intersociety Energy Conversion Engineering Conference, IEEE reference publication 68 C 21 - Energy.

25. Pitts, J.H. and M.H.L. Jester, "Rankine Cycle System Studies for Nuclear Space Power", Intersociety Energy Conversion Engineering Conference, IEEE referency publication 68 C 21 - Energy.

26. Leach, C.E. and B.C. Fryer, "A 7.3 kw(e) Radioisotope Energized Undersea Stirling Engine", Intersociety Energy Conversion Engineering Conference, IEEE reference publication 68 C 21-Energy.

27. Ruehle, William, "The Kernel-Heater Concept for Multikilowatt Radioisotope Power", Intersociety Energy Conversion Engineering Conference, IEEE reference publication 68 C 21 - Energy.

28. Menetrey, W.R., et al, Energy Conversion Systems Reference Handbook: Volume I - General Systems Considerations, Clearinghouse, Dept. of Commerce, Number AD 257 357.

29. Radiological Health Handbook, U.S. Dept. of Health, Education, and Welfare (Public Health Service), Revised Edition, Sept. 1960.

APPENDIX

Table A2.1*

Comparison of Energy Conversion Techniques

Energy Conversion Technique	Typical Max. and Reject Temps.	Est. Plant Eff.	Typical Operating Experience	Advantages	Disadvantages
Thermoelectric	1000°F or 1500°F to $150\ ^\circ$F	5-9%	Several years for a few radioisotope fueled low power ($<$100watt) systems.	No moving parts. Long potential life-time. Rugged. Quiet operation. State-of-the-art.	Low efficiency, large weights. High temperatures. Expensive materials problems.
Thermionic	3000°F to 1200°F	8-15%	Limited, a few tests have run for 8000&10,000hrs. in the laboratory. Most have been shorter.	No moving parts. Light weights. Quiet operation	High temperatures. Limited state-of-the-art. Difficult fuel fabrication.
Water-Rankine	1000°F to $100\ ^\circ$F	10-20%	Few small systems have been built.	Small pump&heat exchanger requirements. Long operating experience in large sizes. Low temperatures	Potential bearing problem and turbine, nozzles, blades in turbines. Little experience in reciprocating.
Mercury-Rankine	1030°F or 1200°F to $560\ ^\circ$F	8-14%	3-3Kw(e) 4100hrs 3-6Kw(e) 7000hrs 40,000hrs total	Good heat transfer properties. Low weight dynamic units. No fluid degradation.	Containment problems. Corrosion/erosion in boiler, bearings.
Organic Rankine	700°F to 290°F	10-25%	1.5Kw(e) 2000hrs	Excellent fluid thermodynamic properties. Good efficiency. Low temperatures	Fluid degradation. Little operating experience.

*From Reference 6.

Closed Cycle Brayton	$1300^{\circ}F$ to $150^{\circ}F$	15-20%	3Kw(e) 60 hrs	No corrosive fluids. High potential reliability.	High temperatures. Low power densities. Sink temperature sensitive.
Stirling(closed)	$900^{\circ}F$ or $1400^{\circ}F$ to $150^{\circ}F$	30-40%	10HP/500 hrs 3Kw(e)1000hrs 3-4Kw(e)2000hrs	Low system cost due to relatively high thermal efficiency.	Seals mechanically complex. Limited operating experience.

Table A2.2*

Comparison of Rankine Cycles

Item	Advantages	Disadvantages
General	Low fluid pumping requirements. Reasonable cycle temperatures. High thermal efficiency.	Developmental bearing technology. Orientation sensitive system design.
Steam Turbine	Reasonable cycle temperatures. Detailed knowledge of water-steam properties.	Potential bearing problems. Low efficiency at low power levels.
Reciprocating Steam Engine	High efficiencies at lower power level than steam turbine.	Limited life. Developmental.
Organic Vapor Turbine	Good thermodynamic characteristics. Low cycle pressures and temperatures. No corrosion. High efficiencies.	Pyrolytic and radiolytic fluid degradation. Potential bearing problems in some designs. Limited operating experience.
Liquid Metal Vapor Turbine	Excellent heat transfer properties. Compact, low weight dynamic units. No fluid degradation.	Mass transfer, corrosion. Developmental. Limited operating experience. Potential bearing problems.

*From Reference 6.

B. High Pressure Superheated Steam Cycle Analysis

The thermodynamic cycle analysis for the assumed high pressure, superheated steam cycle is presented in outline form in the following.

Steam pressure	800 psia
Steam temperature	740°F
Condensing pressure	3 psia

$$N_s = \frac{N(hp)^{0.5}}{H^{1.25}}\left[\frac{550}{\eta\rho}\right]$$

$h_1 = 1363.2$

$h_3 = 932.0$

$$H^{1.25} = \left[(778)(431.2)\right]^{1.25}$$

$$= 8,400,000$$

Assume $\eta = 0.60$, then

$h_{3'}$ = turbine exit enthalpy = 1104.7 Btu/lb

$x_{3'} = 0.982$

$\rho_{3'} = 0.00858$ lb/ft^3

$$N_s = \frac{(24000)(10.71)^{0.5}}{8400000}\left[\frac{550}{(0.60)(0.00858)}\right]^{0.5}$$

$$= 3.06$$

From figure 5.3, η = 60% and from figure 14 of reference 5

$D_s = 7.2$

No. of stages = 4, (multi-staged re-entry type turbine)

However, for this case

$$(\frac{P}{P})_{max} = \frac{800}{3} = 267:1$$

which greatly exceeds the turbine design chart condition of 100:1.

$v_{3'} = 116.5\ ft^3/lb$

$\dot{m} = 0.0293\ lb/sec$

$V_{3'} = 3.42\ ft^3/sec$

$$D = \frac{D_s V_{3'}^{0.5}}{H^{0.25}}$$

$D = 6.76$ in.

C. Low Pressure Superheated Steam Cycle Analysis

Steam pressure	80 psia
Steam temperature	$1200^{\circ}F$
Condensing pressure	1 psia
Condensing temperature	$101.74^{\circ}F$

$h_1 = 1636.2$ Btu/lb

$h_3 = 1124.2$ Btu/lb

Assume $\eta = 0.68$, then

$h_{3'} = 1288.2$ Btu/lb

$v_{3'} = 571.6\ ft^3/lb$

$\rho_{3'} = 0.00175\ lb/ft^3$

$N_s = 5.39$

From figure 5.3, $\eta = 0.68$

No. of stages = 4

From figure 14 of reference 5

$D_s = 6$

Solving for the steam flow rate we get

$\dot{m} = 0.0218\ lb/sec$

$V_{3'} = 12.48\ ft^3/sec$

Therefore

$$D = \frac{D_s V_{3'}^{0.5}}{H^{0.25}}$$

or

$$D = 10.13 \text{ in.}$$

D. Superheated Mercury Cycle Analysis

Mercury pressure	379.4 psia
Mercury temperature	1800°R
Turbine exit pressure	3.23 psia

$h_1 = 186.9$ Btu/lb

$h_3 = 133.9$ Btu/lb

$H = J(h_1 - h_3) = 41{,}200$ ft

Assume $\eta = 0.67$, then

$h_{3'} = 151.4$ Btu/lb

$x_{3'} = 89\%$

$v_{3'} = 14.73$ ft^3/lb

$\rho_{3'} = 0.0679$ lb/ft^3

$N_s = 14.62$

$D_s = 4.2$, single stage, partial admission

$\eta = 0.67$, (check)

$D = 6.25$ in.

For a multi-staged re-entry type turbine, at $N_s = 14.26$

$\eta = 0.77$

Optimum no. of stages = 2

$(P/P)_{max} = 379.4/3.23 = 117{:}1$

which slightly exceeds the design chart condition. Solving for the turbine diameter, we get

$$D = 4.92 \text{ in.}$$

For the single stage turbine the turbine blade height is given by

$$h = (h/D)\ D$$

$$= (0.073)(6.25)$$

$$= 0.456 \text{ in.}$$

where $h/D = 0.073$ from figure 5 of reference 5.

Evaporator Flow Calculations

The schematic arrangement of the evaproating section is shown in figure A7.1. A mass balance on the heat source-boiler is given by, (reference 3)

$$\dot{m}_f = \dot{m}_v \tag{a}$$

$$\dot{m}_v + \dot{m}_r = \dot{m}_i \tag{b}$$

The quality of the vapor-liquid mixture at the separate inlet is given by

$$x_m = \frac{\dot{m}_v}{\dot{m}_v + \dot{m}_r}$$

$$= \frac{\dot{m}_f}{\dot{m}_f + \dot{m}_r}$$

$$= \frac{\dot{m}_f}{\dot{m}_i} \tag{c}$$

The recirculation ratio is the ratio of the recirculation liquid mercury to mercury vapor produced. It is given by modifying eq. (c):

$$\frac{\dot{m}_r}{\dot{m}_v} = \frac{1 - x_m}{x_m} \tag{d}$$

Neglecting changes in kinetic and potential energies an energy balance is as follows:

$$\dot{m}_i h_i = \dot{m}_f h_f + \dot{m}_r h_r \tag{3}$$

or

$$h_i = x_m h_f + (1 - x_m) h_r . \tag{f}$$

Rearranging gives another expression for x_m:

$$x_m = \frac{h_i - h_r}{h_f - h_r} = \frac{h_r - h_i}{h_r - h_f} \tag{g}$$

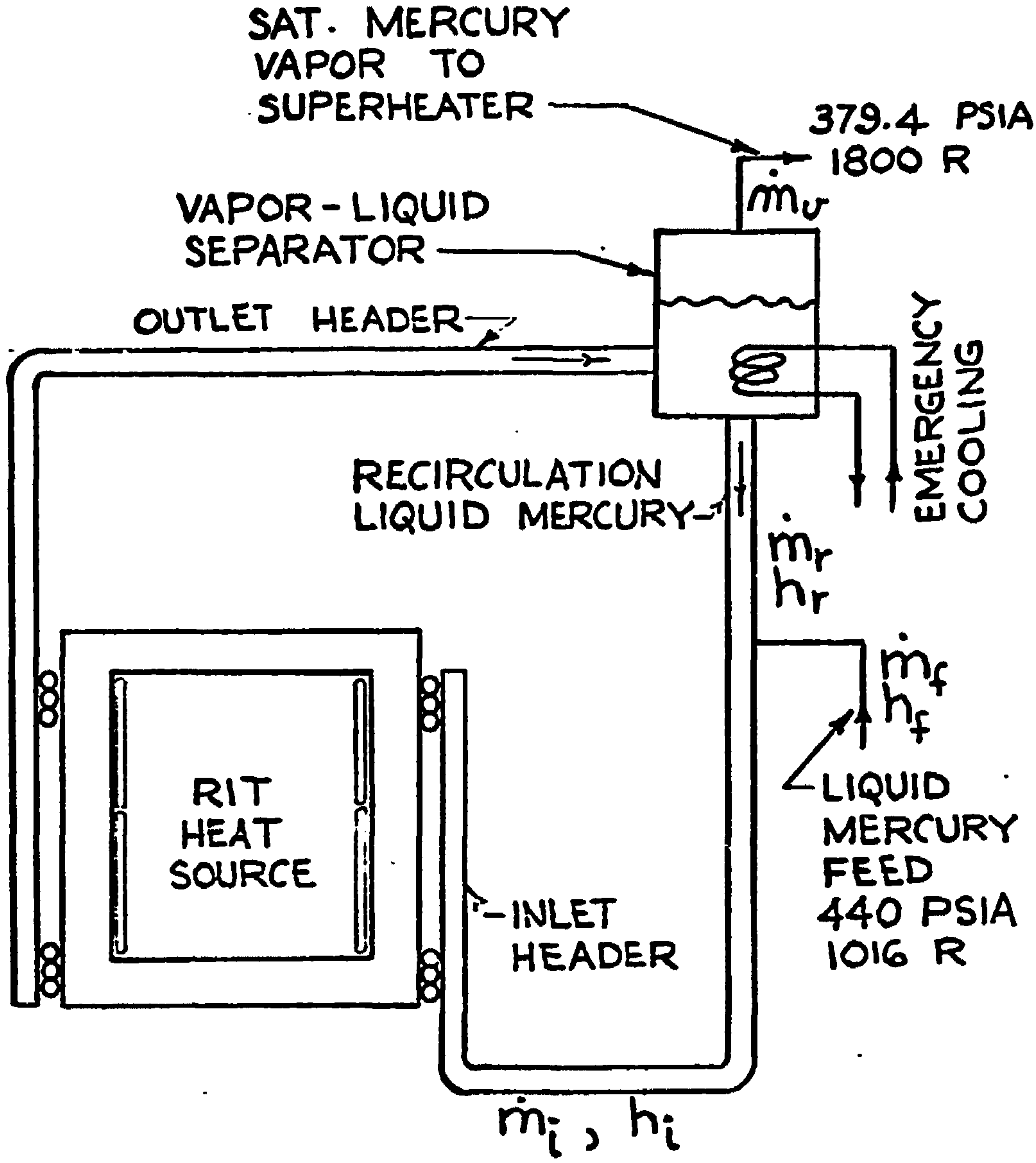

Mercury Boiler Schematic

Figure A7.1

The quantity $h_r - h_i$ denotes the degree of subcooling of the liquid mercury entering the inlet header of the heat source. The void fraction α is defined by

$$\alpha = \frac{\text{volume of vapor in mixture}}{\text{total volume of vapor-liquid mixture}} \, .$$

The slip ratio S is defined as the ratio of the velocity of the vapor V_g to that of the liquid V_f. Thus

$$S = \frac{V_g}{V_f}$$

Also it can be shown that

$$\alpha = \frac{1}{1 + \left[(1 - x)/x \right] \Psi}$$

or

$$x = \frac{1}{1 + \left[(1 - \alpha)/\alpha \right] 1/\Psi}$$

where

$$\Psi = \frac{v_f}{v_g} S$$

From the following figure A7.2 (from fig. 11-17 of reference 3), the value of S may be estimated at 3.2.

Assume that the average inlet velocity to the evaporator tubes is 1.0 ft/sec. Then

$$\Psi = \frac{v_f}{v_g} S$$

$$= \frac{0.00132}{0.2053} (3.2)$$

$$= 0.0206$$

Choose $x_m = 0.10$ then the void fraction is

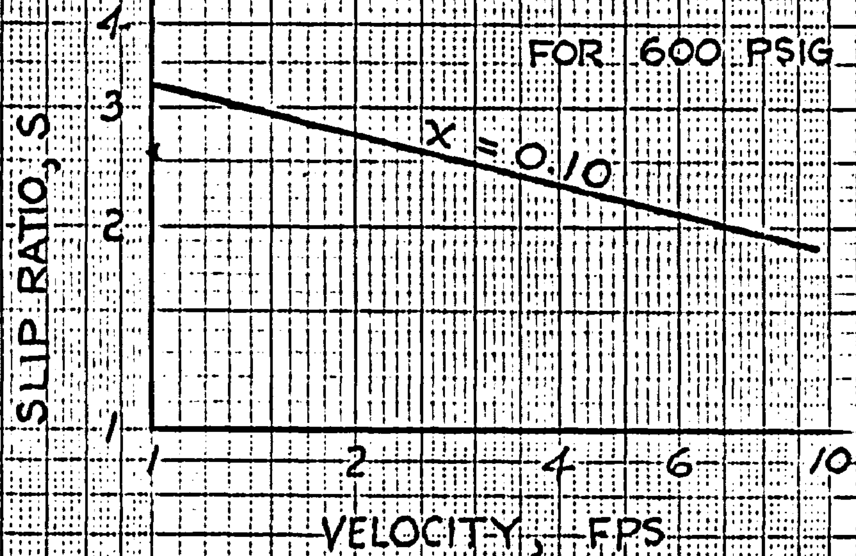

Slip Ratio Curve
(FROM REFERENCE 3)

Figure A7.2

$$\alpha = \frac{1}{1 + \left[\frac{1 - x}{x}\right] \Psi}$$

$$= 0.844$$

The recirculation ratio is

$$\frac{\dot{m}_r}{\dot{m}_v} = \frac{1 - 0.1}{0.1}$$

$$= 9 \; \frac{\text{lb liquid}}{\text{lb vapor}}$$

The total flow through the evaporator tubes is given by

$$\dot{m}_i = (857)(9 + 1)$$

$$= 8570 \text{ lb/hr}$$

The inlet velocity to the tubes, (for 18 tube circuits and for a cross-sectional area of each tube of 0.00025 ft^2)

$$V_i = \frac{\dot{m}_i v_i}{A_i}$$

$$= (8570)(0.00132)\left[\frac{1}{(0.00025)(18)}\right]\left(\frac{1}{3600}\right)$$

$$V_i = 0.7 \text{ ft/sec.}$$

The degree of subcooling entering the evaporating tubes is given by

$$\Delta h_{sub} = x_m(h_r - h_f)$$

$$= 0.1(58.6 - 39.3)$$

$$= 1.93 \text{ Btu/lb}$$

Therefore

$$h_i = 58.6 - 1.9$$

$$= 56.7 \text{ Btu/lb}$$

and

$$c_p \approx 0.032 \text{ Btu/lb }^{o}\text{R}$$

$$\Delta T_{sub} = \frac{1.93}{0.032}$$

$$= 60.3^{o}\text{R}$$

The temperature of the mercury entering the evaporating tubes may be determined from the relation

$$\dot{m}_i c T_i = \dot{m}_r c T_r + \dot{m}_f c T_f$$

or

$$T_i = \frac{1}{\dot{m}_i} (\dot{m}_r T_r + \dot{m}_f T_f)$$

$$= \frac{1}{10} \left[(9)(1600) + (1)(1016) \right]$$

$$T_i = 1542^{o}\text{R}$$

Evaporator Tube Friction Drop

The friction pressure drop for the boiling mercury may be estimated by use of the Darcy equation and a friction multiplier, $\bar{R}$, chapter 11, reference 3). The multiplier is used in order to account for the fact that the friction loss in two phase flow will be greater than that for single phase saturated liquid flow. The multiplier denotes the ratio of pressure drop in two-phase flow to the pressure drop in single phase flow. Thus

$$\bar{R} = \frac{\Delta p_{TP}}{\Delta p_{SP}}$$

Figure A7.3, (from reference 18), provides values of $\bar{R}$ as a function of pressure and exit quality of the flow stream. On the basis of the flow calculations above the exit quality of the mercury from the evaporator

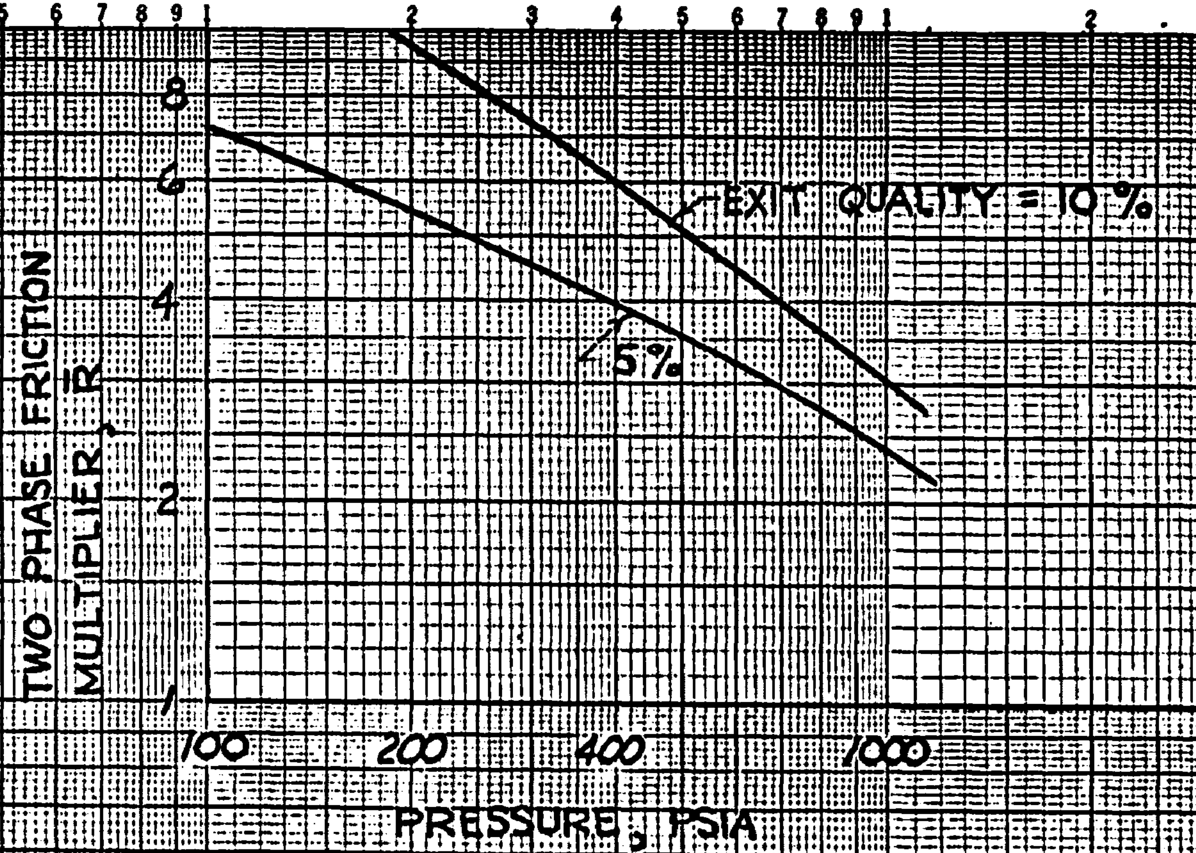

Martinelli-Nelson Friction-Multiplier Correlation (From Ref. 18)

Figure A7.3

tubes is 0.10. Calculations for the pressure drop are as follows:

$$R_e = \frac{D_e V \rho}{\mu}$$

$$\mu = 0.58 \times 10^{-3} \ lb_m/ft \ sec$$

$$\rho = \frac{1}{v} = \frac{1}{0.00124} = 806 \ lb/ft^3$$

$$V = 0.7 \ ft/sec$$

$$D_e = 0.018 \ ft$$

$$R_e = \frac{(0.018)(0.7)(806)(1000)}{(0.58)}$$

$$R_e = 17{,}500$$

$$f = \frac{0.184}{R_e^{\ 0.2}}$$

$$f = 0.026$$

The single phase pressure drop is therefore

$$\Delta p_{SP} = f \frac{L}{D_e} \frac{\rho V^2}{2g_c}$$

$$= (0.026) \frac{(25)(806)(0.7)^2}{(0.018)(2)(32.2)(144)}$$

$$= 1.54 \ lb/in^2$$

From figure A7.3 the two phase friction drop multiplier is five, therefore

$$\Delta p_{TP} = (5)(1.54)$$
$$= 7.7 \ psi$$

Available pressure head. An estimate of the pressure head available, (based on a 3 foot elevation of the separator above the evaporator section), is given by the following:

$$\rho_{downcomer} = \frac{1}{v_{avg.}}$$

$$= \frac{1}{0.00131}$$

$$= 764 \text{ lb/ft}^3$$

The density of the two phase mixture at the top of the riser is

$$v = v_f + xv_{fg}$$

$$= 0.00132 + (0.10)(0.2258 - 0.00132)$$

$$= 0.02377 \text{ ft}^3/\text{lb}$$

$$\rho = \frac{1}{v}$$

$$= 42.1 \text{ ft}^3/\text{lb}$$

The average density in the riser is thus

$$\rho_{avg} = \frac{764 + 42.1}{2}$$

$$= 403 \text{ lb/ft}^3$$

The pressure head available is then given by

$$\Delta p = \gamma h$$

$$= (764 - 403)(3)(1/144)$$

$$= 7.53 \text{ psi}$$

Since this is approximately the same as the friction loss the evaporating tube arrangement having 18 tube circuits of 1/8" diameter tubes (inside diameter, 0.215 inches) will be satisfactory.

Alternate Temperature Field Analysis

For the range of r of interest here the exponential function $e^{-\mu(r-r_1)}$ may be represented approximately by the function $(r_1/r)^{20}$. The value of each function for various radius positions is given in table A7.1

Table A7.1

Function Values

Radius Position	$e^{-\mu(r-r_1)}$	$(r_1/r)^{20}$
r_1	1	1.0
$r_1 + 0.1$	0.053	0.0515
$r_1 + 0.2$	0.0028	0.0039
$r_1 + 0.3$	0.00015	0.0004
$r_1 + 0.4$	0.000008	0.00005

Using the function $(r_1/r)^{20}$ in place of the exponential function in the differential temperature equation for the cylindrical heat flow model with internal generation results in an equation which has the following solution

$$t - t_M = \frac{\mu r_1^2 I_1}{19k}\left[\left(\frac{1}{19}\right)\left\{\left(\frac{r_1}{r_2}\right)^{19} - \left(\frac{r_1}{r}\right)^{19}\right\} + \ln\frac{r_2}{r}\right]$$

Substituting in values for the parameters results in

$$t_1 - t_M = 85.4^{\circ}F$$

for the temperature drop across the tungsten shield. This result compares closely with the value obtained in Chapter VII using the exponential attenuation function.

Temperature Drop Calculation for Cylinder Model

Assuming No Internal Heat Source in the Shield

The applicable differential equation is

$$\frac{d^2t}{dr^2} + \frac{1}{r}\frac{dt}{dr} = 0$$

The boundary conditions are

$$-kA\frac{dt}{dr} = q_i \qquad \text{at } r = r_1$$

$$t = t_M \qquad \text{at } r = r_2.$$

where r_1 is the inside radius of the cylinder and r_2 is the outside radius of the cylinder. Assume a solution of the form

$$t = C_1 + C_2 \ln r$$

Substituting the boundary conditions into the differential equation produces

$$t_M = C_1 + C_2 \ln r_2$$

$$-kA\left.\frac{dt}{dr}\right|_{r = r_1} = -kA\frac{C_2}{r_1} = q_i$$

therefore

$$C_2 = -\frac{q_i r_1}{kA}$$

$$C_1 = t_M + \frac{q_i r_1}{kA}\ln r_2$$

and

$$t - t_M = \frac{q_i r_1}{kA}\ln\frac{r_2}{r}$$

where $A = 2\pi r_1 \ell$

thus

$$t_1 - t_M = \frac{q_i}{2\pi k\ell}\ln\frac{r_2}{r}$$

$$= \frac{(158000)(12)}{(2\pi)(65.1)(18.4)}\ln\frac{12}{8}$$

$$= 102^{o}F$$

Detailed Analysis: One Dimensional, Flat Slab, Heat Flow Model

The arrangement of the materials is shown schematically in figure A7.4.

For the fuel portion the heat flow may be depicted as illustrated in figure A7.5. The heat generated in the layer of thickness dx is equal to the heat crossing plane (x + dx) minus the heat crossing plane x. Thus

$$q_1''' \ A \ dx = q_{x \ + \ dx} - q_x$$

where q_1''' is the volumetric thermal source strength. But

$$q_x = - k_1 A \frac{dt}{dx}$$

and

$$q_{x \ + \ dx} = q_x + \frac{dq_x}{dx} dx$$

$$= - k_1 A \frac{dt}{dx} + (- k_1 A \frac{d^2t}{dx^2} dx)$$

Therefore

$$q_1''' \ A \ dx = - k_1 A \frac{d^2t}{dx^2} dx$$

or

$$\frac{d^2t}{dx^2} = - \frac{q_1'''}{k_1}$$

The latter equation may be integrated twice to give

$$\frac{dt}{dx} = - \frac{q_1'''}{k_1} x + C_{1,1}$$

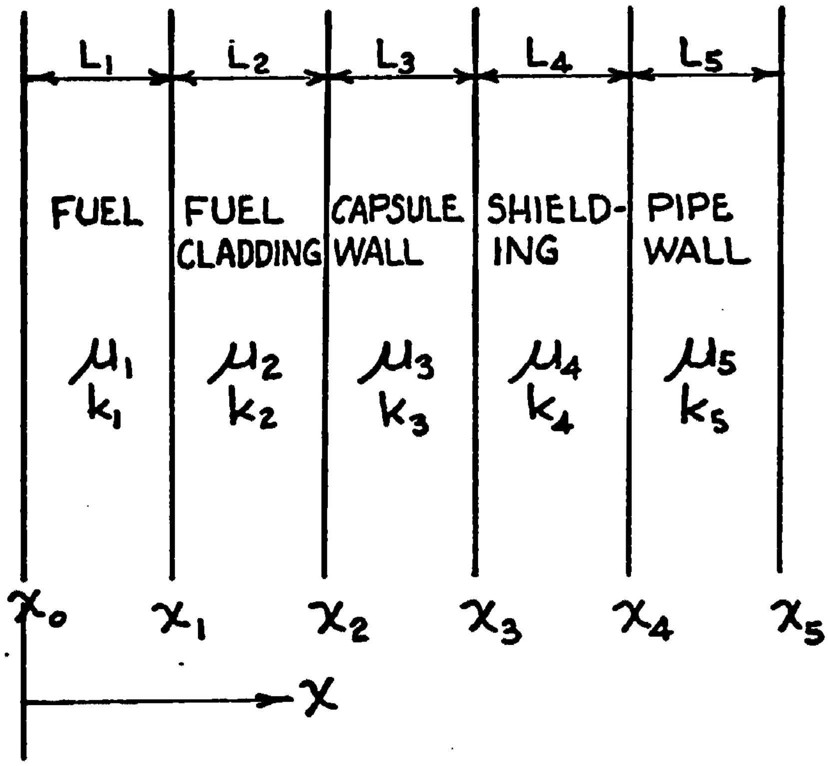

Flat Slab Model of Heat Source

Figure A7.4

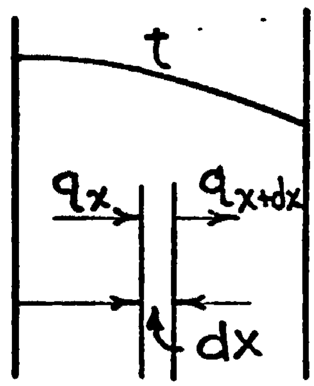

Fuel Heat Flow

Figure A7.5

and

$$t_1 = -\frac{q_1''' x^2}{2k_1} + C_{1,1} + C_{1,2} \tag{1}$$

For the materials other than the fuel the heat generated is a function of the position x. Thus we may write

$$q''' = q_S''' e^{-\mu x}$$

where q_S''' is the volumetric thermal source strength at the left hand surface of the particular material. Thus the differential equation for these materials would be

$$\frac{d^2t}{dx^2} = -\frac{q_S''' e^{-\mu x}}{k}$$

Integrating twice results in

$$\frac{dt}{dx} = \frac{q_S''' e^{-\mu x}}{\mu k} + C_1$$

and

$$t = -\frac{q_S''' e^{-\mu x}}{\mu^2 k} + C_1 x + C_2$$

Thus the temperature expression for material two becomes

$$t_2 = -\frac{q_2''' e^{-\mu_2 x}}{\mu_2^2 k_2} + C_{2,1} x + C_{2,2} \tag{2}$$

where $x_1 \le x \le x_2$

Similarily for the other materials we may write

$$t_3 = -\frac{q_3''' e^{-\mu_3 x}}{\mu_3^2 k_3} + C_{3,1} x + C_{3,2} \tag{3}$$

where $x_2 \le x \le x_3$

$$t_4 = - \frac{\dot{q}_4''' e^{-\mu_4 x}}{\mu_4^2 k_4} + C_{4,1} x + C_{4,2} \tag{4}$$

where $x_3 \le x \le x_4$

$$t_5 = - \frac{q_5''' e^{-\mu_5 x}}{\mu_5^2 k_5} + C_{5,1} x + C_{5,2} \tag{5}$$

where $x_4 \le x \le x_5$

If it is assumed that the surface on the left is an adiabatic surface and assuming that the inside surface of the pipe is approximately the same as the temperature of the mercury, or other fluid which removes heat energy from the heat source subsystem, then the boundary conditions for the temperature equations may be written as

$$\left. \frac{dt_1}{dx} \right|_{x = 0} = 0 \tag{6}$$

$$\left. t_5 \right|_{x = x_5} = t_M \tag{7}$$

$$\left. t_1 \right|_{x = x_1} = \left. t_2 \right|_{x = x_1} \tag{8}$$

$$\left. t_2 \right|_{x = x_2} = \left. t_3 \right|_{x = x_2} \tag{9}$$

$$\left. t_3 \right|_{x = x_3} = \left. t_4 \right|_{x = x_4} \tag{10}$$

$$\left. t_4 \right|_{x = x_4} = \left. t_5 \right|_{x = x_4} \tag{11}$$

$$\left. - k_1 \frac{dt_1}{dx} \right|_{x = x_1} = \left. - k_2 \frac{dt_2}{dx} \right|_{x = x_1} \tag{12}$$

$$- k_2 \frac{dt_2}{dx}\bigg|_{x = x_2} = - k_3 \frac{dt_3}{dx}\bigg|_{x = x_2} \tag{13}$$

$$- k_3 \frac{dt_3}{dx}\bigg|_{x = x_3} = - k_4 \frac{dt_4}{dx}\bigg|_{x = x_3} \tag{14}$$

$$- k_4 \frac{dt_4}{dx}\bigg|_{x = x_4} = - k_5 \frac{dt_5}{dx}\bigg|_{x = x_4} \tag{15}$$

Let

$$A_1 \equiv - \frac{q_1'''}{2k_1}$$

$$A_2 \equiv - \frac{q_2'''}{\mu_2^2 k_2}$$

$$A_3 \equiv - \frac{q_3'''}{\mu_3^2 k_3}$$

$$A_4 \equiv - \frac{q_4'''}{\mu_4^2 k_4}$$

$$A_5 \equiv - \frac{q_5'''}{\mu_5^2 k_5}$$

and substitute the above five temperature equations into the boundary conditions to obtain the following expressions for the constants of integration

$$C_{1,1} = 0 \tag{16}$$

$$C_{2,1} = \frac{2k_1 A_1 L_1}{k_2} + A_2 \mu_2 \tag{17}$$

$$C_{3,1} = - \frac{k_2 A_2 \mu_2 e^{-\mu_2 L_2}}{k_3} + \frac{k_2 C_{2,1}}{k_3} + A_3 \mu_3 \tag{18}$$

$$C_{4,1} = -\frac{k_3 A_3 \mu_3 e^{-\mu_3 L_3}}{k_4} + \frac{k_3 C_{3,1}}{k_4} + A_4 \mu_4 \tag{19}$$

$$C_{5,1} = -\frac{k_4 A_4 \mu_4 e^{-\mu_4 L_4}}{k_5} + \frac{k_4 C_{4,1}}{k_5} + A_5 \mu_5 \tag{20}$$

$$C_{5,2} = t_M - A_5 e^{-\mu_5 L_5} - C_{5,1} L_5 \tag{21}$$

$$C_{4,2} = A_5 + C_{5,2} - C_{4,1} L_4 - A_4 e^{-\mu_4 L_4} \tag{22}$$

$$C_{3,2} = A_4 + C_{4,2} - C_{3,1} L_3 - A_3 e^{-\mu_3 L_3} \tag{23}$$

$$C_{2,2} = A_3 + C_{3,2} - C_{2,1} L_2 - A_2 e^{-\mu_2 L_2} \tag{24}$$

$$C_{1,2} = A_2 + C_{2,2} - A_1 L_1^2 \tag{25}$$

The required heat source energy production is

$$q = \frac{(125,700)(1.10)}{(0.875)}$$

$$= 158000 \text{ Btu/hr}$$

For a fuel volume of 105 cu in., or 0.0608 cu ft the energy generation rate of the fuel is

$$q_g''' = \frac{158000}{0.0608}$$

$$= 2,600,000 \text{ Btu/hr ft}^3$$

The average thermal source strength for the fuel may then be determined by

$$\begin{aligned} q_1''' &= \frac{1}{L_1} \int_0^{L_1} q_g'''(1 - e^{-\mu_1 x})\, dx \\ &= q_g'''\left[1 + \frac{e^{-\mu_1 L_1} - 1}{\mu_1 L_1}\right] \end{aligned} \tag{26}$$

The material thickness and necessary physical properties are given in table A7.2.

Table A7.2

Material Parameters

Material	Thickness, ft	μ ft^{-1}	k Btu/hr ft°F
1. Fuel (Cobalt 60)	0.0104	15.85	11.84
2. Fuel Cladding (Nickel)	0.00416	10.0	37.5
3. Capsule Wall (Stainless Steel)	0.0104	8.5	10.7
4. Shielding (Tungsten)	0.3333	29.4	65.1
5. Pipe Wall (Carbon Steel)	0.0079	8.4	18.8

Numerical Results

Substitution of values into equation (26) yields

$$q_1''' = 187{,}000 \text{ Btu/hr ft}^3$$

The energy absorbed in the fuel is thus

$$q_{fuel} = (187000 \text{ Btu/hr ft}^3)(0.0608 \text{ ft}^3)$$

$$= 11{,}380 \text{ Btu/hr}$$

Therefore the energy flux to the fuel cladding is given by

$$q_{cladding} = 158000 - 11380$$

$$= 146{,}620 \text{ Btu/hr}$$

The fuel surface area is

$$A = (46.7 \text{ in.})(20.4 \text{ in.})/144$$

$$= 6.61 \text{ ft}^2$$

The intensity of the energy flux (gamma ray energy flux) to the fuel cladding is

$$I_2 = \frac{146620}{6.61}$$

$$= 22,200 \text{ Btu/hr ft}^2$$

Therefore

$$q_2''' = \mu_2 I_2$$

$$= (10)(22,200)$$

$$= 222,000 \text{ Btu/hr ft}^3$$

The intensity of the gamma ray energy flux to the capsule wall surface is given by

$$I_3 = I_2 \ e^{-\mu_2 L_2}$$

$$= (22,200)e^{-(10)(0.00416)}$$

$$= 21,300 \text{ Btu/hr ft}^2$$

Thus

$$q_3''' = \mu_3 I_3$$

$$= (8.5)(21,300)$$

$$q_3''' = 181,000 \text{ Btu/hr ft}^3$$

Similarly

$$q_4''' = 573,000 \text{ Btu/hr ft}^3$$

and

$$q_5''' = 9.18 \text{ Btu/hr ft}^3$$

Solving for the constants of integration we get

$$C_{1,1} = 0$$

$$C_{2,1} = -643\ ^{o}F/ft$$

$$C_{3,1} = -2252\ ^{o}F/ft$$

$$C_{4,1} = -370\ ^{o}F/ft$$

$$C_{5,1} = -1281\ ^{o}F/ft$$

$$C_{5,2} = t_M + 10.1\ ^{o}F$$

$$C_{4,2} = t_M + 133.3\ ^{o}F$$

$$C_{3,2} = t_M + 360.7\ ^{o}F$$

$$C_{2,2} = t_M + 186.2\ ^{o}F$$

$$C_{1,2} = t_M + 127{,}8\ ^{o}F$$

Upon stubstituting for the constants of integration in the temperature equations we obtain

$$t_1 = -7180x^2 + t_M + 127.8 \qquad 0 \le x \le x_1$$

$$t_2 = -59.2e^{-10.0x} - 643x + t_M + 186.2 \qquad x_1 \le x \le x_2$$

$$t_3 = -234e^{-8.5x} - 2252x + t_M + 360.7 \qquad x_2 \le x \le x_3$$

$$t_4 = -10.19e^{-29.4x} - 370x + t_M + 133.3 \qquad x_3 \le x \le x_4$$

$$t_5 = -0.00692e^{-8.4x} - 1281x + t_M + 10.1 \qquad x_4 \le x \le x_5$$

From these equations the temperatures at the boundaries and interfaces may be obtained. These temperatures are as follows:

$$t_1\Big|_{x = 0} = t_M + 127.8^{o}F$$

$$t_1\Big|_{x = L_1} = t_M + 127^{o}F$$

$$t_2\big|_{x = L_2} = t_M + 126.7^{\circ}F$$

$$t_3\big|_{x = L_3} = t_M + 123.1^{\circ}F$$

$$t_4\big|_{x = L_4} = t_M + 10.1$$

$$t_5\big|_{x = L_5} = t_M$$

Thus the total temperature drop across the five materials is 127.8°F. The temperature across the tungsten shield is 113°F, or 92 per cent of the total.

Any air or gas gap would introduce a comparatively large temperature drop in the heat transfer path and is therefore to be avoided. Maintaining good thermal contact between the outer heat source wall and the mercury tubes will be a problem. Powdered graphite will be packed around the tubes as a means of enhancing the heat transfer from the heat source shield to the tube.